1-1-1988

The determination of the mechanical behavior of polyamic acid/ polyimide coatings/

Charles L. Bauer
University of Massachusetts Amherst

THE DETERMINATION OF THE MECHANICAL BEHAVIOR OF POLYAMIC ACID/POLYIMIDE COATINGS

A Dissertation Presented

by

Charles L. Bauer

Submitted to the Graduate School of the
University of Massachusetts in partial fulfillment
of the requirements for the degree of

DOCTOR OF PHILOSOPHY

May 1988

Polymer Science and Engineering

THE DETERMINATION OF THE MECHANICAL BEHAVIOR OF POLYAMIC ACID/POLYIMIDE COATINGS

A Dissertation Presented

by

Charles L. Bauer

Approved as to style and content by:

Richard J. Farris, Chairperson of Committee

Julio M. Ottino, Committee Member

James A. Donovan, Committee Member

William J. MacKnight, Acting Department Head
Polymer Science and Engineering

In memory of my Dad

ACKNOWLEDGMENTS

I was very apprehensive about my choice of careers after completing my undergraduate degree. However, by the end of my first year at UMass, I realized that I had made the right decision and now feel comfortable in the field I have chosen.

I owe much to my advisor, Dr. Richard J. Farris, for allowing me the opportunity to study polymer mechanics and engineering. This may not seem like much, but for him to permit an "organic chemistry" person to join his group was a risk to everyone.

I would also like to thank Drs. Julio Ottino and James Donovan for serving on my committee. They were especially cooperative in helping me complete the graduate school requirements during my last few months here. The faculty and support staff deserve my thanks for their assistance, expertise and guidance.

My special thanks go to my friends in the Amherst area and my family. They are the people that make graduate school bearable during the rough times.

Finally, I would like to acknowledge the support of IBM, East Fishkill and in particular, Drs. Robert Lacombe and Peter Geldermans. They helped to initiate this work and allowed me access to their facilities to prepare samples during the early stages of my research.

ABSTRACT

THE DETERMINATION OF THE MECHANICAL BEHAVIOR OF POLYAMIC ACID/POLYIMIDE COATINGS

MAY 1988

Charles L. Bauer, B.S., Carnegie Mellon University

Ph.D., University of Massachusetts

Directed by: Professor Richard J. Farris

The dimensional constraints imposed on polymeric coatings may significantly influence the final stress state in the coatings. These stresses may be sufficiently large to cause failure of the coating, such as delamination or cracking. For many polymeric coating materials the development of such stresses is dependent on the processing history of the coating. To accurately design devices that incorporate these types of coatings, the properties must be characterized as a function of the thermal and solvent history.

Many specialty polymeric coatings are used by the microelectronics industry. One class of materials commonly used are polyimides, which may be formed from a polyamic acid solution. Large residual stresses may develop in polyimide coatings because of the many processing stages required to form the fully cured material.

The development of the stresses and mechanical properties in polyamic acid/polyimide coatings based on pyromellitic dianhydride and oxydianiline (PI5878 from DuPont) was studied as a function of processing history. Using techniques such as the propagating wave method and the Impulse Method, the stress, mass and modulus of the polyamic acid coating were determined as a function of temperature and time. For a coating under a two dimensional

constraint, the stress due to solvent removal from the coating and subsequent imidization may be as large as 30 MPa. The solvent removal is dependent on temperature and stress in the polyamic acid coating. An energy balance approach qualitatively describes this coupled behavior. Mechanical properties such as modulus and thermal expansion coefficient were obtained throughout the processing of these coatings. The modulus of the polyamic acid coating was 2 GPa compared to 3 GPa for the fully cured polyimide. The thermal expansion coefficient at 25° C is 4.9 x 10^{-5} cm/cm/° C for the polyamic acid and 1.8 x 10^{-5} cm/cm/° C for the polyimide. Using a high pressure gas dilatometer, Poisson's ratio for the polyimide was determined to be 0.34 at 1% strain. The surface energy of adhesion for a 200° C cured PI5878 on glass was determined to be 1.6 Nm^{-1} from a novel self-delamination technique.

TABLE OF CONTENTS

LIST OF TABLES

LIST OF FIGURES

CHAPTER 1

INTRODUCTION

1.1 Polymeric Coatings

Polymeric coatings have varied commercial applications. In most cases a thin coating is used as an insulating or protective layer such as a wire coating or enamel paint. These coatings are typically categorized as strong or weak materials and as well or poorly adhering coatings. Classifying coatings merely by their tensile strength or adhesion to substrates does not provide a reliable usage criterion. Strong coatings usually have high moduli and thus will develop higher residual stresses than weaker coatings with a relatively low moduli. It is these stresses which can lead to failure of the coating, such as cracking or delamination. To select the best coating system, the strength and adhesion of the material must be compared to the stress level in the coating.

Stresses in a coating develop from solidification of the coating or differences in thermal expansion and swelling between the coating and substrate. Solidification processes include polymerization, crystallization or solvent removal. Each of these creates a volume change in the material. If the material is unconstrained no stresses will develop. However, if the material cannot freely contract or expand in all directions, as with polymeric coatings applied to a rigid substrates, internal stresses will develop. Since many of the solidification processes occur at elevated temperatures, on cooling to room temperature,

thermal stresses develop. Additional exposure to temperature and solvents can also change the stress state in the coating.

Consequently, the stress level in a coating will be a function of the processing history. This has been demonstrated by Perera and Eynde with the drying of an epoxy/polyamide varnish.[1] The final residual stress in the films could be varied by exposing several of these coatings to identical thermal and moisture environments, but in different sequences.

To illustrate such thermal history dependence, the applied stress on a Du Pont Kapton-H polyimide film was obtained as a function of temperature, Figure 1.1. The film was initially stressed to 10 MPa, heated to 100° C and cooled. The cycle is reversible and linear. On reheating to 300° C and cooling to room temperature, the reference state has shifted and the stress at room temperature is greater than the initial value. Another shift in the stress-free reference temperature is observed on heating the sample to 400° C. This demonstrates that for a fully cured and annealed polyimide material the final stress state is a function of the processing history. An incremental approach to elasticity is one of the simplest methods to describe such behavior. This method incorporates a shifting stress-free reference state by allowing the mechanical properties to depend on variables such as temperature and concentration.

The Kapton material used in the above example represents a relatively new class of coating materials, polyimides, which have found wide use in the microelectronics industry.[2,3] A typical electronic package is illustrated in Figure 1.2 and shows the complicated layered structures incorporating polyimides. These polyimides are applied as liquid coatings and are subjected to harsh processing environments (temperature swings of 400° C and washing with several organic solvents) to remove solvent and cure the polyimide material.

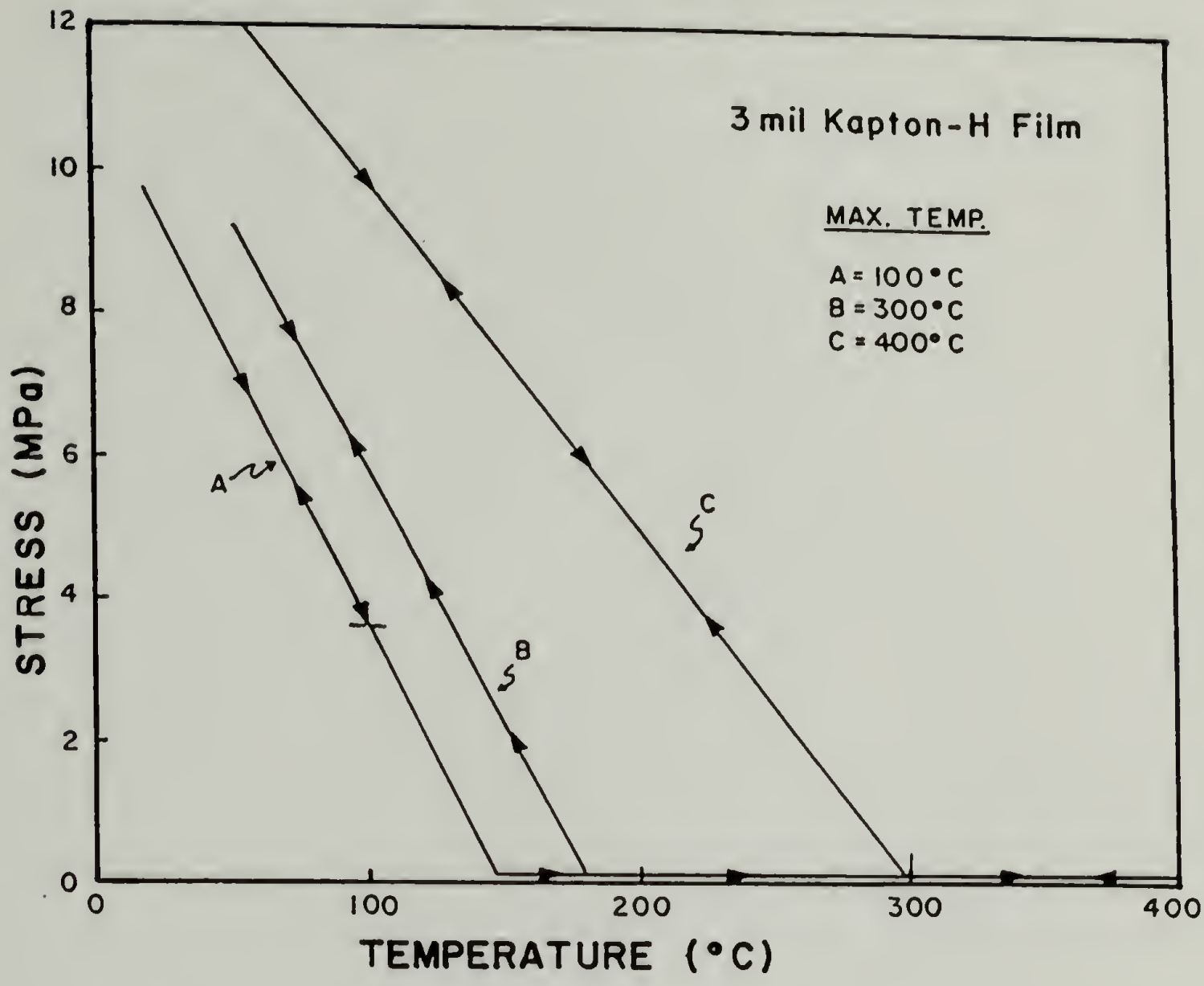

Figure 1.1. Stress versus temperature for a Kapton film held at constant length.

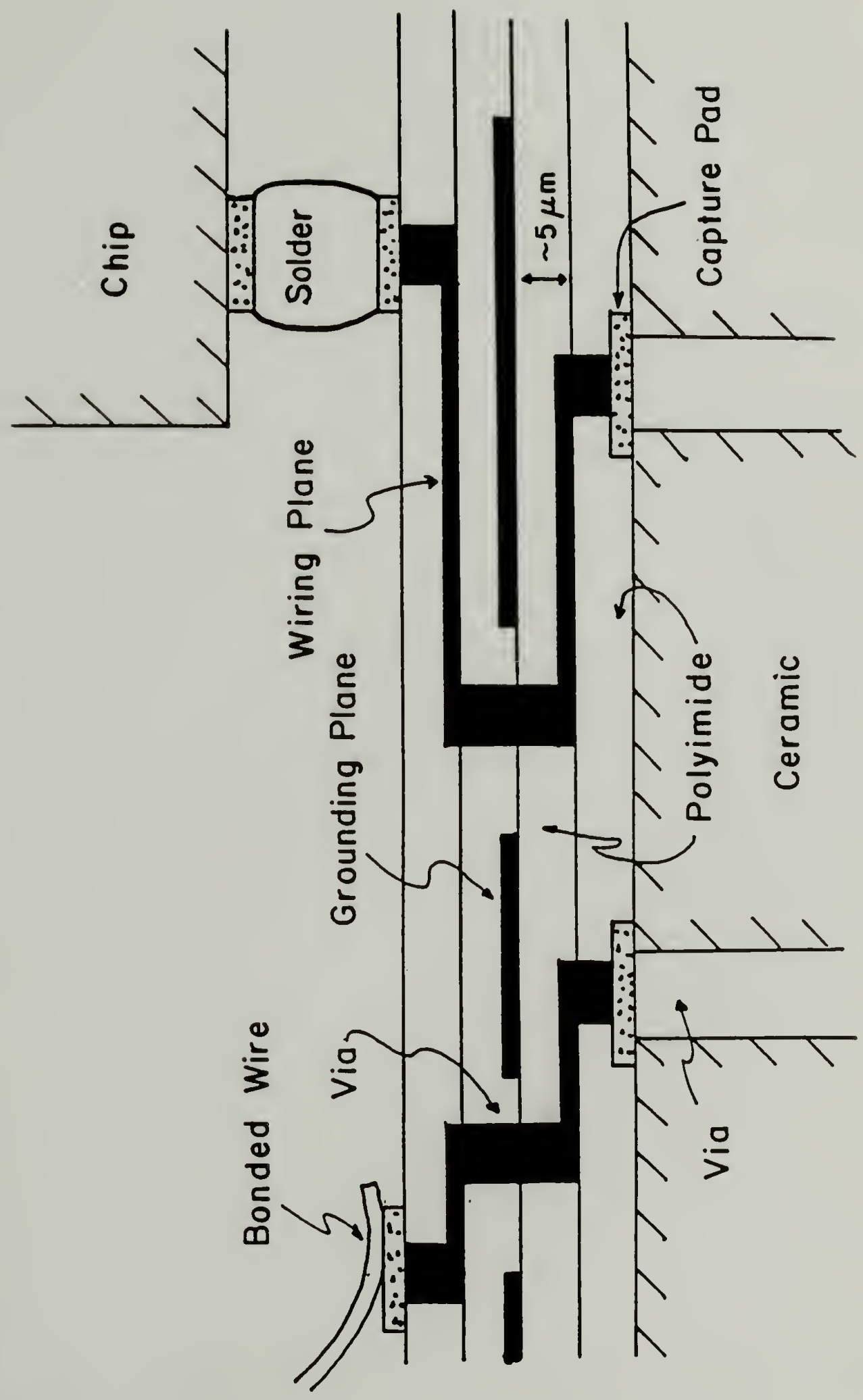

Figure 1.2. Illustration of an electronic package, not drawn to scale.

Such processing conditions may give rise to large residual stresses in the polyimide coating which can lead to failure of the structure, especially delamination. This is extremely important near corners in the electronic package where triaxial stresses may develop due to the three dimensional constraint. Therefore, it is necessary to understand how the mechanical properties and state of stress depend on processing history to adequately design electronic packages with these materials.

1.2 Dissertation Overview

The overall objective of this work is to obtain the necessary information to determine the influence of thermal and solvent history on the state of stress in polyimide coatings. This problem was divided into two areas: 1) the study of the development of the mechanical properties and stresses during film formation; and 2) the mechanical characterization of fully cured polyimide films as a function of thermal and solvent treatments. The emphasis of this thesis was placed on the study of the early processing stages of polyimide coatings, that is, solvent removal and initial imidization.

To accomplish these goals it was necessary to develop and adapt many techniques to measure the mechanical properties and shrinkage stresses during processing. Many of these methods are useful for studying any thin coating, film or fiber.

Before presenting the results of this work, a brief review of polyimides and stresses in coatings will be presented in Chapter 2. The development of the stresses and properties in polyimide films during film formation is addressed in

Chapter 3. The determination of the mechanical properties of polyimide films, such as Poisson's ratio, is presented in Chapter 4. Because one of the dominant failure mechanism for polyimide coatings is delamination, it is necessary to describe the adhesion of polyimides to substrates. A novel method for determining the surface energy of adhesion for coatings will be discussed in Chapter 5. This research is then summarized in Chapter 6.

CHAPTER 2

BACKGROUND

2.1 Introduction

Aromatic polyimides are a relatively new class of high strength, thermally stable polymers. They were initially used as protective coatings and wire insulators. One of the most commercially successful polyimides is Kapton-H manufactured by DuPont. This material has a tensile modulus of 3.0 GPa (430 kpsi), an ultimate tensile strength of 172 MPa (25 kpsi) and no definable glass transition temperature or melting point.[4] These features along with the electrical properties of polyimides (such as a dielectric constant of 3.5 for 1 mil Kapton-H) make them desirable materials in microelectronic components.

Polyimides have varied uses in the microelectronics industry such as fabrication aids, adhesives, and interlevel insulators.[3] For these applications, thin polyimide (PI) films between 5 and 15 μm are generally prepared by spin- or spray-coating either a soluble PI or a polyamic acid (PAA, a precursor to PI) in solution onto a substrate. The solvent is removed and several heat treatments are usually performed to obtain the PI coating. Since the coating is dimensionally constrained, large residual stresses may develop during these processing steps.

2.2 Polyimides

Polyimides may be prepared in the melt by the condensation reaction of a diamine salt and a tetracarboxylic acid. However, the most common synthesis of polyimides involves a two step reaction of a dianhydride with a diamine in a polar solvent.[5] One example is the condensation reaction of pyromellitic dianhydride (PMDA) and oxydianiline (ODA) (Figure 2.1). The first step forms a soluble polyamic acid, poly[N,N'-bis(phenoxyphenyl)-pyromellitamic acid]. At this stage, the material can be processed into films or coatings. After partial solvent removal, it is converted into the polyimide with water emitted as a by-product. This conversion process is accomplished thermally by heating the material at elevated temperatures or chemically with a combination of dehydrating agent and basic catalyst (e.g. acetic anhydride and pyridine mixture). Thermal imidization is rapid at temperatures greater than 150° C and conversion may be followed using infrared spectroscopy by observing the disappearance of the N-H stretching at 3247 cm^{-1} and the appearance of the imide bands at 1776 and 722 cm^{-1}.[2,5,6] Conversion of polyamic acid to polyimide has also been studied using microdielectrometry and X-ray photoelectron spectroscopy.[7,8] Curing up to 400° C in nitrogen is performed to improve properties.

Polyimide films based on PMDA-ODA are a yellow, transparent material and have a modulus of 3 GPa and a tensile strength of 170 MPa. Those films cured at 400° C have no definable glass transition temperature below 400° C and exhibit less than 1.5% weight loss up to 500° C under nitrogen.[5] The material rapidly degrades at this temperature if exposed to air.

This polyimide is insoluble and processing must be accomplished during the polyamic acid stage. By varying the structure of the diamine or dianhydride,

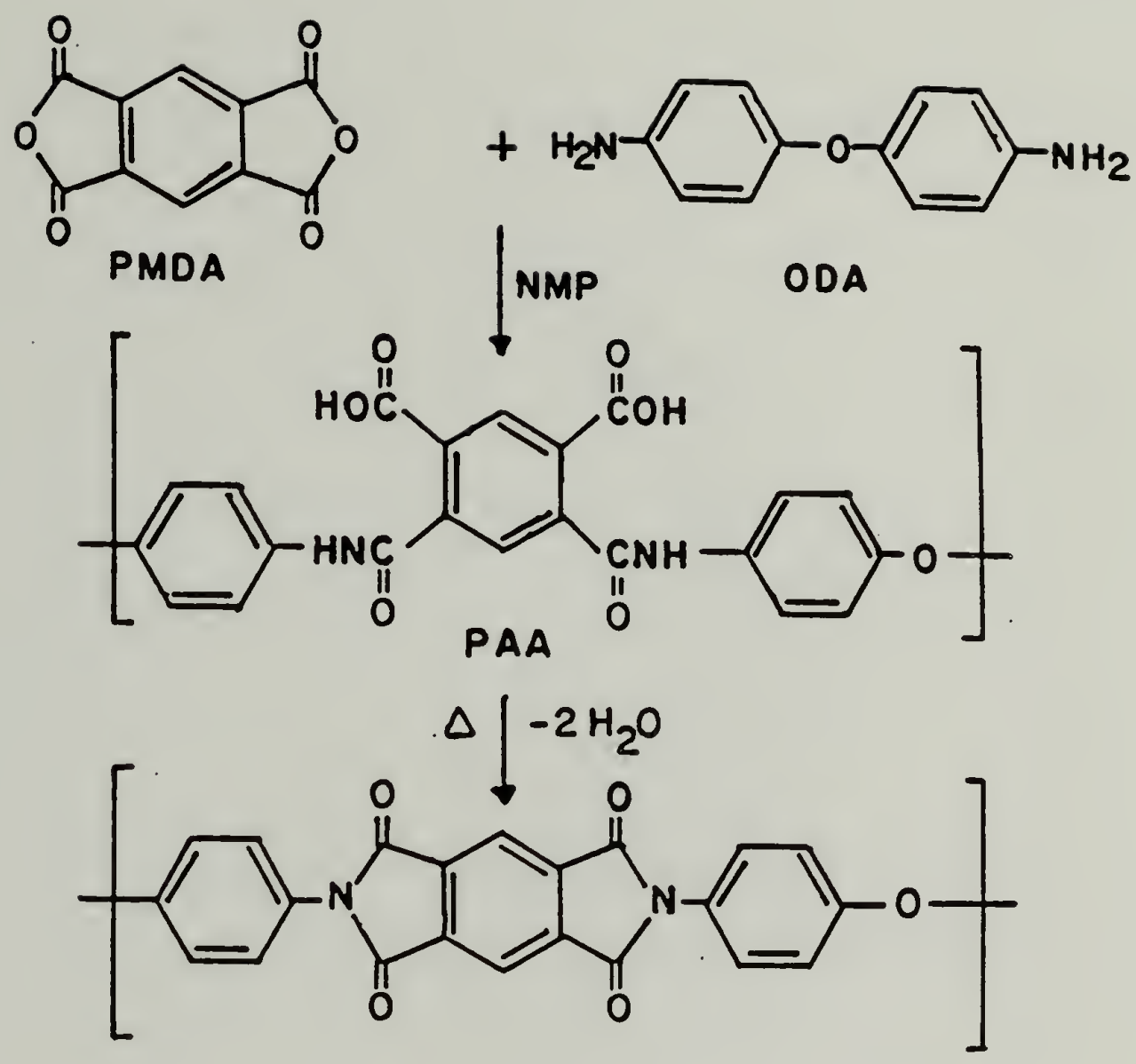

Figure 2.1. Reaction scheme for formation of a polyimide.

polyimides of varying properties may be synthesized. If less rigid or flexible chemical spacer units are incorporated into the structure, soluble polyimides may be prepared, such as Ciba-Geigy's Probimide series. Such polyimide systems may then exhibit a glass transition and melting point. Palmese and Gillham have correlated the glass transition to the temperature and time of cure for a polyamic acid/polyimide sysytem based on benzophenone tetracarboxylic acid dianhydride.[9] The physical properties of various other polyimides are summarized in the reviews by Adrova and Sroog.[2,5]

Because of its commercial success, most of the characterization and structure-property relationships have been performed on the polyimide based on PMDA-ODA, poly[N,N'-bis(phenoxyphenyl)-pyromellitimide]. Several investigators have studied the dynamic mechanical behavior of this polyimide to understand the relaxation processes in the films.[10-15] Results of these experiments show two major relaxation peaks at -80° and at 80° C. The lower temperature peak is attributed to water content while the higher is associated with intramolecular movements such as aromatic ring oscillations. At temperatures less then 0° C the dynamic modulus increases with increasing water content, but at temperatures greater than 27° C it is insensitive to water content.[11] At the low temperatures, water acts like a hard filler, thus accounting for the increase in modulus with water content.[15] Bernier showed that the mechanical relaxation spectrum of dried films is relatively insensitive to dimethylformamide, dimethylacetate and dimethylsulfoxide treatments, while water greatly alters the spectrum.[11]

Until recently it has been difficult to define the physical structure or morphology of films made from PMDA-ODA. In general, polyimides of this type are considered to have a linear structure. Due to the good thermal properties,

dielectric behavior and diffusion behavior of polyimides some researchers have suggested the presence of crosslinks in the material.[16,17] However, the observed behavior may be attributed to strong physical crosslinks as opposed to actual chemical crosslinks such as from amide linkages across chains. This is supported by solution characterization of PAA/PI systems.[18] For the PMDA-ODA system it was shown that there is little change in molecular weight on imidization of the PAA and no evidence was observed for crosslinking in samples cured up to 300° C. To characterize the fully cured PI, sulfuric acid was used as the solvent and this may destroy any of the chemical crosslinks. Since there is no degradation of the polymer chains in the PI as shown by molecular weight comparisons with the PAA precursor, it is unlikely that crosslinks, if present, would be preferentially destroyed.

Because of the rigid aromatic rings in the PMDA-ODA polyimide, the polymer can only freely twist around the ether linkages. From theoretical calculations and X-ray diffraction studies, the C-O-C bond angle is about 130° such that a planar zig-zag structure may result with a distance between ether oxygens of 18 Å.[19,20] Despite such regularity, a crystalline unit cell has only been defined for PI fibers and not films. From X-ray diffraction studies of PMDA-ODA polyimide processed as fibers, a rhombic unit cell is obtained with cell dimensions of a = 6.31, b = 3.97, and c = 32 Å.[21,22]

In PI films, a long range order has not been noted although short range order has been observed in the form of molecular aggregation as detected using small angle X-ray scattering.[20,23,24] Isoda has found that the molecular aggregation creates a two phase structure which can be controlled by the imidization temperature. The two phase structure is formed at high temperatures but at low temperatures, only an amorphous structure is

observed.[20] Recent results by Takahashi using wide angle X-ray diffraction and Russell using small angle X-ray diffraction have indicated that the aggregation or smectic-like structure is initially developed in the condensed state of the PAA and preserved upon imidization, after which, annealing improves the structure.[24,25]

Orientation of thin PI films was first detected by Ikeda.[10] He observed ordering of the PI chains parallel to the film surface. Using integrated optics and wide angle X-ray diffraction, Russell reported in-plane orientation in thin PI films that were spin-coated onto substrates and that the method of imidization has the greatest effect on the orientation of the film.[26] In a latter study, Russell examined the void content in such thin films using small angle X-ray diffraction. He found voids of 50 to 150 Å in radius with a void volume fraction less than 0.0007.[27]

Orientation will effect the properties of the PI film. During processing Kapton is stretched more in one direction resulting in anisotropy in the plane of the film with the principal axis approximately 45° to the machine direction.[28,29] For spin-coated, sprayed or cast films, the properties are assumed to be isotropic in the plane since they can randomly orient during processing, although some radial orientation may exist due to spinning. The properties normal to the plane will be different from those in the plane.

The effect of chemical environments on the properties of PI films has been studied primarily with diffusion and gas adsorption experiments.[30-38] Very little work has been published on the effect of liquid environments on polyimides. The degradation and aging of Kapton in water has been reported. The tensile strength decreases by 28% after 1000 hr. exposure to water.[3] Recently Kapton has been shown to undergo hydrolytic degradation at a rate which obeys an

Arrhenius expression with respect to temperature.[39] The rate was unaltered by stressing the film. Researchers at McDonnell Douglas Corp. have shown that the time to fail of slightly strained Kapton films in 70° C water was an inverse function of the strain. However, by annealing highly strained samples at 210° C the samples did not fail upon immersion in water.[40,41]

2.3 Stresses in Coatings

2.3.1 Constraints in Coatings

Residual stresses in materials most often arise from volumetric changes due to thermal expansion, swelling, inelastic processes, or solidification processes. These processes include solvent removal, crystallization or chemical reactions such as polymerization. For a linear, isotropic, homogeneous material whose properties are changing with time, the relation between these effects and the stress may be expressed using an incremental approach:

$$E[d\epsilon_{ij} - \delta_{ij}(\alpha\, dT + \beta\, dc + \tau\, dt)] = (1 + \nu)d\sigma_{ij} - \nu\,\delta_{ij}\, d\sigma_{kk}, \qquad (2.1)$$

with

E = tensile modulus,

α = linear thermal expansion coefficient,

β = linear swelling coefficient,

τ = linear rate of shrinkage due to polymerization,

d = differential or incremental operator,

T = temperature,

c = concentration,

t = time,

ν = Poisson's ratio,

δ_{ij} = Kronecker delta,

ϵ_{ij} = strain,

σ_{ij} = stress.

This allows the properties such as modulus and Poisson's ratio to vary as a function of temperature, concentration, time, degree of polymerization, etc. and accounts for a shifting stress free state. If the rates of deformation are slow, viscoelastic effects may be neglected. Equation 2.1 still contains time effects but no viscoelastic effects.

To illustrate the effects of constraints, assume there are no changes in concentration or solidification effects. Equation 2.1 reduces to eqn. 2.2.

$$E[d\epsilon_{ij} - \delta_{ij}\alpha dT) = (1 + \nu)d\sigma_{ij} - \nu\delta_{ij}\, d\sigma_{kk} \qquad (2.2)$$

For a one dimensional constraint only, such that $d\epsilon_{11} = 0$ and $d\sigma_{22} = d\sigma_{33} = 0$, it can be shown that $d\sigma_{11} = -E\alpha dT$. For biaxially constrained materials, where $d\epsilon_{11} = d\epsilon_{22} = 0$ and $d\sigma_{33} = 0$ it is shown that:

$$d\sigma_{11} = d\sigma_{22} = -E\alpha dT/(1 - \nu). \qquad (2.3)$$

Thus the stresses in the media are increased by a factor of $1/(1 - \nu)$, compared to those in the one dimensionally constrained case. The dependence on Poisson's ratio is markedly observed when a material is volumetrically constrained, $d\epsilon_{11} = d\epsilon_{22} = d\epsilon_{33} = 0$. This gives eqn. 2.4.

$$d\sigma_{11} = d\sigma_{22} = d\sigma_{33} = -E\alpha dT/(1 - 2\nu) \qquad (2.4)$$

As ν approaches 0.5 the stresses increase without bound.

The importance of these constraints may be demonstrated for a Kapton polyimide with E = 3 GPa and ν = 0.34. If a 1% thermal strain is assumed to be applied to the sample ($\Delta T \approx 350^\circ$ C), the stress equals 30 MPa for a one dimensional constraint. With a biaxial constraint the stress becomes 45 MPa and

94 MPa for a volumetrically constrained sample. In comparison, the reported yield stress is 70 MPa. Solely by increasing the number of constraints may cause irreversible deformation or failure.

In most cases coatings applied to substrates are only under two-dimensional constraints. As the simplest case consider a thin coating attached to a rigid infinite plate (see Figure 2.2). Since the thin coating is adhered to the substrate it can freely expand and contract normal to the plate, thus away from the edges, plane stress conditions may be applied i.e. $d\sigma_{33} = d\sigma_{13} = d\sigma_{23} = 0$. Therefore, there are no stresses acting at the interface trying to detach the film. The stress-strain relations for the coating are

$$d\epsilon^{c}_{11} = (d\sigma^{c}_{11} - \nu^{c}\, d\sigma^{c}_{22})/E^{c} + \alpha^{c}\, dT, \tag{2.5a}$$

$$d\epsilon^{c}_{22} = (d\sigma^{c}_{22} - \nu^{c}\, d\sigma^{c}_{11})/E^{c} + \alpha^{c}\, dT. \tag{2.5b}$$

Similarly for the substrate

$$d\epsilon^{s}_{11} = (d\sigma^{s}_{11} - \nu^{s}\, d\sigma^{s}_{22})/E^{s} + \alpha^{s}\, dT, \tag{2.6a}$$

$$d\epsilon^{s}_{22} = (d\sigma^{s}_{22} - \nu^{s}\, d\sigma^{s}_{11})/E^{s} + \alpha^{s}\, dT. \tag{2.6b}$$

At the interface $d\epsilon^{c}_{11} = d\epsilon^{s}_{11}$ and $d\epsilon^{c}_{22} = d\epsilon^{s}_{22}$, then eqns. 2.5 and 2.6 become

$$(d\sigma^{c}_{11} - \nu^{c}\, d\sigma^{c}_{22})/E^{c} - (d\sigma^{s}_{11} - \nu^{s}\, d\sigma^{s}_{22})/E^{s} = (\alpha^{s} - \alpha^{c})dT, \tag{2.7a}$$

$$(d\sigma^{c}_{22} - \nu^{c}\, d\sigma^{c}_{11})/E^{c} - (d\sigma^{s}_{22} - \nu^{s}\, d\sigma^{s}_{11})/E^{s} = (\alpha^{s} - \alpha^{c})dT. \tag{2.7b}$$

A solution for the stresses may be obtained by considering a force balance in all directions. The solution is simplified for a flexible coating on a stiff substrate, where $t^{s}E^{s} >> t^{c}E^{c}$ (t^{s} and t^{c} are the thicknesses of the substrate and coating, respectively), hence eqn. 2.7 reduces to eqn. 8.

$$(d\sigma^{c}_{11} - \nu^{c}\, d\sigma^{c}_{22})/E^{c} = (\alpha^{s} - \alpha^{c})dT \tag{2.8a}$$

$$(d\sigma^{c}_{22} - \nu^{c}\, d\sigma^{c}_{11})/E^{c} = (\alpha^{s} - \alpha^{c})dT \tag{2.8b}$$

Solving for the stresses with this assumption gives eqn. 2.9.

$$d\sigma^{c}_{11} = d\sigma^{c}_{22} = E^{c}(\alpha^{s} - \alpha^{c})dT/(1 - \nu^{c}) \tag{2.9}$$

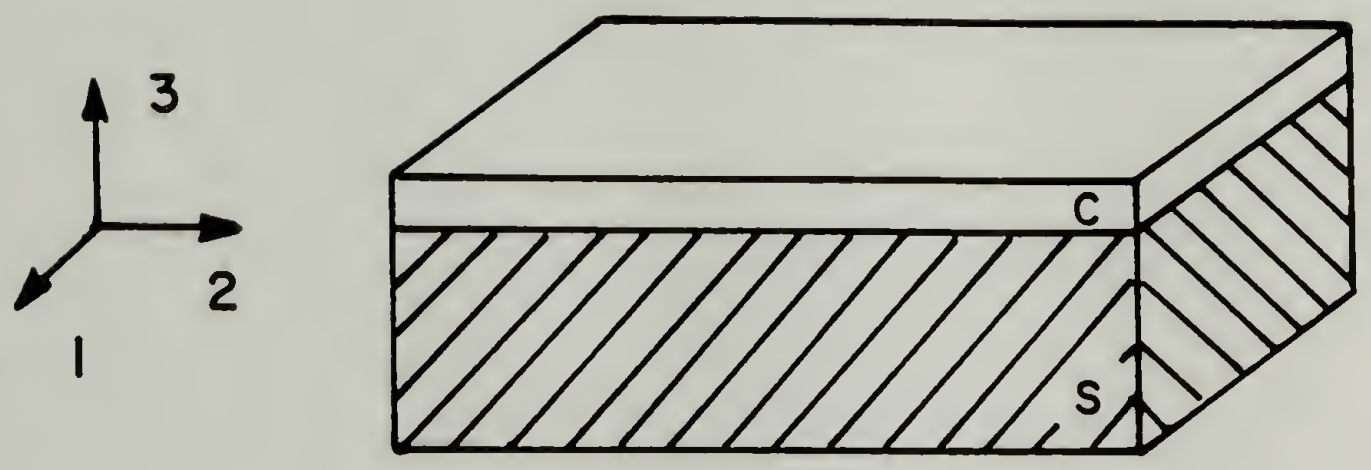

Figure 2.2. Illustration of a coating (C) on a substrate (S).

Then

$$\sigma^{c}_{11}(T_f) = \sigma^{c}_{22}(T_f) = \int_{T_i}^{T_f} E^{c}(\alpha^{s} - \alpha^{c})/(1 - \nu^{c})\, dT + \sigma(T_i) \qquad (2.10)$$

The integral is simple to resolve if E, α, and ν are independent of temperature and the traditional result from linear thermoelasticity is recovered. However, for most polymer coatings this may not be the case and the temperature dependence of the properties must be known to properly evaluate the stresses. A similar equation would result if swelling and solidification displacements were included. The properties would then be functions of temperature, concentration, and time.

The above analysis does not account for the influence of free edges on the stress distribution in the coating. This may be corrected by satisfying the equilibrium equations for static conditions at the edges:

$$\partial\sigma_{ij}/\partial x_j = 0. \qquad (2.11)$$

For the two dimensional case illustrated in Figure 2.3 these become

$$(\partial\sigma_{11}/\partial x_1) + (\partial\sigma_{13}/\partial x_3) = 0 \qquad (2.12a)$$

$$(\partial\sigma_{13}/\partial x_1) + (\partial\sigma_{33}/\partial x_3) = 0 \qquad (2.12b)$$

with the conditions

$\sigma_{11} = 0$ at $x_1 = 0$,

$\sigma_{13} = 0$ at $x_3 = t$, the thickness of the coating,

$\left.\begin{aligned} \sigma_{11} &= \sigma_o \\ \sigma_{13} &= 0 \\ \sigma_{13} &= 0 \end{aligned}\right\}$ away from the edge, $x_1 >> 0$,

σ_o = residual stress in film.

The solution to this problem has been worked out by Aleck using the principle of least work.[42] The approximate solution indicates the shear and normal stresses decay to approximately zero by the distance of one coating thickness into the film. Thus for a 10 μm film on glass, approximately 10 μm into the film away

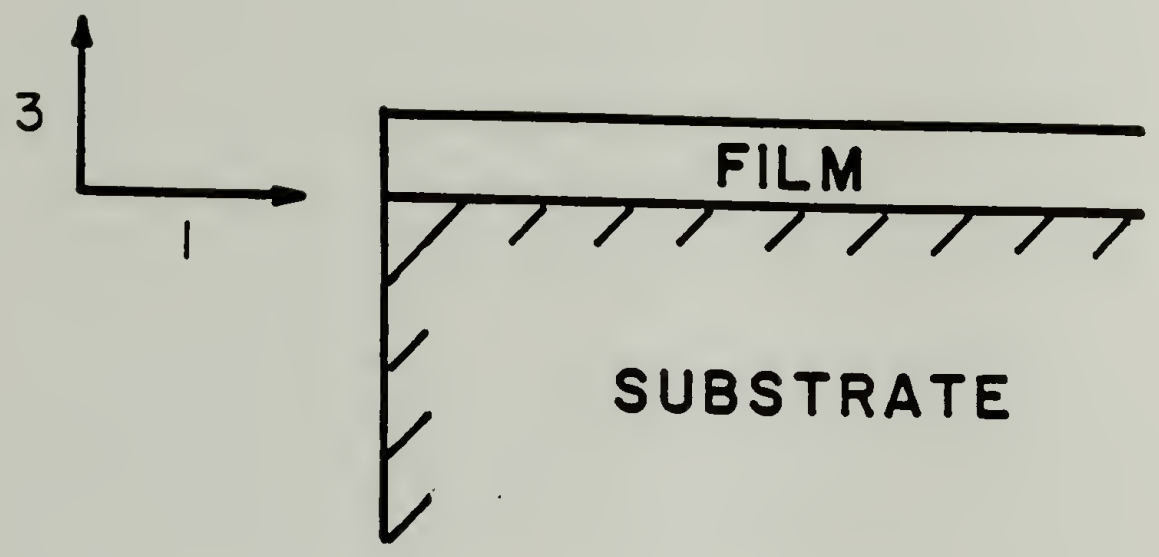

Stresses at Interface:

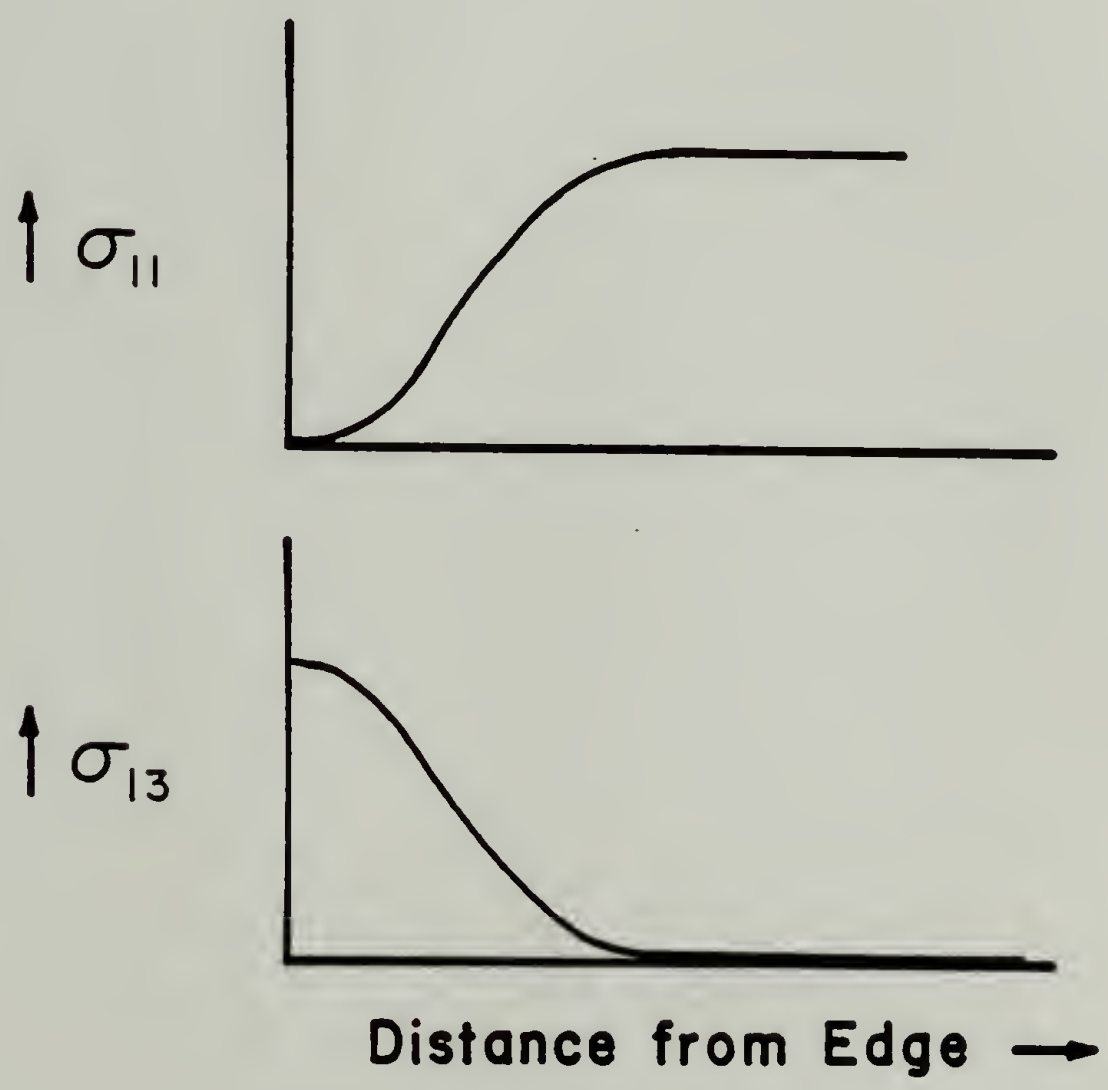

Figure 2.3. Shear (σ_{13}) and normal (σ_{11}) stresses at the interface of a coating and substrate as a function of position on the substrate.

from the free edge $\sigma_{13} = \sigma_{33} = 0$ and the analysis for stresses in eqn 2.10 is applicable. Therefore the stresses acting on the interface between the coating and substrate are zero away from the edge. The stresses that exist are in the plane of the coating and do not act to debond the coating.

2.3.2 Development of Stresses in Solvent-Based Coatings

Stresses in solvent-based coatings arise from the differential shrinkage between the thin film coatings and the corresponding substrates. Initially after coating a flat, planar substrate, stresses do not develop as solvent is removed since the liquid freely shrinks. When sufficient solvent has evaporated, the material gels or solidifies. As further solvent evaporates after this critical concentration, the film shrinks and develops stresses in the plane. Therefore the internal stresses are not related to the concentration of the initial liquid coating but the concentration at which the material can first sustain a load. This solidification may be related to molecular motion which resembles the glass transition in solid polymers.[43]

The stress will continue to increase as solvent is continually removed. Because of the strong interplay between stress and solvent concentration a steady state stress level and residual solvent content may be attained.[44,45] The kinetics and solvent mass transport behavior of water based coatings has been studied and modeled.[46-50] Croll has shown that for polystyrene and poly(isobutyl methacrylate) coatings cast from toluene, the residual stresses are independent of final coating thickness and depend only on the amount of solvent evaporated and not the transport phenomena.[51] He used these results to obtain a theory which correlates the volume of solvent lost to a volumetric change in the film.

Additional solvent may be removed by exposing the material to higher temperatures. This increases shrinkage stresses by removing additional solvent but also by inducing other solidification processes such as polymerization and thermal annealing. In the formation of polyimide films, the material undergoes a solvent removal step plus several thermal treatments to cyclize the polymer and anneal it. Each of these processes may contribute to the development of residual stress.

Several methods have been developed to determine the residual stresses in coatings.[52] Initially these were only applied to brittle coatings such as vapor deposited metals. The work by Corcoran helped popularize beam bending techniques to measure residual stresses in organic coatings.[53] Historically, this has become the primary method of determining stresses in solvent-based polymer coatings.[45,54-56] These techniques assume linear elastic behavior of both the coating and beam materials. From the change in the deflection of the beam due to the coating, the residual stress in the coating may be calculated if the mechanical properties of the materials are known.

CHAPTER 3

FILM FORMATION

3.1 Introduction

Polyimide coatings based on PMDA-ODA are commonly used in industry. To prepare these coatings, a solution of the polyamic acid is cast, sprayed or spin-coated onto a substrate. Following a solvent removal step, several thermal treatments are used to convert the polyamic acid (PAA) to polyimide (PI) and anneal the material. This chapter will discuss the development of stresses and properties in films of these materials during the solvent removal stage and initial imidization.

Using axially constrained coatings on very soft substrates it was possible to directly assess the change in stress due to solvent removal. Primarily two techniques were used: thermomechanical experiments (force-temperature) and the propagating wave method. From both these methods the force on a sample as a function of temperature and time is obtained. In addition, the propagating wave technique allows measurement of mass per unit length as a function of time and temperature. Application of the Impulse Method to coated rubber fibers used in the propagating wave technique also allows a measure of the modulus during processing.

3.2 Experimental Procedures

3.2.1 Tensile Testing

Tensile properties were obtained using either an Instron Universal Testing Machine or a TMI Tensilon STM-20 Tensile Tester. The elongation rate for the tests generally was 10%/min. Tensile tests were performed on various thin films (15 μm in thickness) by first mounting the samples on manila tabs. A window, 8 cm x 1 cm, was cut into a manila sheet, 10 cm x 1.5 cm. Since the manila sheet is much stiffer than the film, this technique prevents damaging the film prior to testing. The thin film sample was placed on top of this opening and then glued in place with a short manila tab using Devcon 5 min. epoxy. After curing overnight the samples were placed into the tensile tester, gripped, and then the window frames were cut off prior to testing.

3.2.2 Thermomechanical Experiments

Force as a function of temperature was obtained by placing a sample in a vertical glass oven and gripping both ends, with one end attached to a load cell and the other to an adjustable mount. A slow nitrogen flow was introduced through the bottom and a resistance temperature device was placed near the middle of the sample to measure the temperature. Output from the probe and load cell was digitally recorded on a Bascom-Turner Instrument model 4000. See Figures 3.1 and 3.2. With a sample in place, several heating and cooling cycles were performed at various loads.

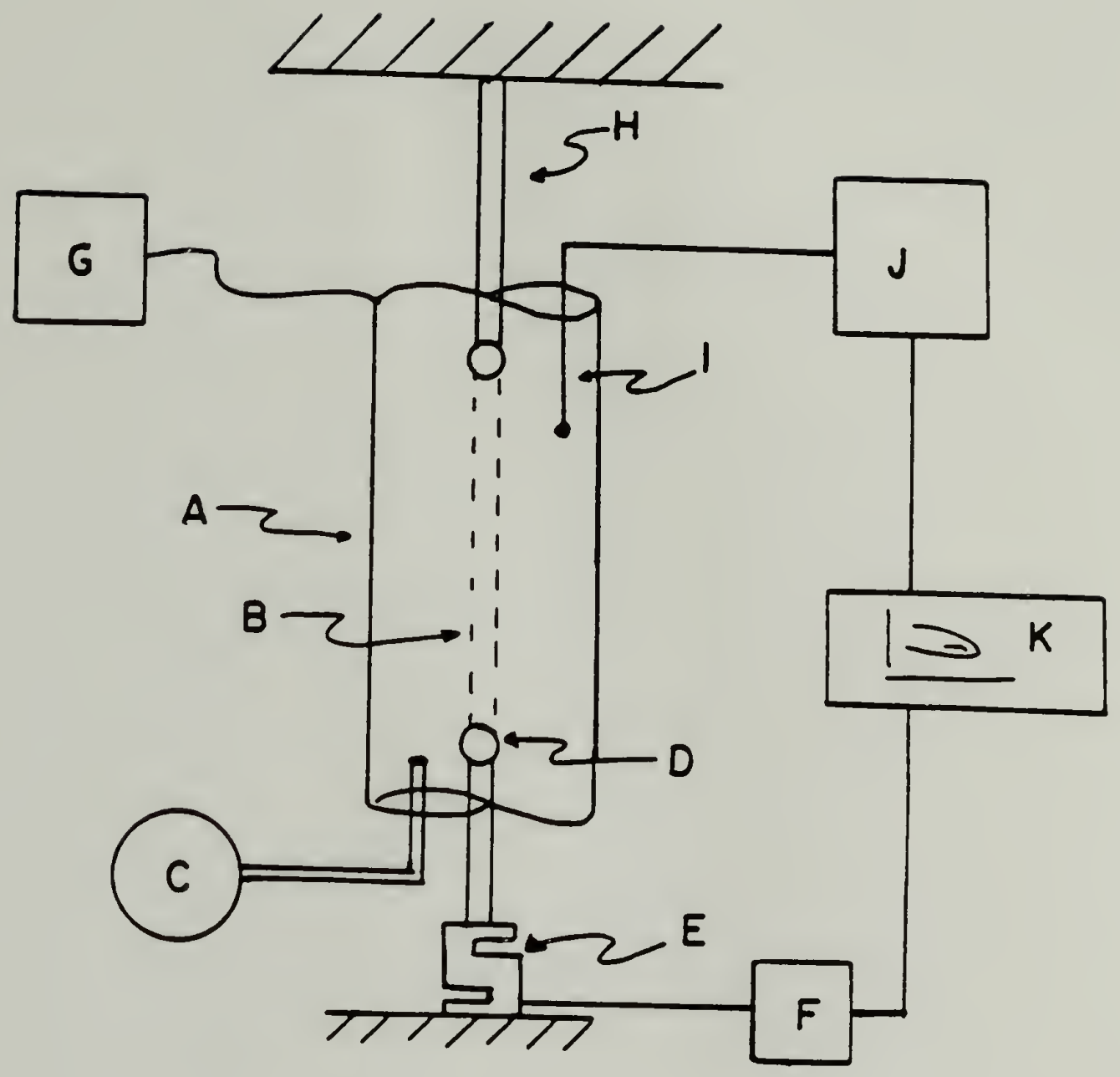

Figure 3.1. Schematic diagram of force-temperature apparatus. A = oven, B = sample, C = nitrogen source, D = clamp, E = load cell, F = amplifier, G = heating control, H = adjustable clamp, I = temperature probe, J = temperature readout, K = recorder.

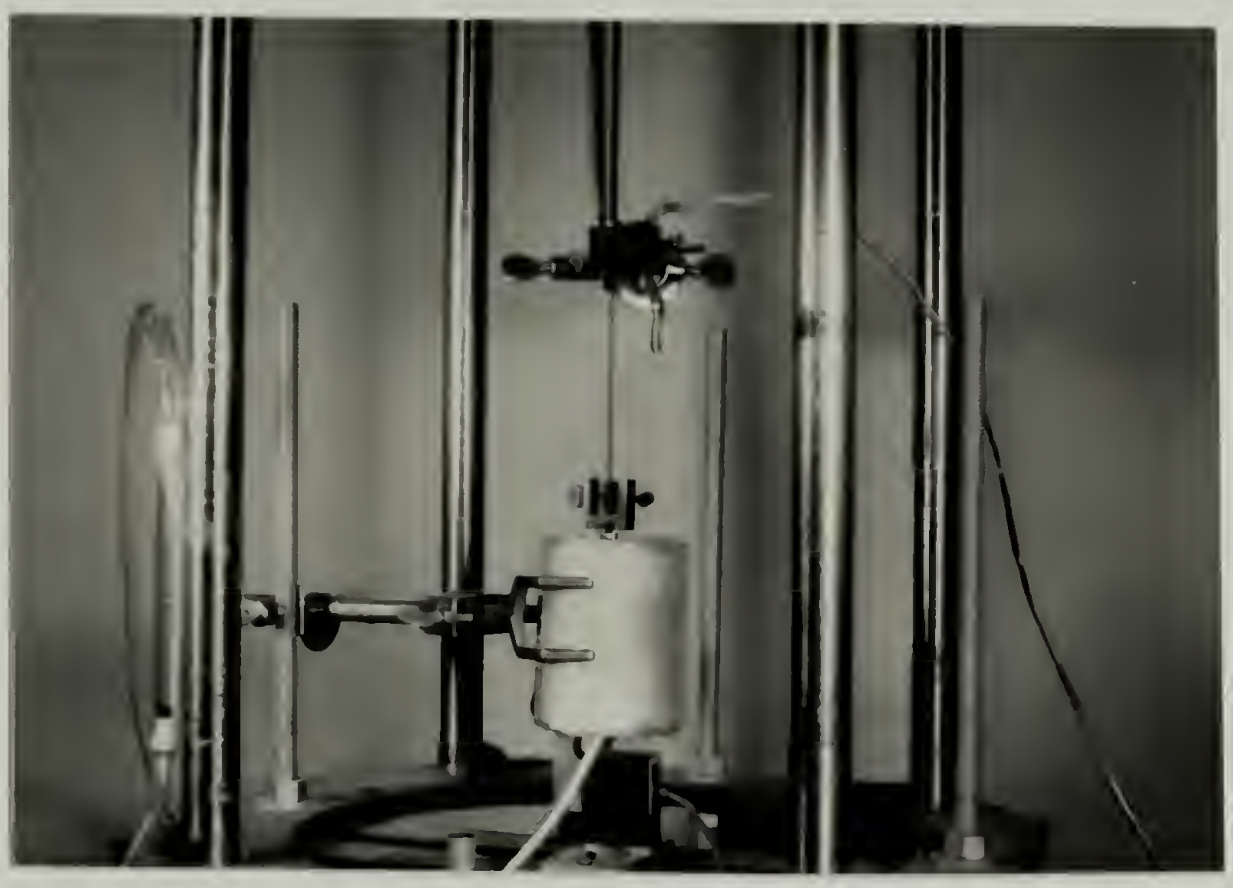

Figure 3.2. Photograph of force-temperature apparatus.

To obtain displacement (strain) as a function of temperature, the load cell in the above apparatus was replaced with a linear variable differential transformer (LVDT). The specimen was maintained at constant load using weights.

Samples for the thermomechanical experiments consisted of either a thin film of polyamic acid or polyimide or a rubber sheet coated with polyamic acid. The ends of the rubber strip (6 cm x 1.5 cm x 0.25 mm) were glued between aluminum foil (Figures 3.3 and 3.4). This was then dipped into a 15% PAA/85% NMP solution and placed into the force temperature apparatus, gripping only the aluminum tabs. The sample was sufficiently long to provide an even coating on the rubber with this method. This arrangement allows direct measurement of the shrinkage forces during solidification of the coating. The rubber serves only as a soft, flexible support for the liquid coating.

The PAA solution was a DuPont material, PI5878 (lot #G976379 and #G0034217443, 20,000 MW), based on PMDA-ODA. As received, the PI5878 is approximately 25% solids and this was diluted to the designated concentration using N-methylpyrrolidinone (Aldrich #M7960-3)(NMP). A solvent removal temperature of 85° C was typically chosen since this is the recommended industrial drying temperature for these PAA coatings.

3.2.3 Propagating Wave Technique

Using the propagating wave technique, the mass/length and stress on a sample are obtained as a function of time and/or temperature.[57] In this method a traveling wave is applied to the sample and by measuring the velocity of this

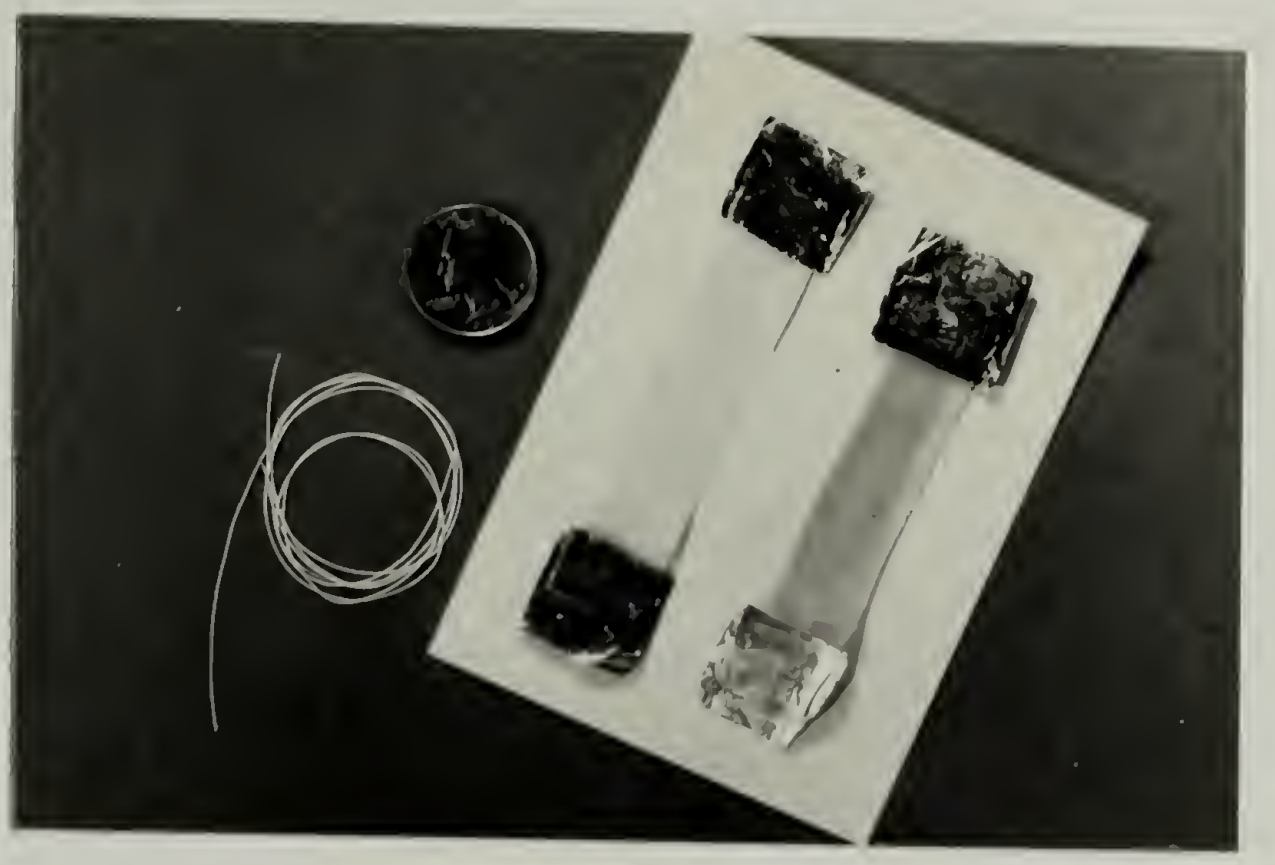

Figure 3.3. Photograph of samples for force-temperature experiments.

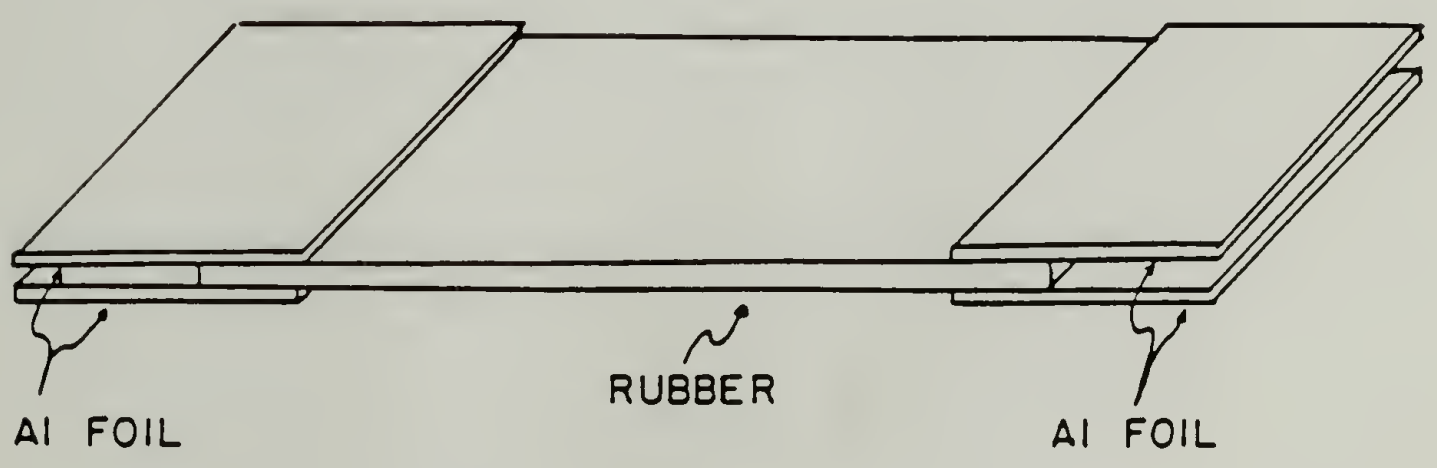

Figure 3.4. Sample for F-T apparatus.

wave and the tension on the sample, the mass per unit length is obtained. Samples may consist of long, thin ribbons or coated rubber fibers.

The one-dimensional wave equation for a flexible, vibrating string may be written as:[58]

$$\partial^2 u/\partial t^2 = (F/m_l)(\partial^2 u/\partial x^2) \qquad (3.1)$$

where

u = deflection of the string out of the plane,

x = position along string,

F = tension on string,

t = time,

m_l = mass per unit length of string.

It can be shown that F/m_l is the square of the velocity of a traveling transverse wave, v, along the string. Therefore:

$$\text{mass/length} = \text{tension}/(\text{velocity})^2. \qquad (3.2)$$

A schematic of the apparatus is shown in Figure 3.5. A sample threaded through an oven is held at constant length with one end attached to a load cell. Two sensors at a fixed distance apart are located near the sample to detect movement of the sample. These sensors are a single-mode laser transmitter-receiver pair which are positioned to act as switches. The coated rubber fiber sample is placed between the transmitter-receiver pair, opening the circuit. Movement of the sample outside the sensor completes the circuit.

A wave is initiated at D and the time for the wave to travel from one sensor to the other is measured by using the sensors to trigger a Nicolet digital oscilloscope. From the time delay and length of travel, the velocity of the initiated wave is calculated. The load on the sample is simultaneously recorded when the wave is initiated. Then, using equation 3.2, the mass/length is obtained.

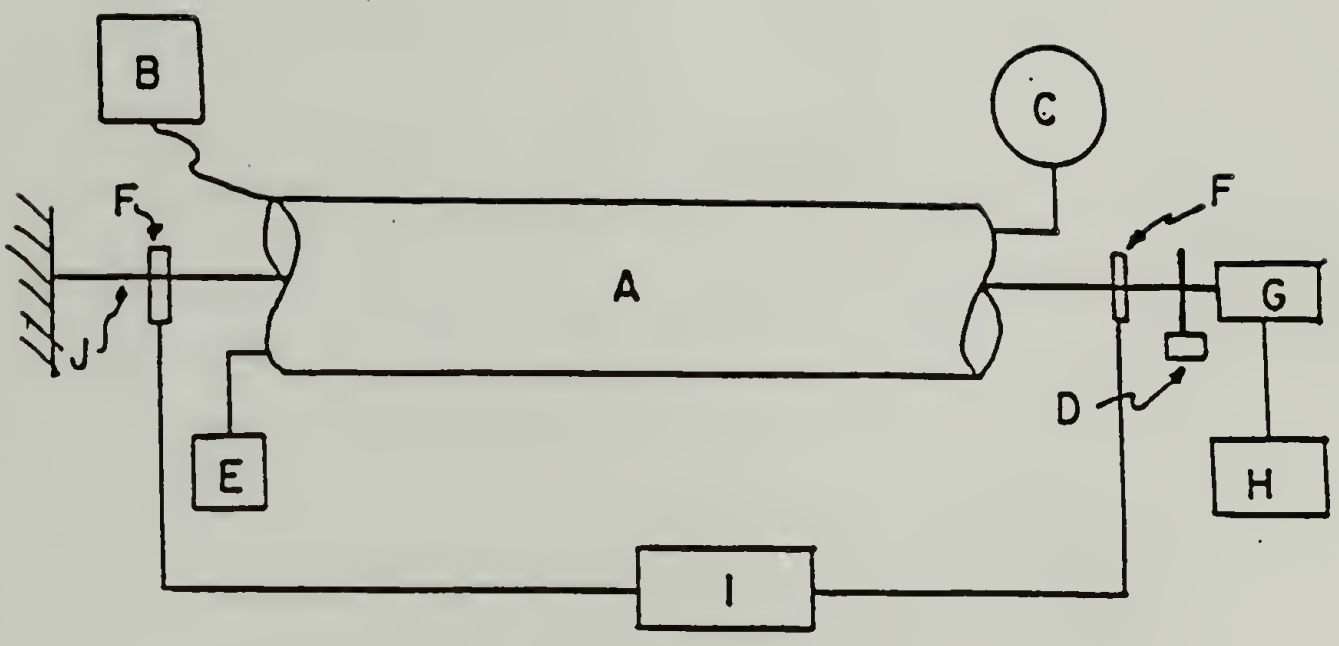

Figure 3.5. Schematic diagram for propagating wave apparatus. A = oven, B = heating control, C = nitrogen source, D = striker, E = temperature probe, F = vibration sensor, G = load cell, H = amplifier and readout, I = recorder for vibration sensors, J = sample.

The experimental apparatus also allows the sample to be heated in nitrogen. Then changes in load and mass/length may be measured as a function of time and temperature. For monofilament threads, there is a 1% error in determining the mass/length.

For the propagating wave technique, long threads of natural rubber 320 μm in diameter from Globe Rubber Co. were coated with a 25% PAA solution and mounted in the apparatus. There was no change in the mechanical integrity of the rubber fibers after soaking for one hour in NMP. The fibers were coated by passing the threads through a barrel filled with the PAA solution and fitted with a wire drawing die. The validity of this method of measuring mass/length was confirmed by comparing results from this technique with those obtained by directly weighing a coated sample having a known length.

3.2.4 Impulse Method/Propagating Wave Technique

The Impulse Method was used to obtain changes in the elastic modulus of a sample during processing. This method has been developed by Farris and Vratsanos.[59] For uniaxial deformations that start and end at the same strain the equilibrium modulus, E_{eq}, is related to the stress response, $\sigma(t)$, and the strain history, $\epsilon(t)$, by equation 3.3.

$$Eeq = \frac{\int_0^\infty \sigma(t)dt}{\int_0^\infty \epsilon(t)dt} \qquad (3.3)$$

This method was used in conjunction with the propagating wave technique. The propagating wave apparatus was adapted with an axial pulsing mechanism to

apply a step strain to the sample (Figures 3.6 and 3.7). This apparatus consists of a double ended Clippard miniature air cylinder to pulse the sample with a Schaevitz 50DCD linear variable differential transformer attached to one end to measure displacement. This mechanism was attached to the sample in place of the rigid support in the wave apparatus. Hub clamps placed on the air cylinder shaft allow adjustments to be made in the applied displacements. Output from the load cell and LVDT is collected by an IBM-AT personal computer. The plotted strain values from the computer are only relative changes since the computer programs do not allow zeroing of the LVDT signal.

3.2.5 Thermal Expansion

Thermal expansion behavior was obtained using a Perkin Elmer TMA-1 equipped with a film extension analysis probe.

3.3 Solvent Removal

3.3.1 Thermomechanical Results

Results from a force-temperature experiment for a PAA solution coated rubber sample are shown in Figure 3.8. In the first cycle, an initial load of approximately 100g is applied to the sample. Since the coating is still in a liquid state, the rubber supports the entire load. At this force, the rubber strip is just below its thermoelastic inversion point. Therefore, with increasing temperature a positive thermal expansion is observed causing a slight decrease in force. The response of a rubber sheet soaked for 1 hour in NMP shows little change in stress

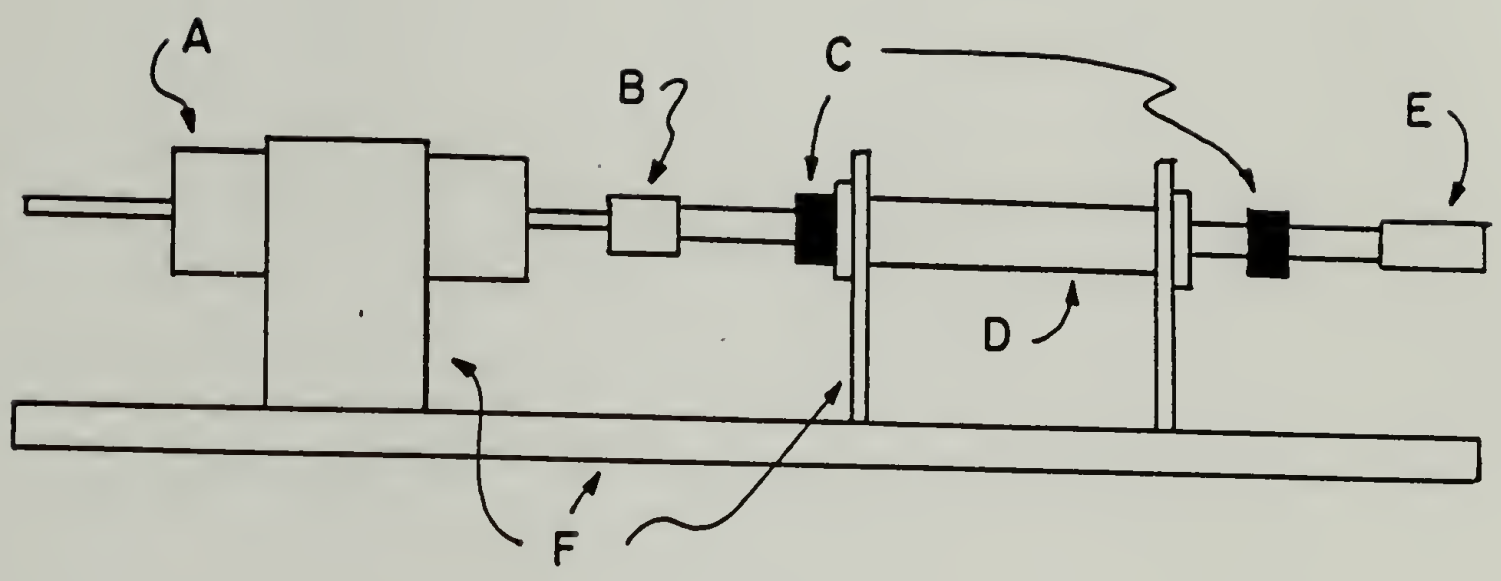

Figure 3.6. Schematic diagram for pulsing apparatus. A = LVDT, B = coupler, C = hub clamps, D = air cylinder, E = sample holder, F = supports.

Figure 3.7. Photograph of propagating wave instrument with pulsing apparatus

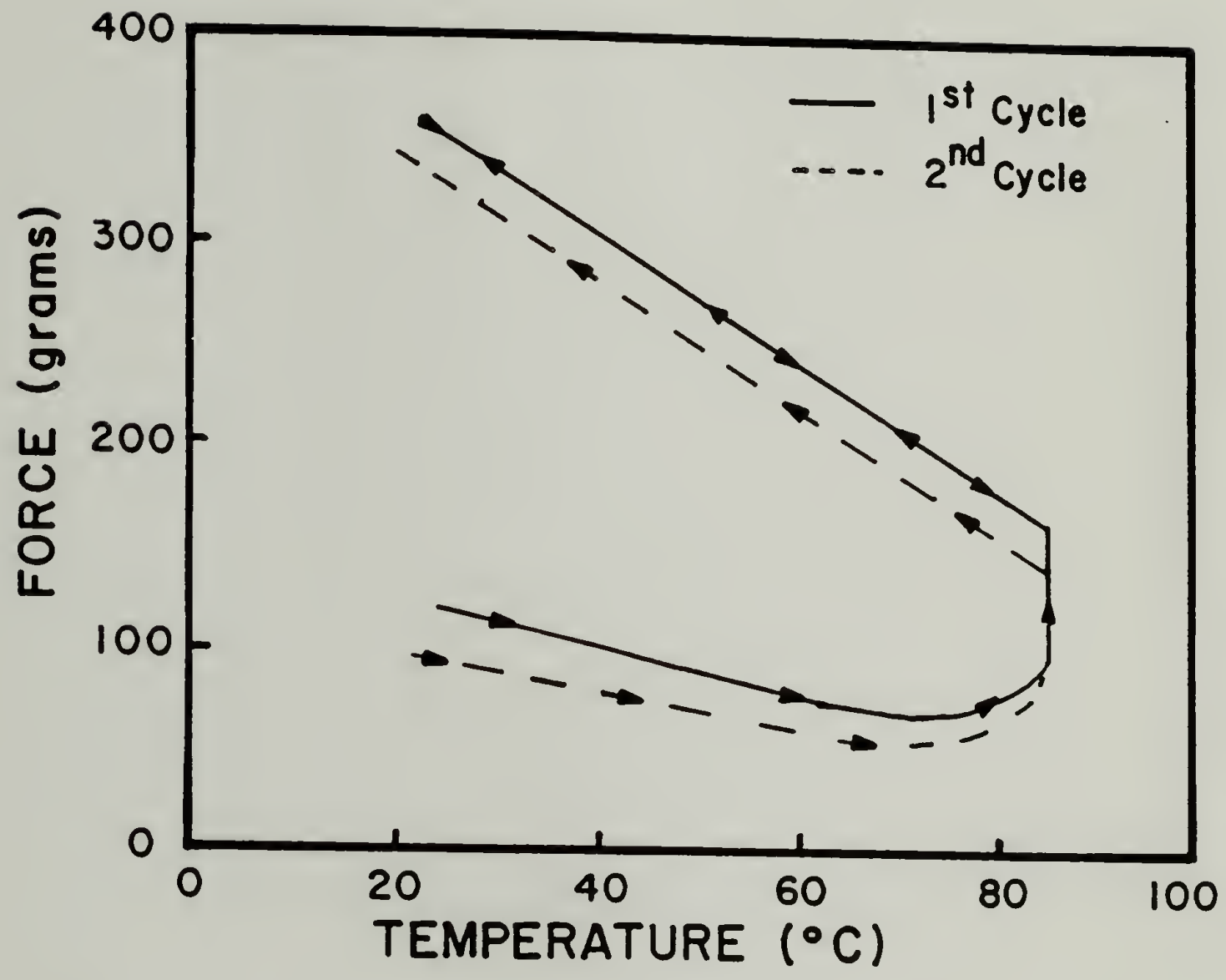

Figure 3.8. Force versus temperature for a PAA solution on rubber.

with temperature; therefore, its changes with force may be neglected (Figure 3.9). For the PAA coated rubber in Figure 3.8, at temperatures greater than 60° C the force begins to increase with increasing temperature. This indicates that the coating has passed its critical concentration point and can now support a load. The shrinkage stress observed is due to solvent loss in the coating and not to any changes in the rubber support. The temperature is increased to 85° C and held at this value several hours until no further increase in force is observed. When slowly cooled to room temperature, the force (at 25° C has increased by 250g due to solvent loss in the PAA film. Using the final coating dimensions (the films had an average thickness of 10 μm), this corresponds to a change in stress of 8 MPa. After each of these runs infrared spectra were obtained. The N-H stretching band was always present and there was no indication of the imide absorbance at 1776 and 722 cm^{-1} (see Appendix). Thus no conversion to polyimide has occurred in these films.

In the second cycle, the load is manually reduced to 100g by adjusting one of the mounts on the apparatus. A similar heating cycle is performed and the resulting force-temperature trace parallels that in the previous cycle. If instead the load was left unchanged after the first cycle (at 375g) and reheated, the heating/cooling curve reversibly follows the upper path (cooling) of cycle 1 (between 375g at 25° C and 165g at 85° C).

Figure 3.10 shows a similar experiment as in Figure 3.8 on another sample. In this example the stress and temperature are plotted as functions of time. In the first run, after 5 hours at 85° C the stress has reached a steady state value of 9.3 MPa. After this run the stress was reduced to 1 MPa and heated to 85° C. This figure illustrates that the rate of stress increase for the second run is slower

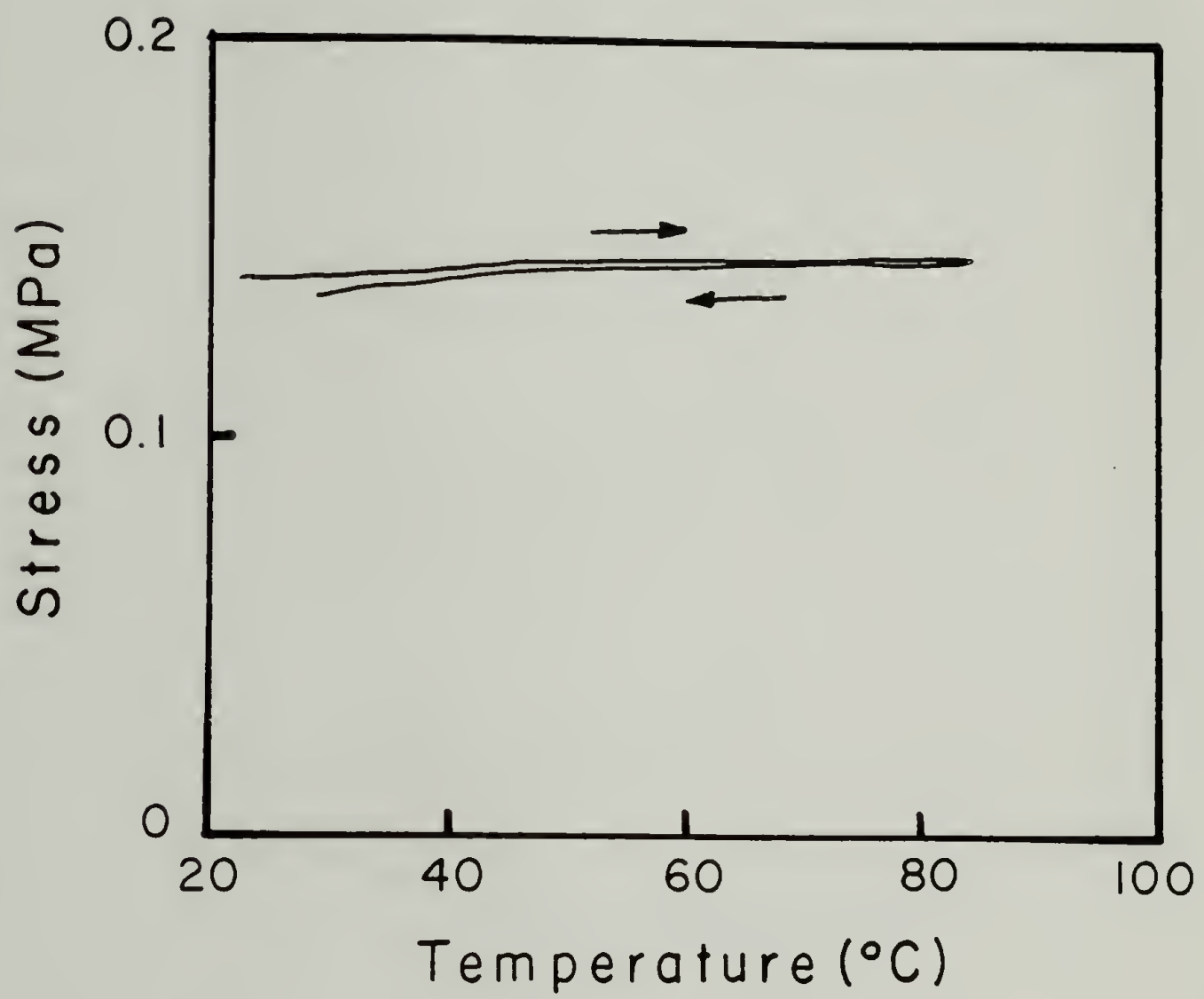

Figure 3.9. Stress versus temperature for rubber sheet used in thermomechanical experiments.

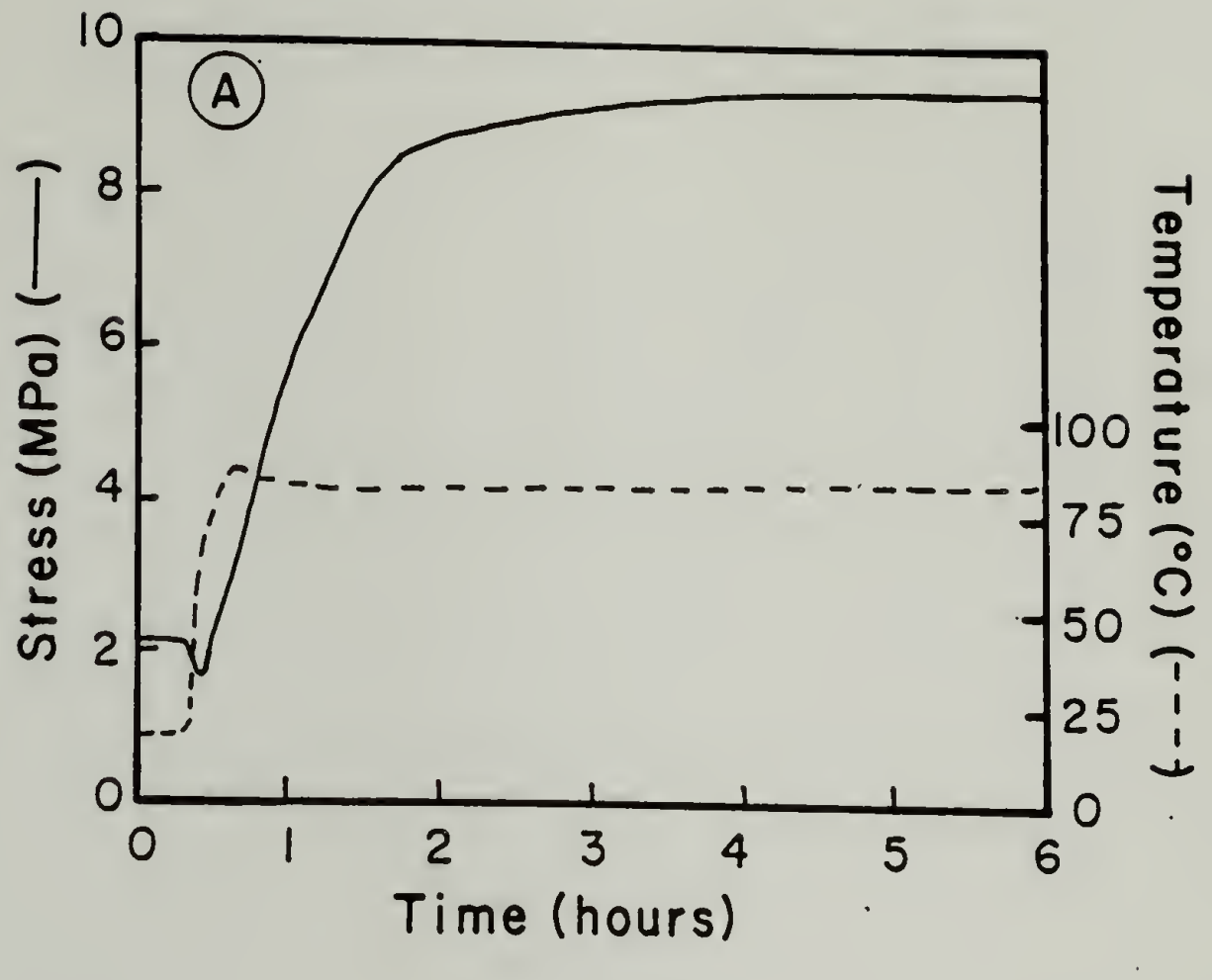

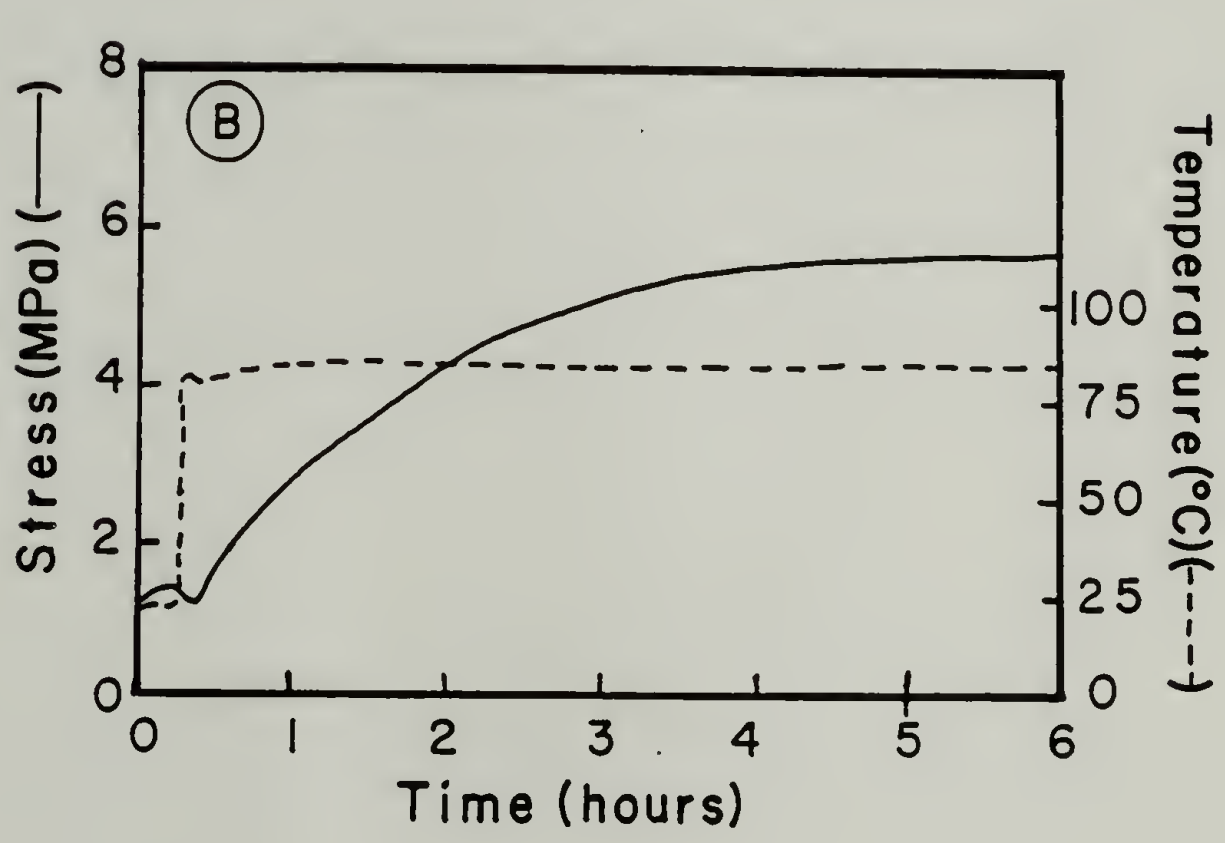

Figure 3.10. Stress and temperature versus time for a PAA coating on rubber. A - First cycle. B - second cycle, stress reduced manually to 1 MPa before starting second cycle.

than in the first run. After 6 hours the stress reaches a steady state value of about 6 MPa. These results demonstrate that the observed behavior in Figure 3.8 is free from non-equilibrium effects.

Stress recovery experiments were performed on these coated samples to investigate the viscoelastic effects. A stress of 8 MPa is applied to the sample and the film undergoes a 30% relaxation. If the stress in suddenly reduced to 1 MPa, a small increase in stress to 2 MPa occurs. Thus, recovery effects do not account for the stress increase observed in Figure 3.8 in the second cycle.

Another PAA solution coated rubber sample was placed in the force-temperature apparatus and the results of a sequence of experiments is illustrated in Figure 3.11. The heating-cooling schedule of cycle A is identical to that of cycle 1 in Figure 3.8. For the second cycle the starting force is manually increased to twice the room temperature value. The heating and cooling trace for B is linear and reversible. No increase in force is observed after residing at 80° C for 1 hour. At the end of cycle B the force is reduced to 50g, the starting level in cycle A. Heating to 80° C, an increase in force is observed similar to that in run A.

Figure 3.12 represents a composite set of results for similar experiments. The procedure is identical to the previous one, that is, the PAA solution coated sample is heated rapidly to the elevated temperature and held at this temperature until no observed increase in force, then cooled. After cycle 1 the load is not adjusted before heating the sample as shown in cycle 2. After this run, the force was then decreased to 50g and on heating to 85° C the path follows that from the first cycle (cycle 3). After each cycle the coating was removed from the rubber sample and modulus and thermal expansion coefficient were obtained. These results are shown in Table 3.1.

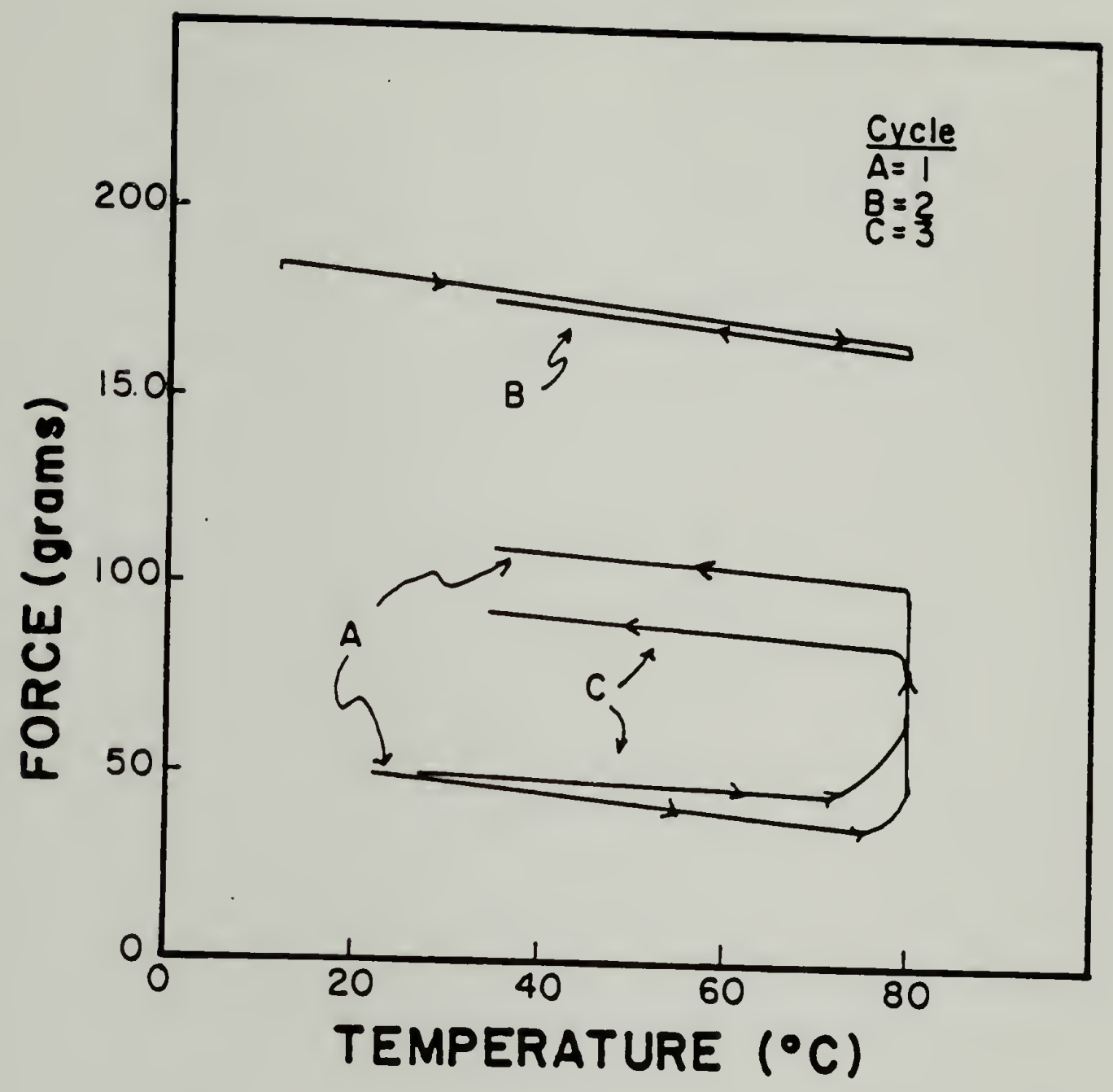

Figure 3.11. Force versus temperature for a PAA solution on rubber.

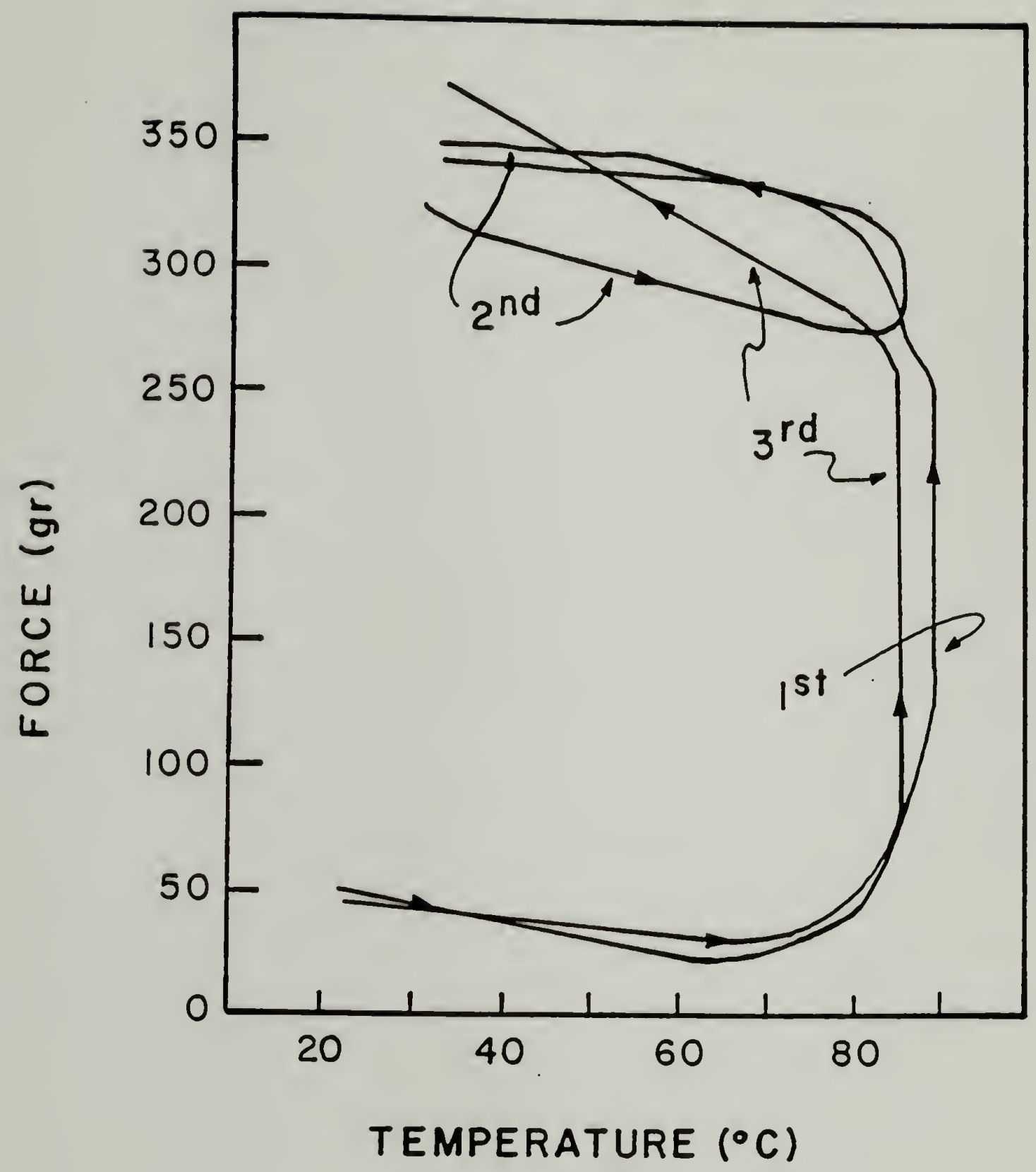

Figure 3.12. Force versus temperature for a PAA solution on rubber. 1st, 2nd and 3rd indicate heating cycle.

Table 3.1. Properties of force-temperature cycled PAA films

Cycle number	E ± 10% (GPa)	$\alpha \times 10^5$ (cm/cm/° C)
1	1.50	4.9
2	2.20	3.3
3	1.80	3.4

The tensile modulus of the PAA films is about 2 GPa in comparison to fully cured PI films which have a modulus of 3 GPa. Subsequent heating cycles do not drastically alter this property; however the tensile strength increases from 28 ± 4 MPa for PAA to 113 ± 12 MPa for PI films. A slight decrease in expansion coefficient is observed only after the first cycle. These results indicate that the stress increase is due primarily to solvent loss.

To demonstrate that this technique is applicable to other materials and the results are not inherent only to PI5878 material, thermomechanical experiments were performed using a polyimide solution from Ciba-Geigy, Probimide 293. This material is a soluble polyimide in gamma-butyrolactone (GBL) with the general chemical structure shown in Figure 3.13. An 18% solids solution of this polymer, CG293, in GBL was coated onto rubber substrates as in the previous experiments and mounted in the thermomechanical apparatus. Results of a sequence of heating/cooling cycles on a sample are shown in Figure 3.14. The maximum temperature for solvent removal was chosen to be 50° C. This is one recommended drying temperature for this material and is lower than that for PI5878. Although GBL and NMP have about the same boiling point, GBL has a lower heat of vaporization at room temperature than NMP.[60]

In the first cycle of Figure 3.14, the initial applied load was again 50g. The sample was heated to 50° C and kept at this temperature until there is no further

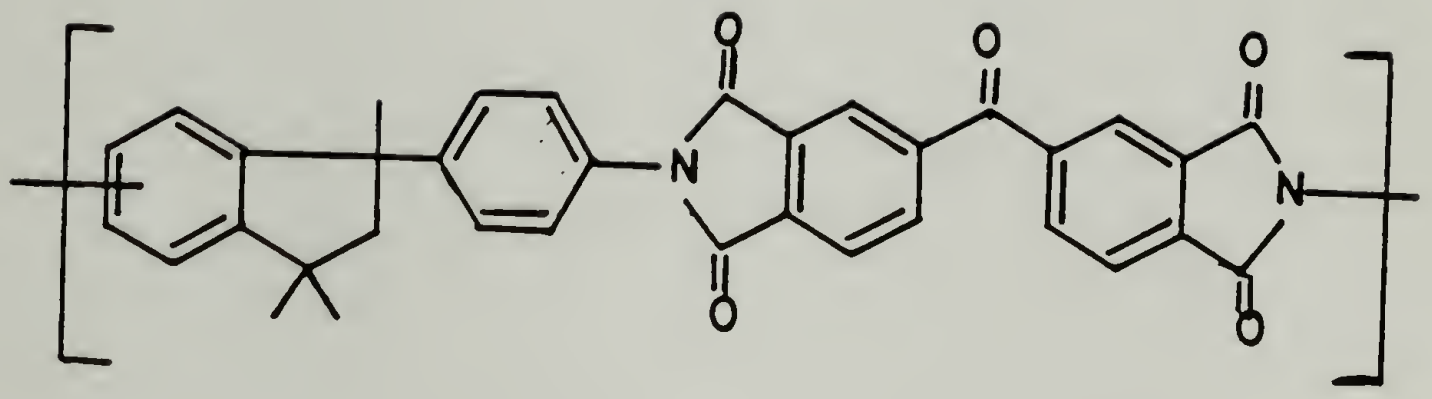

Figure 3.13. Ciba-Geigy Probimide 293.

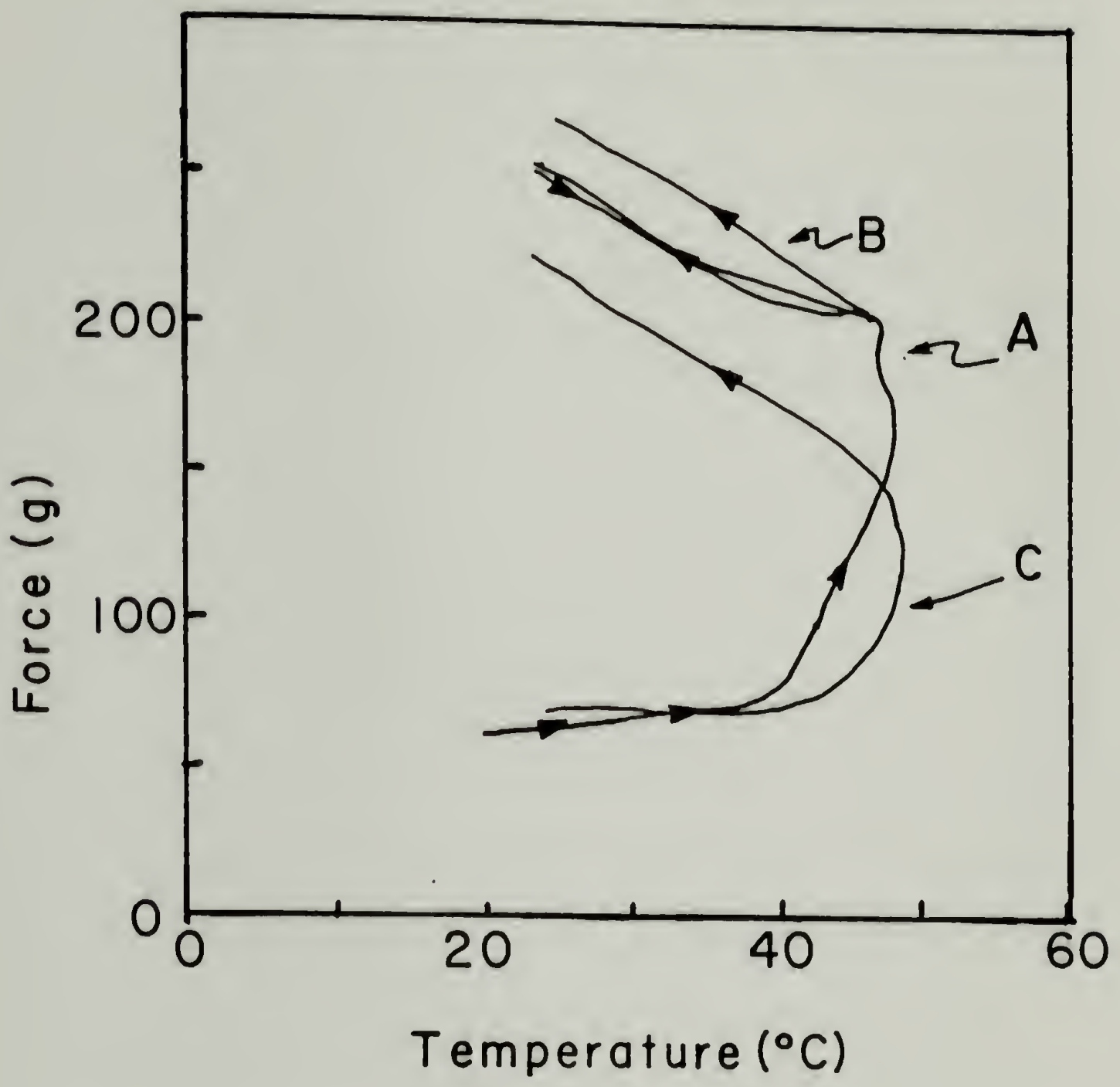

Figure 3.14. Force versus temperature for CG293 solution on rubber. A = first cycle, B = second cycle, C = third cycle.

increase in force. The sample was cooled to room temperature, reheated to 50° C, and subsequently cooled back to room temperature after 1 hour. For cycle C the load was manually reduced to 50g and heated in the same manner as for cycle A. The resultant force-temperature curves for this material are identical in shape to the PI5878 material. There is approximately a 150g increase in force due to solvent loss which is about 9.5 MPa of stress on the coating.

Similar force-temperature experiments were also attempted using a Miniwax Polyurethane Clear Satin Finish containing 42% solids. Due to the softness of this material, it was difficult to observe any dependence of solvent removal on stress. A force-temperature profile for this coating is shown in Figure 3.15. The change of stress on the 110 μm thick coating due to solvent removal at 60° C is only 0.325 MPa.

Using force-temperature experiments, the effect of a change in temperature on the stress in a solvent-based coating was studied. Figure 3.16 shows results from such an experiment plotting stress and temperature as a function of time. The thermal cycling procedure again is the same as in the previous experiments discussed above. For this experiment the highest temperature during the first cycle was 60° C. On cooling to room temperature, the stress reached 10 MPa. At this temperature, a steady stress state was attained after 9 hours, almost twice as long as when the temperature was 85° C. After this time the temperature was increased to 80° C. Initially on increasing the temperature there is a decrease in stress which is due to thermal expansion. After this initial drop the stress again increased while the temperature was held constant. Eventually the stress leveled off at 8 MPa. This increase is due to further solvent evaporation and subsequent material shrinkage. The additional drying is influenced by two factors. First, since the change in stress due to

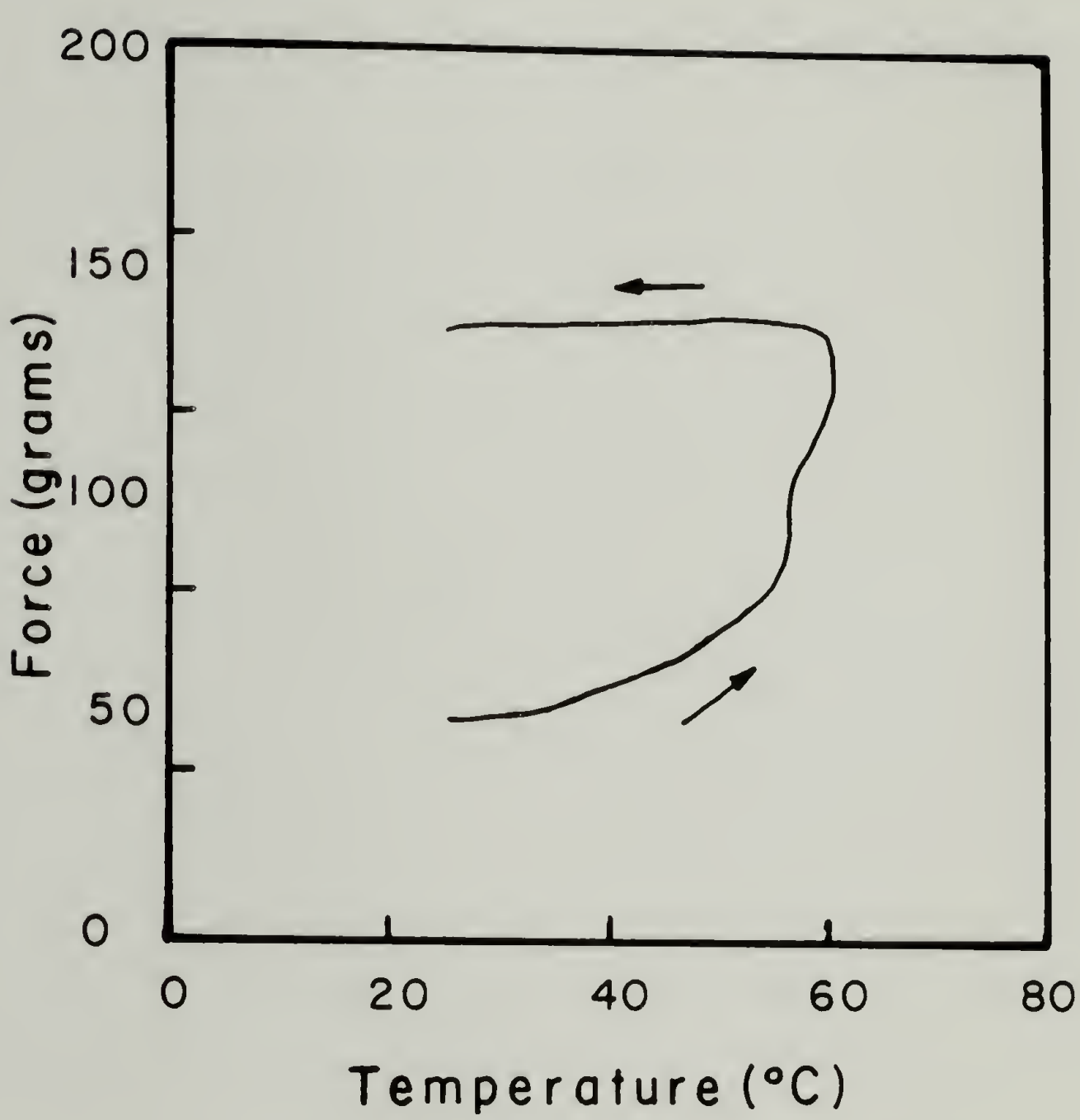

Figure 3.15. Force versus temperature for a 110 μm polyurethane coating on rubber.

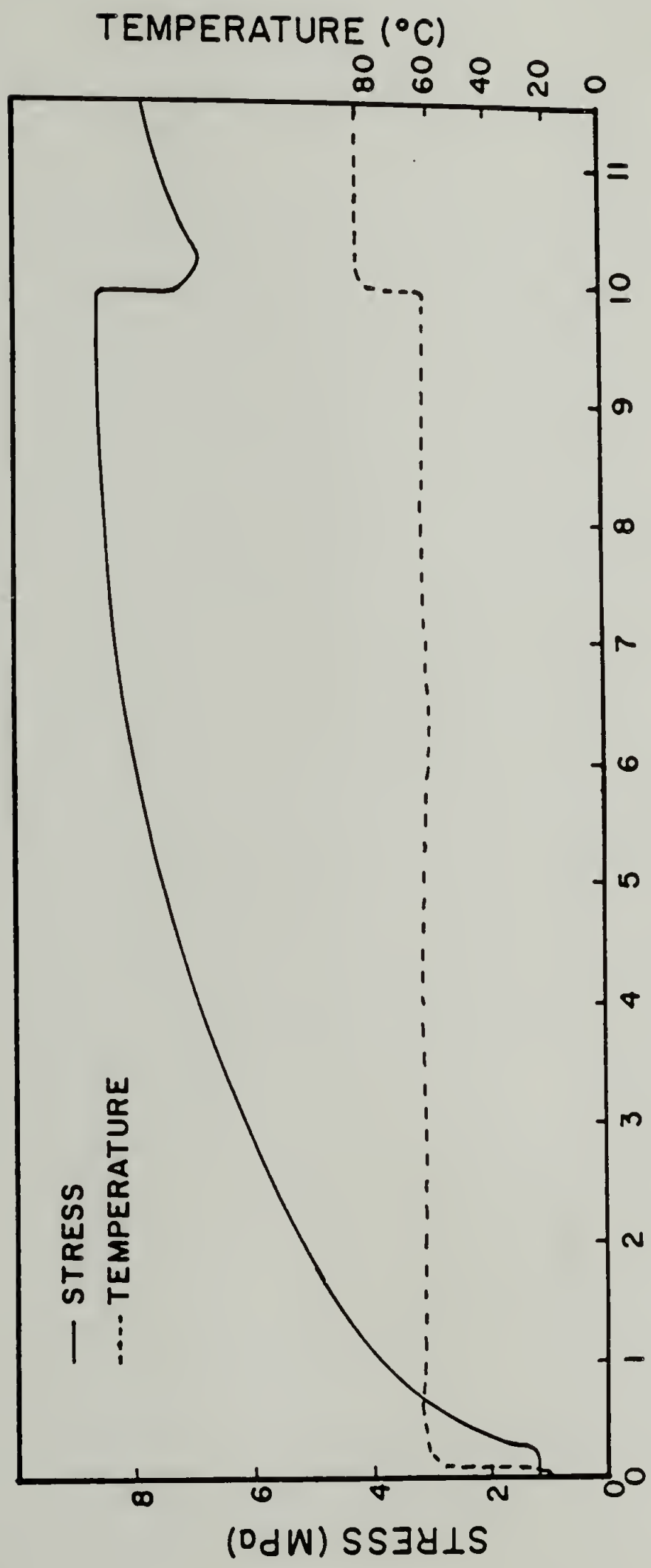

Figure 3.16. Stress and temperature versus time for a PAA coating on rubber.

temperature is equivalent to a change caused by a mechanical deformation, then as observed above, a reduction in stress allows further solvent to be removed. Secondly, the higher temperature increases the driving force for solvent evaporation.

To further investigate the effect of temperature on the solvent removal process, strain and temperature as functions of time at constant stress were obtained. Results are illustrated in Figure 3.17. A constant load of 115g was applied to the sample. On heating at 65° C, the strain decreased with time as expected. After 10 hr. the strain leveled at -6.5%. When the temperature was increased to 90° C the strain increases by 0.04% due to thermal expansion. This corresponds to a thermal expansion coefficient of 3×10^{-5} cm/cm/° C; whereas the measured value of the expansion coefficient for PAA (Table 3.1) was approximately 3.4×10^{-5} cm/cm/° C. Further heating at 90° C results in a decrease in strain which must be due to shrinkage and not creep. After the equilibrium strain has been reached, if the applied load is increased there is no additional change of strain with time due to solvent loss; but if it is decreased, the strain again decreases with time.

These thermomechanical experiments illustrate the strong coupling among equilibrium solvent concentration, stress and temperature. Clearly the stress level plays an important role.

3.3.2 Propagating Wave Results

Using the propagating wave technique, the changes in stress may be correlated directly with solvent mass loss. This technique was utilized for several experiments using a long, thin PAA coated rubber fiber. These experiments

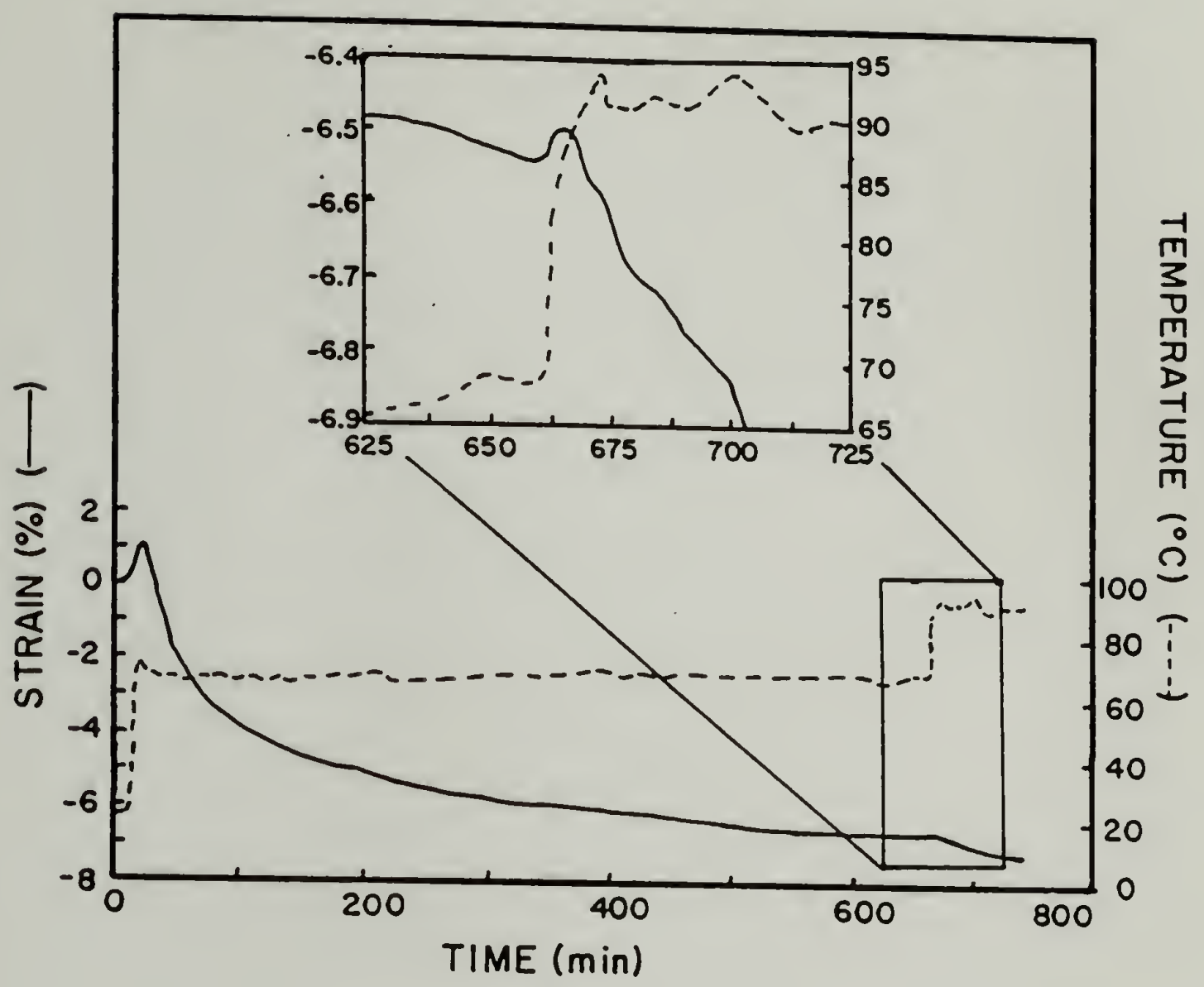

Figure 3.17. Strain and temperature versus time for a PAA coating on rubber.

duplicated the thermomechanical experiments while allowing the corresponding mass loss to be determined for each sample. One such experiment is presented in Figure 3.18. Since the sample was partially dried at the start of this experiment, the load applied to the sample was assumed to be carried only by the PAA coating which has a thickness of approximately 15 μm. When the cycles were completed, the PAA coating was removed and the rubber alone was tested in the instrument. With this, the change in stress and mass of the coated sample with temperature was corrected to account for response of the rubber substrate to temperature.

In the first cycle, a stress of 6.8 MPa is applied to the sample and it is rapidly heated to 87° C and held at this temperature for two hours before cooling to room temperature. Again an increase in room temperature stress is observed. From the corresponding mass/length data in Figure 3.18B, this increase in stress can definitely be related to loss of solvent from the PAA coating. The second heating cycle was accomplished without changing the level of stress on the sample. Upon completing this cycle, another increase in stress is noted along with a decrease in the mass/length.

Since in the first cycle the sample was only heated for two hours, it did not reach a steady stress state as observed in the thermomechanical experiments after 4 hours. Therefore, additional shrinkage is expected in the second cycle. For this run the sample was kept at the elevated temperature until there was no observable loss in mass or increase in stress. Before beginning the third cycle, the load was manually reduced to 8.3 MPa. Upon heating, the stress-temperature curve overlapped that of the second run, with the stress increasing by 5.5 MPa to 11.8 MPa. There was additional mass loss corresponding to this increase, but its magnitude was not as large as in the previous cycles. This may be attributed to

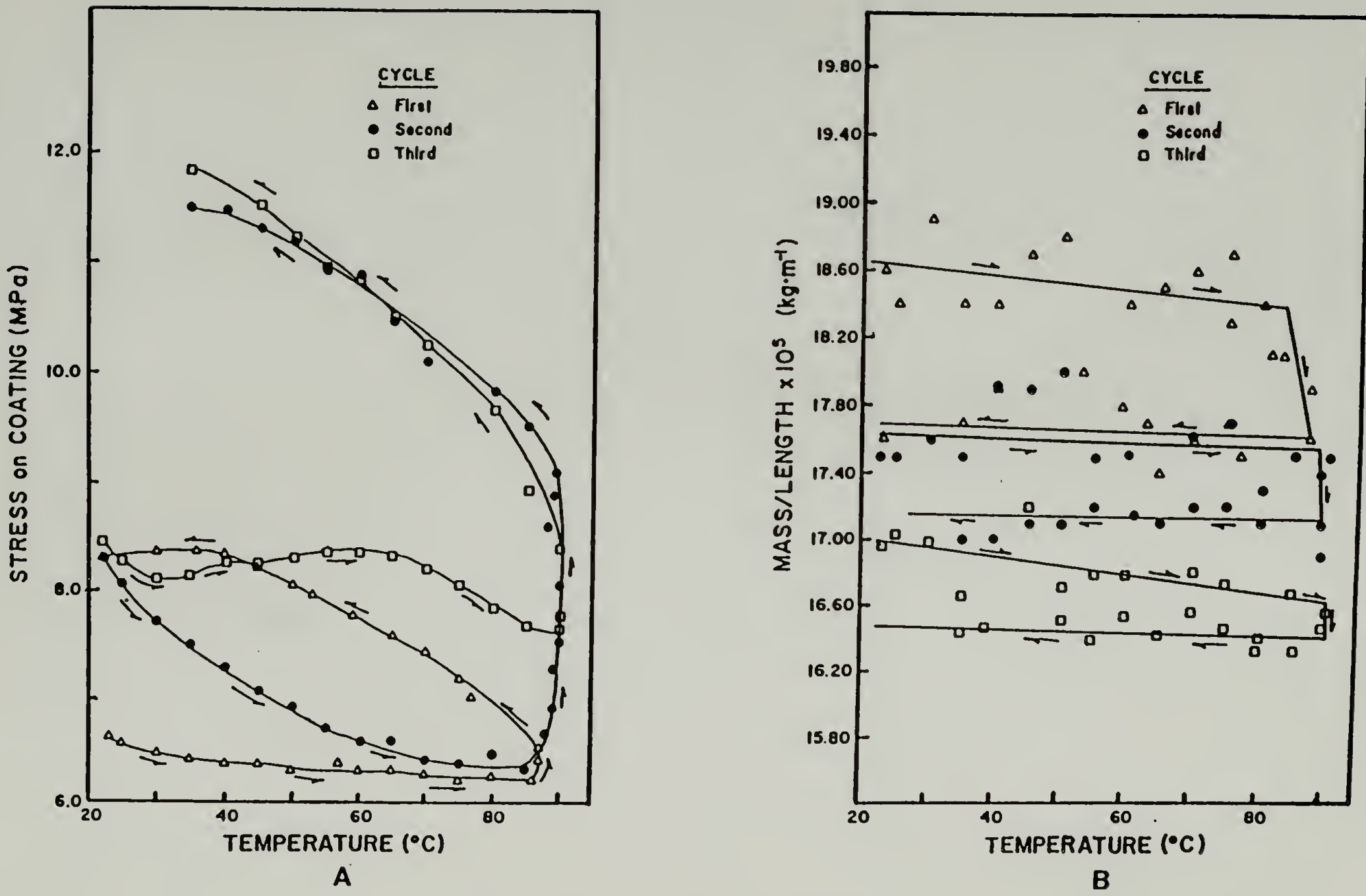

Figure 3.18. Drying of a PAA coated rubber fiber. Load manually reduced to 8.3 MPa at the start of the third cycle. A) Stress on coating versus temperature. B) Mass/length of coated fiber versus temperature.

the increase in stiffness of the coating after each successive thermal treatment. Therefore it requires less of a volumetric change to create the same stress change.

A series of these experiments is summarized in Figure 3.19. The following heating/cooling schedule was used:

Cycle 1: After air drying the sample for 30 min. in air it is placed in the instrument and a deformation is applied (8 MPa). The sample is rapidly heated to 85° C and kept at this level until there is no observed change in mass/length or stress, after which the sample is cooled to room temperature.

Cycle 2: After cycle 1 the sample is then immediately reheated to 85° C. It is cooled to room temperature when the 'no change' condition is satisfied.

Cycle 3: The stress is manually reduced to the initial starting value in cycle 1 (8 MPa) and then heated in the same manner.

Figure 3.19 presents the initial and final room temperature stress and mass/length values. In the first cycle the stress increased by 100%, from approximately 8 to 16 MPa. The mass/length of the PAA decreased from 8.0 to 7.5×10^{-5} kg/m. From separate weighing experiments it was found that a coated rubber fiber loses 32 wt% during the 30 min. air drying. With this value and by taking into account the mass/length of the rubber support (approximately 5.3×10^{-5} kg/m), the mass/length change for only the coating was calculated to be 32% during the first cycle and an overall weight loss to be 54%. In cycle 2 there

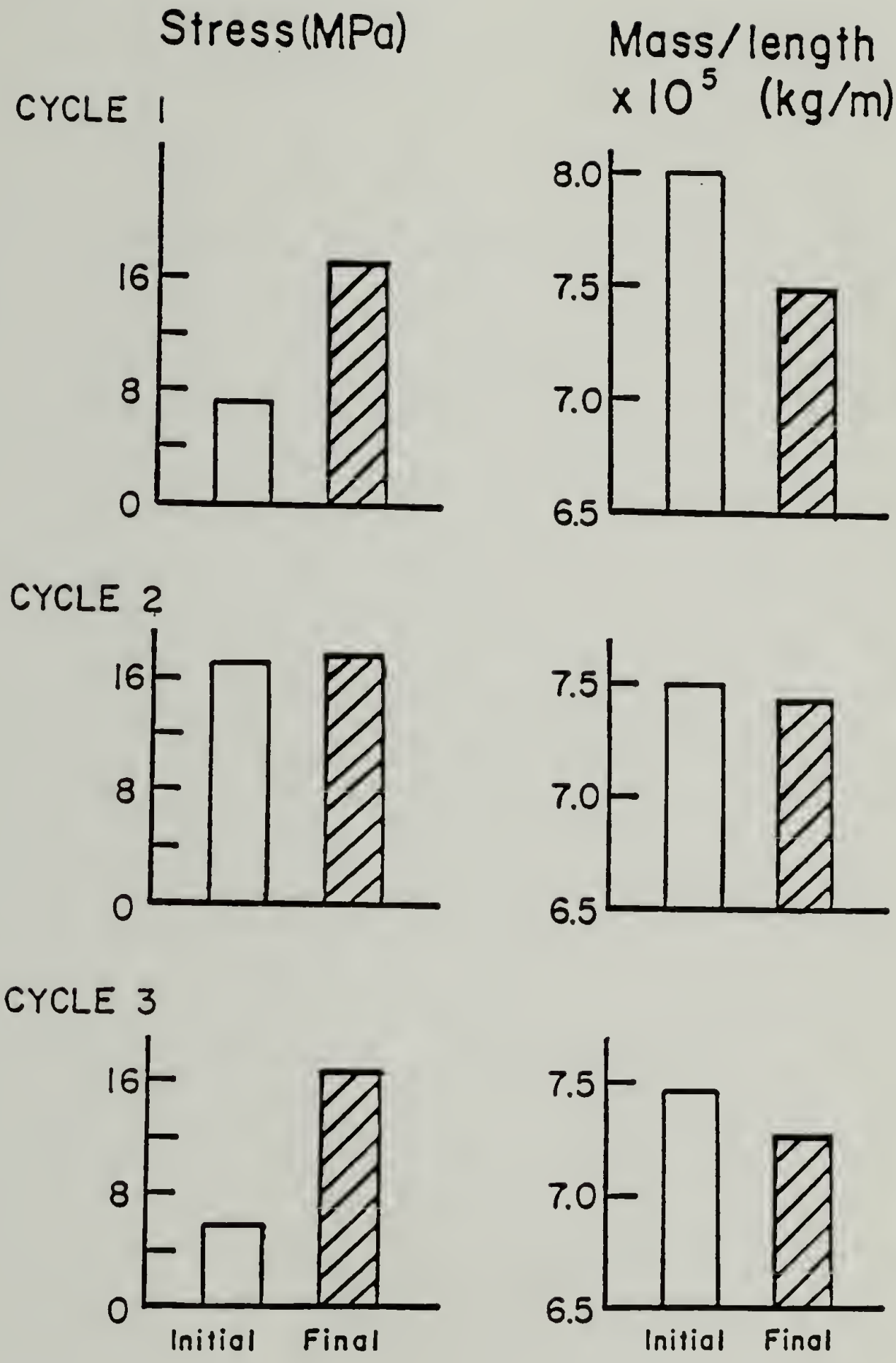

Figure 3.19. Graphic representation of room temperature stress on coating and mass/length of coated fiber for the drying of a PAA coated rubber fibers at 85° C.

was a slight increase in stress accompanied by a change in mass/length of 6%. After cycle 3 the stress returned to the upper value of 16 MPa. Along with this increase there was a 17% loss of mass during the cycle. At the end of these cycles the total mass loss was 64%. The original PAA solution was 74% solvent. Therefore, even after all these thermal treatments all the solvent could not be removed.

3.3.3 Impulse/Propagating Wave Results

To obtain changes of equilibrium modulus during the drying process, the Impulse Method was applied to polyimide samples. The Impulse Method was initially applied to a Kapton ribbon to demonstrate that the apparatus would provide reliable results. The stress response to a box strain is illustrated in Figure 3.20. After integrating over time and applying equation 3.3, the equilibrium modulus was determined to be 2.96 GPa at 22° C. Standard tensile tests give 3 GPa for the modulus. Therefore, it appears that this technique may be applied to long ribbons or fibers providing the sample is always in tension.

A typical stress response for a step strain applied to a coated rubber fiber is shown in Figure 3.21. Using equation 3.3, the equilibrium modulus was determined to be 598 MPa. A series of such pulses was performed during the drying of a PAA coated rubber fiber to yield the change in modulus with temperature (Figure 3.22) The modulus increases from 100 MPa initially to 2 GPa at 80° C due to solvent removal. Because of instrument noise and difficulties in data acquisition, many samples had to be discarded. Better instrumentation and data collection procedures are needed to improve this technique.

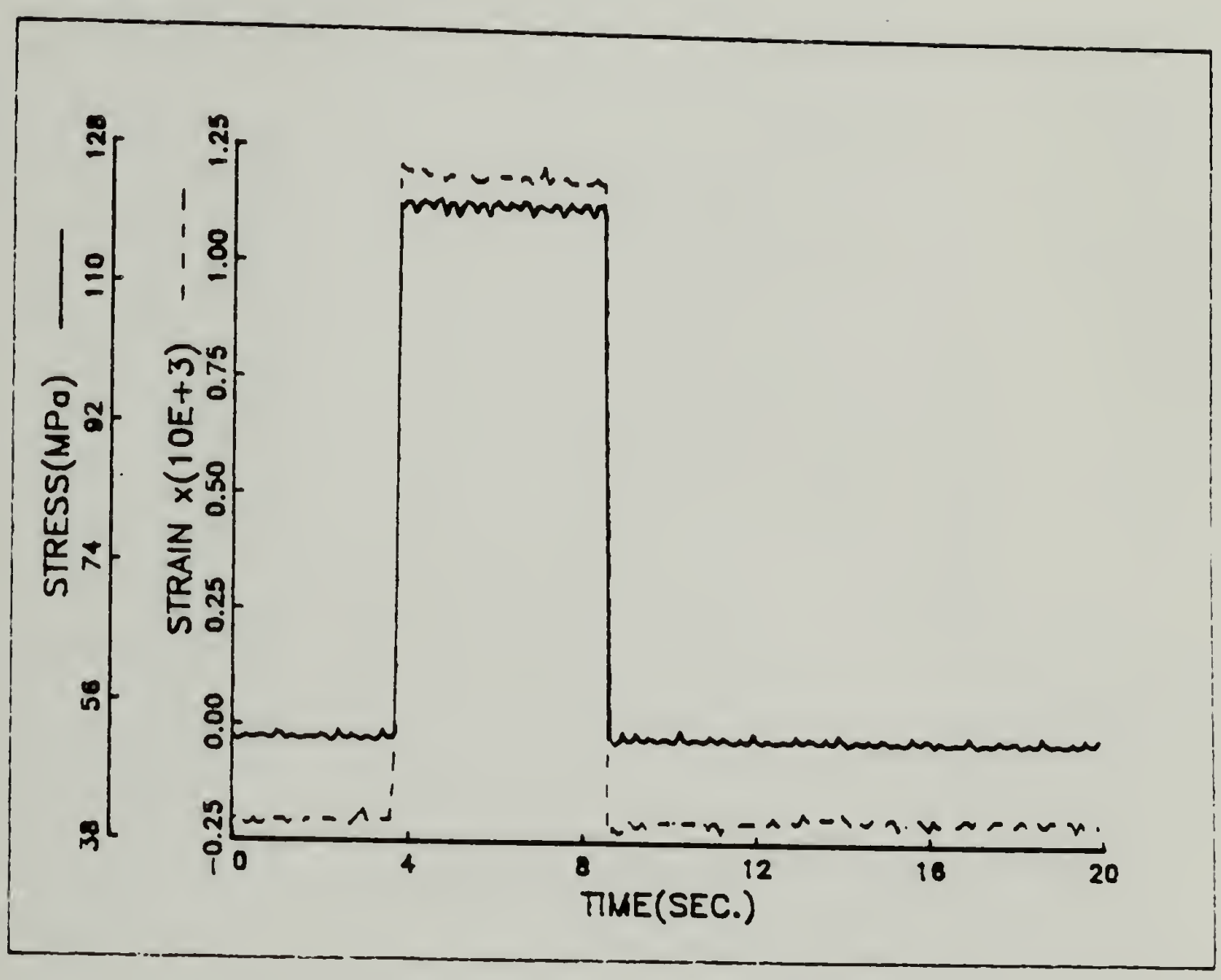

Figure 3.20. Stress response to a uniaxial pulse deformation applied to a Kapton ribbon.

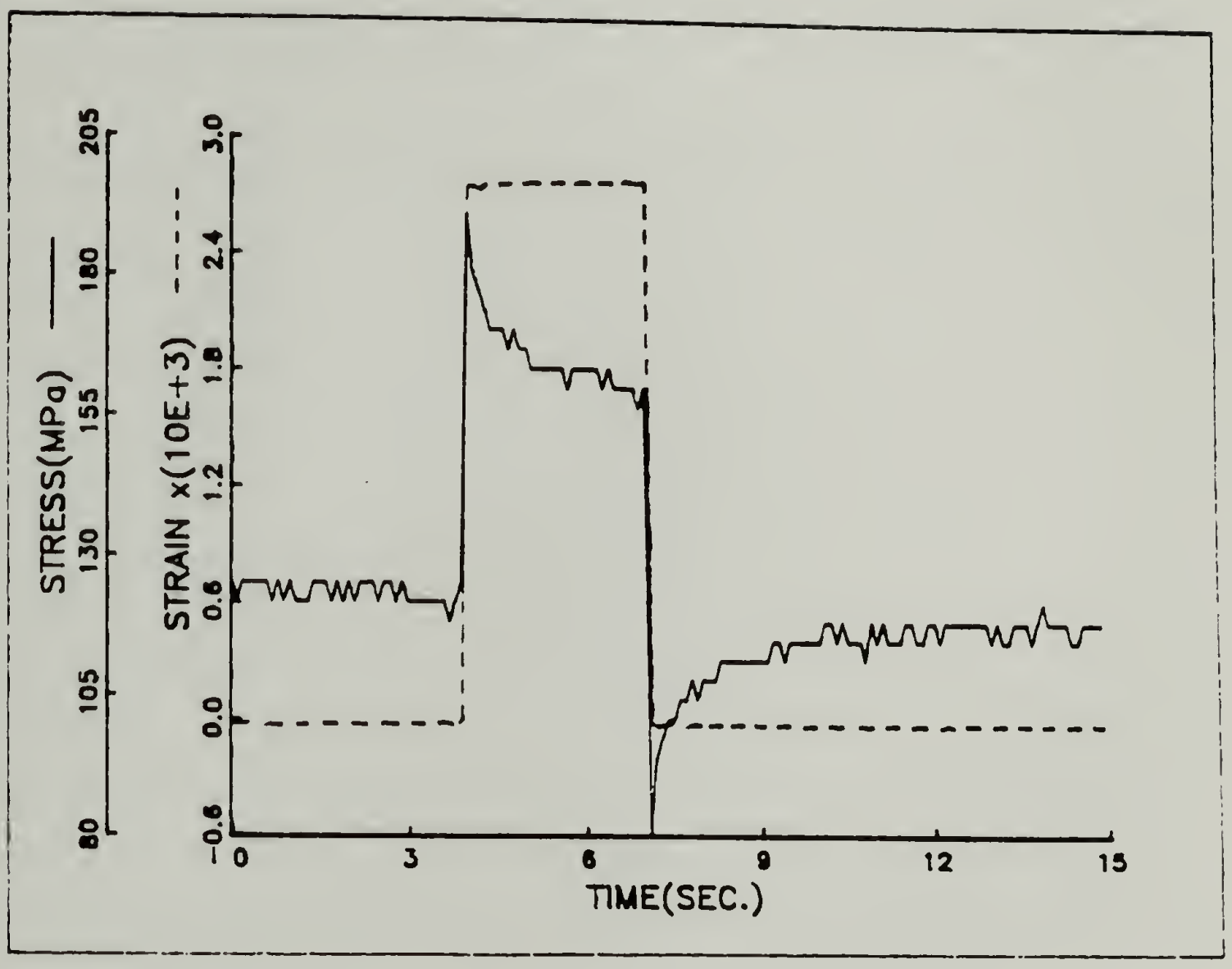

Figure 3.21. Stress response to a uniaxial pulse deformation applied to a PAA coating on a rubber fiber. Pulse #48, E_{eq} = 598 MPa, T = 89° C.

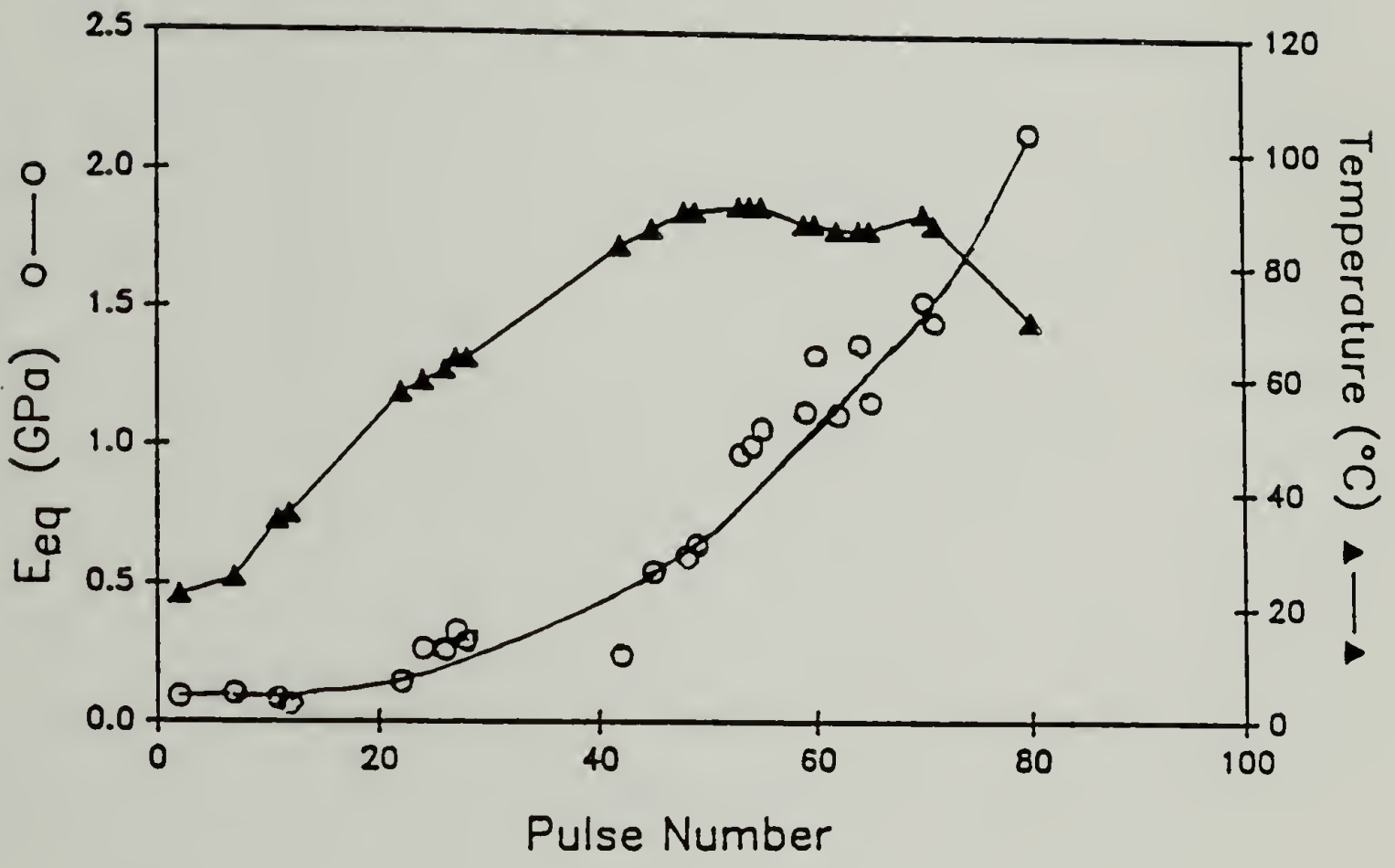

Figure 3.22. Equilibrium modulus of PAA and temperature versus pulse number during the drying of a PAA coated rubber fiber.

This method was then applied with the propagating wave technique to allow simultaneous measurement of the stress on a coating, mass loss and equilibrium modulus as a function of time or temperature during solvent removal. This is illustrated in Figure 3.23. As solvent is removed the mass of the coating decreases (24%), the stress increases (to 13 MPa) and the equilibrium modulus increases (to 1.66 GPa). As with the thermomechanical experiments, the load was manually decreased at the start of the second cycle and the sample was reheated to 85° C. The change in stress and mass/length were identical to that of the first cycle. However, due to the large scatter in data impulse method, no change in modulus was detected.

3.4 Initial Imidization

Using force-temperature experiments and the propagating wave/impulse method, the property changes due to imidization of the PAA at 150° C were obtained. In Figure 3.24 a PAA sample spin coated on a glass plate and dried at 85° C for 30 min. on the plate was used in the force-temperature apparatus. An initial load of 8 MPa was applied to the sample since this was the measured shrinkage stress due to solvent removal in the earlier experiments. This stress relaxed to 3 MPa before heating to 85° C. On cooling to room temperature the stress increased to 15 MPa. The change in stress with this cycle cannot be directly compared to that from previous force-temperature results since this film was dried initially on a glass plate under a biaxial constraint. The PAA coated on the rubber sheet is only constrained in one direction.

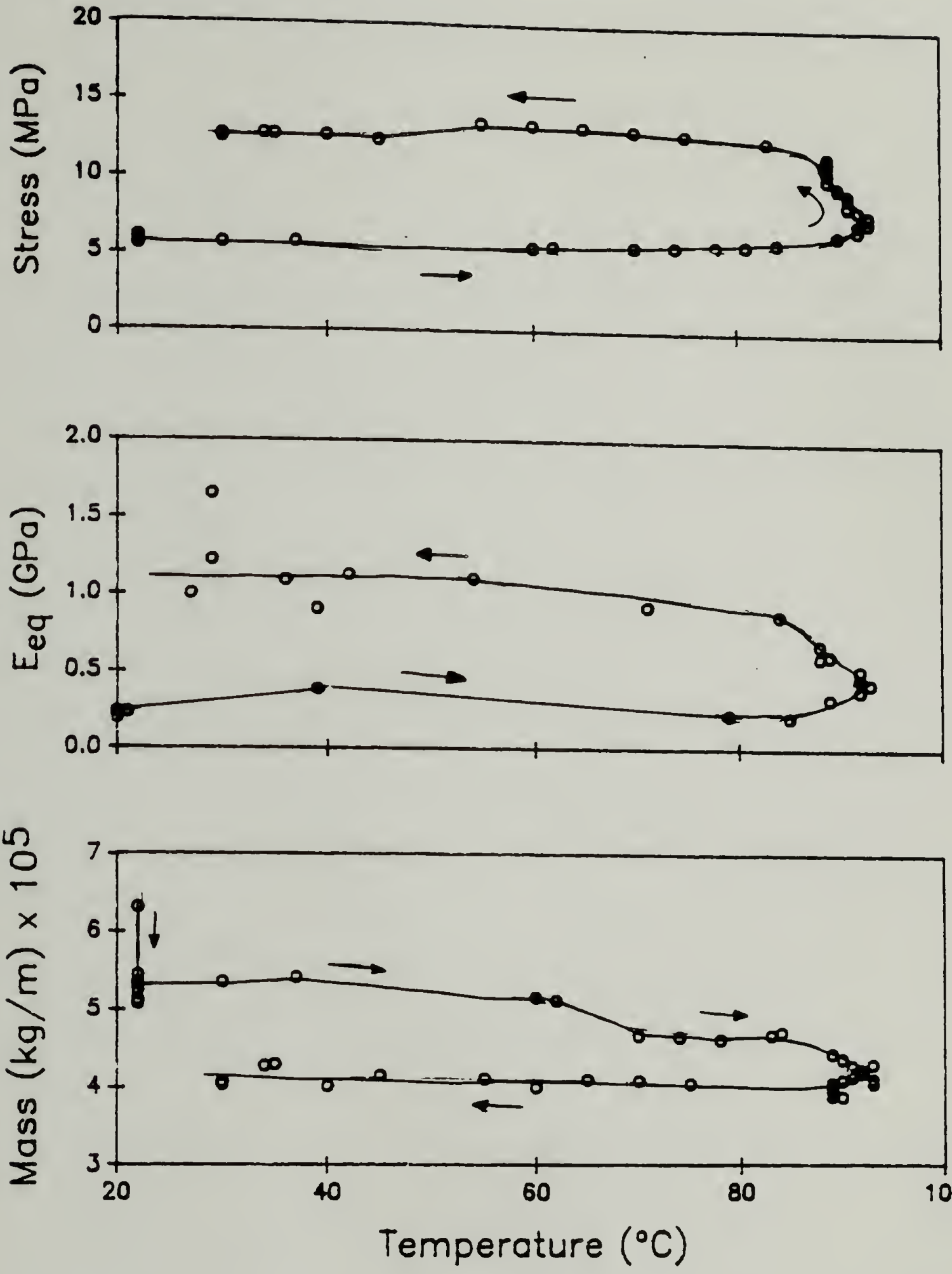

Figure 3.23. Stress, mass/length and equilibrium modulus of a PAA coating as a function of temperature.

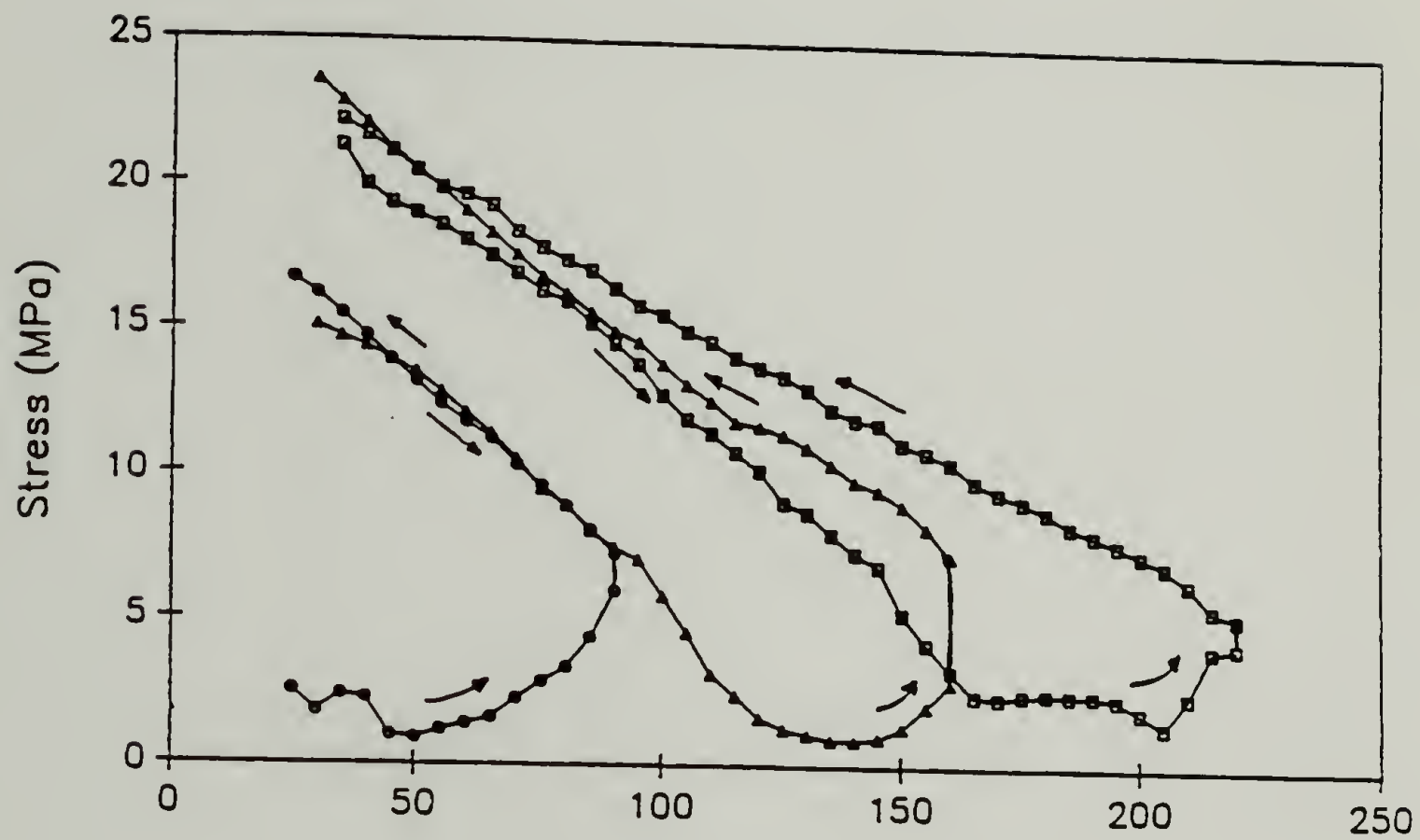

Figure 3.24. Stress versus temperature for a PI5878 free-standing film initially dried at 85° C on a glass plate.

The film was then heated to 155° C and kept at this temperature for 1 hour. A 6 MPa increase in stress occurs. This is caused by further solvent removal and shrinkage due to the imidization (confirmed by infrared spectroscopy, see Appendix).

This sample was then heated to 220° C for 1 hour where an additional increase in stress of 5 MPa occurs. The room temperature stress is the same as when starting, 23 MPa. Due to the curing and annealing at higher temperatures this is attributed to changes in thermal expansion coefficient and modulus with temperature and processing.

A coated rubber sample was used in the propagating wave/impulse method. These results are presented in Figures 3.25 to 3.27. The same thermal cycling was performed as for the 85° C dried film. The stress on the coating increased from 4 MPa to 12 MPa due to solvent drying at 85° C with a corresponding mass loss of 0.8×10^{-5} kg/m. The modulus increased from 230 MPa to approximately 2.8 GPa for this step. In the second cycle, the sample was heated to 166° C for 60 min. There is a noticeable increase in stress and decrease in mass. There appears to be a slight increase in modulus due to this thermal treatment but because of the large scatter this is difficult to quantify. On examining this sample after testing a non-uniform coating was found. Therefore these results using this technique are only qualitative and reflect the relative trends in behavior due to further solvent removal and imidization at higher temperature.

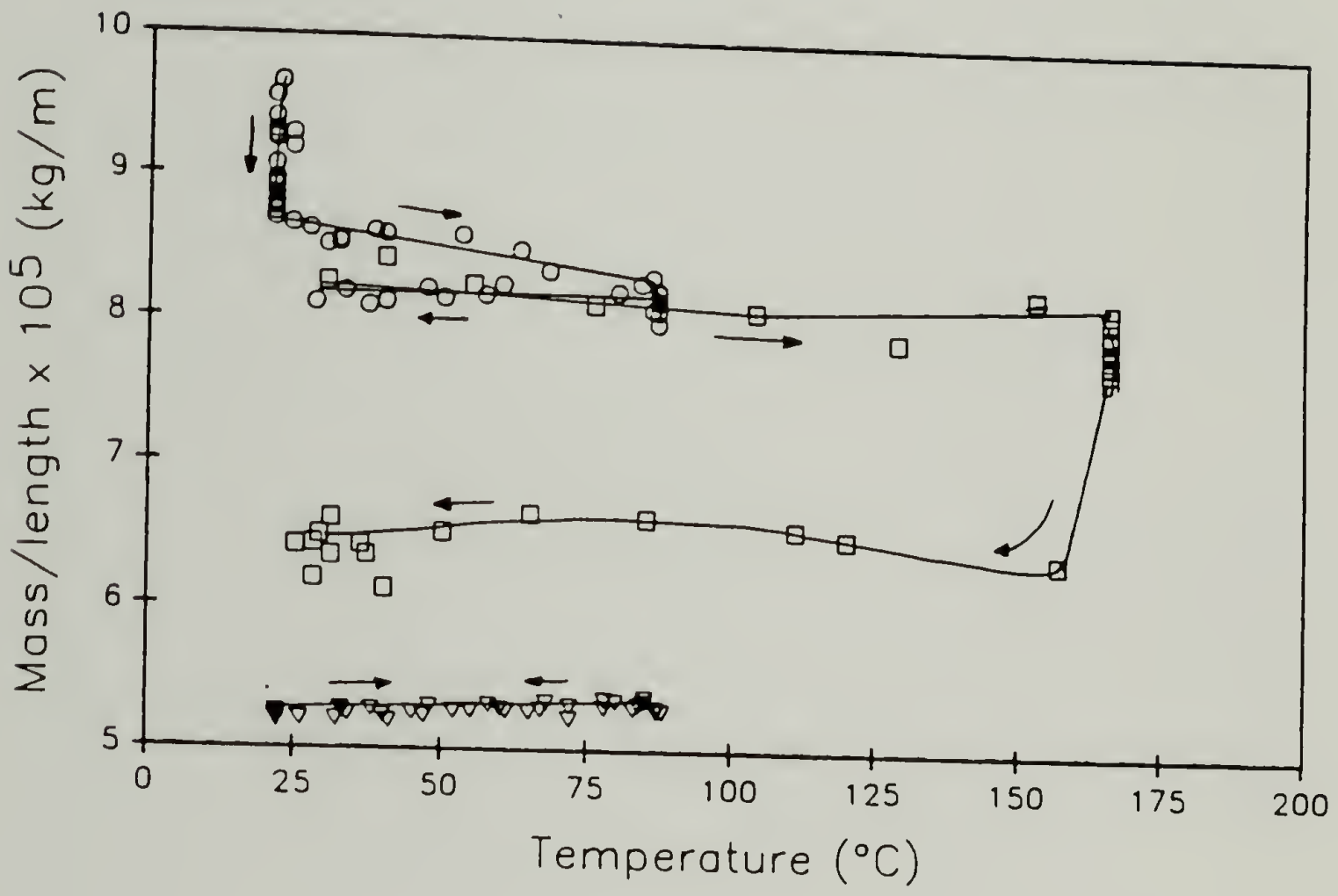

Figure 3.25. Mass/length of rubber fiber and PAA coated rubber fiber during drying. ○ - first cycle, □ - second cycle, ▽ - rubber fiber only.

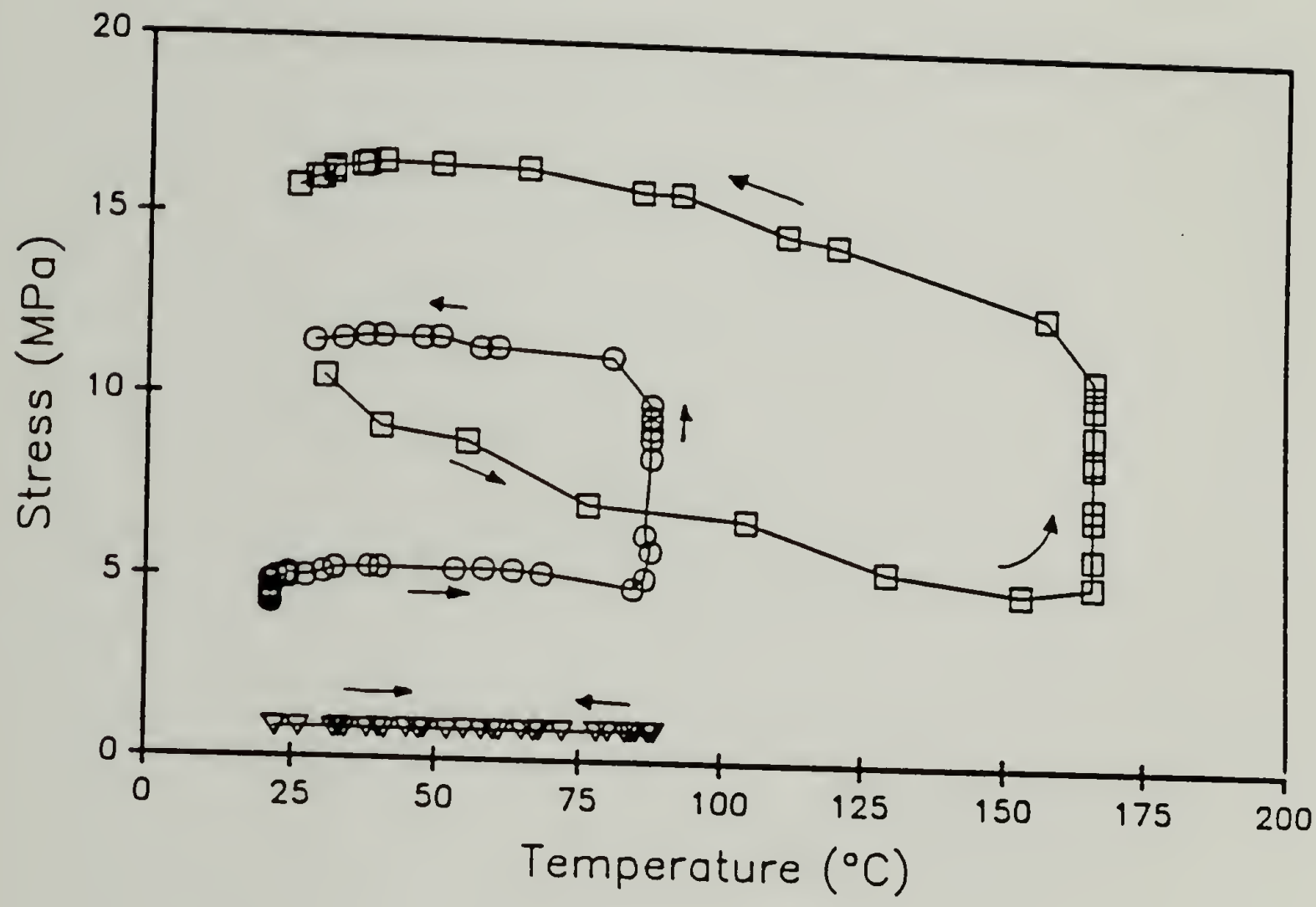

Figure 3.26. Stress on rubber fiber and PAA coating during drying. ○ - first cycle, □ - second cycle, ▽ - rubber fiber only.

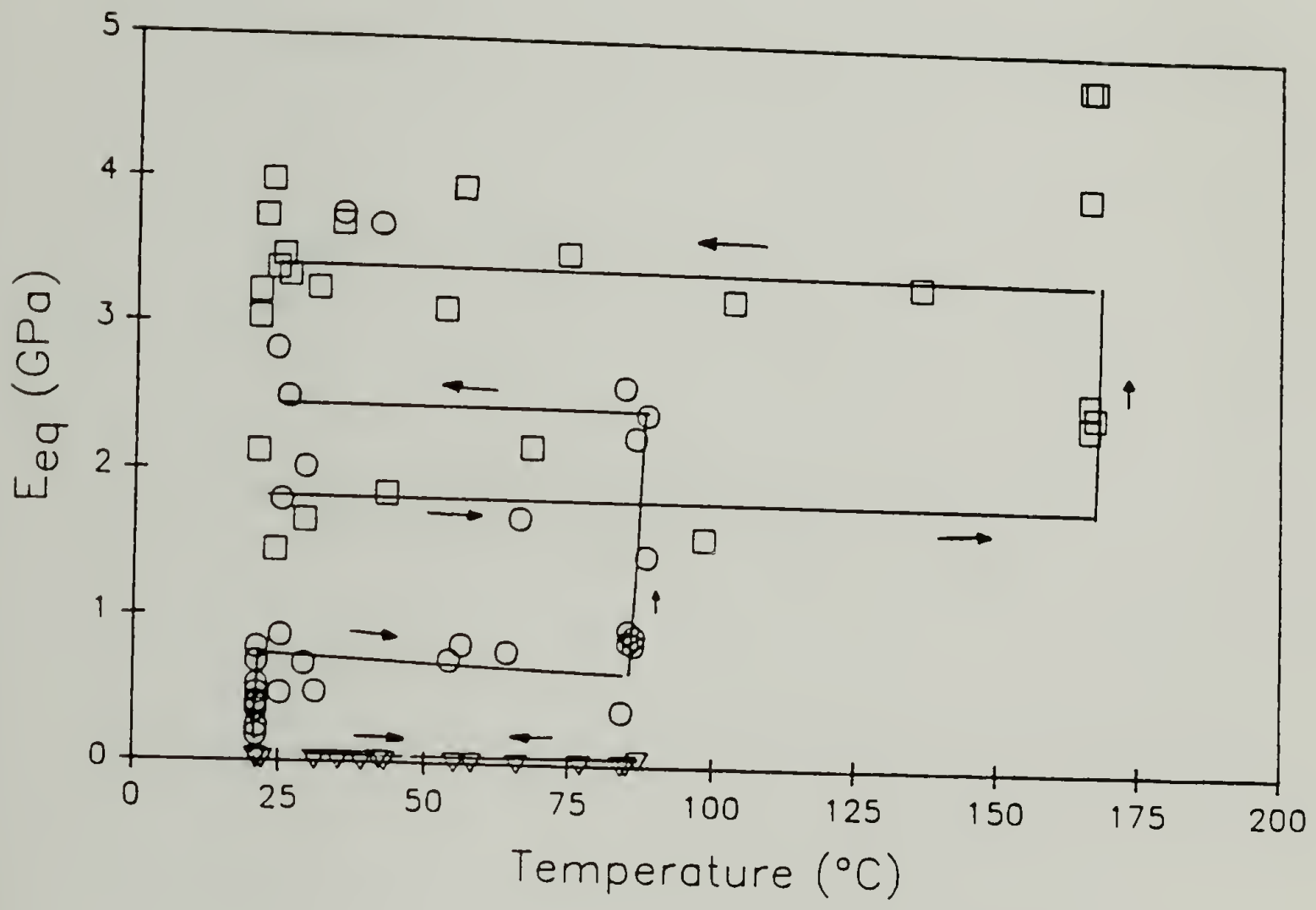

Figure 3.27. Equilibrium modulus of rubber fiber and PAA coating during drying. ○ - first cycle, □ - second cycle, ▽ - rubber fiber only.

3.5 Discussion

3.5.1 Solvent Removal and Imidization

The force-temperature experiments and propagating wave/impulse technique provide a direct means of measuring the development of stress in a solvent-based coating. Since the coating is applied to all sides of the flexible rubber support, there is no bending of the sample. It is then possible to keep the coating at constant strain which is a realistic situation for most coatings. Other techniques to measure residual stresses in coatings such as beam bending methods, follow the deflection of a beam due to shrinkage of an applied coating. These bending techniques suffer from several drawbacks. One, the coatings are not held at constant strain since the substrate curves due to shrinkage of the coating. Secondly, two dimensional bending forces occur and it is difficult to analyze or extrapolate the observed behavior to the two dimensional case, especially for large deflections. Finally and most importantly, is the assuption of linear elastic behavior.

With a one dimensional constraint, shrinkage stresses due to solvent removal in PMDA-ODA films are approximately 8 MPa as determined from thermomechanical experiments. For a biaxial constrained system these stresses would approach 16 MPa. A maximum stress of 16 MPa due to solvent evaporation at 85° C was obtained for PAA coated on rubber fibers. This cylindrical geometry constrains the coating in approximately two dimensions. Therefore the results from the propagating wave method support those from force-temperature experiments. In comparison, using an X-ray double crystal

lattice curvature technique, Goldsmith et al. and Geldermans et al. reported a shrinkage stress of 23 MPa due to solvent removal.[61,62] This is a bending method but does hold the sample in two dimensions.

For the soluble polyimide from Ciba-Geigy it was found that a uniaxially constrained film develops shrinkage stresses of 9.5 MPa.

From the force-temperature and propagating wave results, the solvent removal in films is dependent on the stress level in the coating. At a given temperature, as solvent is removed from the coating, the stress level in the coating increases. This continues until a certain critical stress level is reached in the film, after which no more solvent may be removed at this temperature. Only by reducing the stress in the material or by increasing the temperature may more solvent be removed. If the stress is reduced, additional solvent will be evaporated until the shrinkage stress reaches the same critical value. Even after several such reductions in stress it is difficult to remove all the solvent in the material. Increasing the temperature may also remove more solvent.

Chow et al. have investigated such solvent removal effects on stress using poly-N-vinylcarbazole films solvent cast on Mylar or Kapton.[63] They reported that the residual strains are developed mainly during the initial drying stage at room temperature in a vacuum oven and that additional drying at 150° C for 6 hours had little effect on the strains but reduced the residual solvent content by an order of magnitude.

The observed stress coupled solvent removal behavior suggests that a balance occurs between the driving force of solvent removal and that of the energy due to the stress in the sample. To remove more solvent, more energy must be added to the system such as by increasing the temperature or reducing the holding force attributed to the stress level. If either of these is not altered,

then additional solvent cannot be removed. This implies that in processing these coatings there is an optimum length of time for the solvent removal step and any additional solvent drying at a given temperature will not release further solvent. Furthermore, for PAA coatings, the trapped solvent may be beneficial to the coating by facilitating the imidization process.[64]

It is difficult to explain the stress-dependent solvent removal behavior at the molecular level. Work by Brekner and Feger has shown that PAA forms two complexes with NMP which have characteristic stoichiometric ratios and decomplexation temperatures.[65,66] It is probable that the energy due to the residual stress field may effect or couple with this behavior.

An additional shrinkage stress of 6 MPa was observed on heating the PAA films to 155° C. If this is added to that due to the solvent removal step the total shrinkage is 14 MPa or approximately 28 MPa in a biaxially constrained material. It has been reported that on curing these types of polyimides at 150° C, 55 MPa of stress is developed. On thermally curing these up to 400° C the room temperature stress decreases to 30 MPa.[62] This change in stress was attributed to differences in thermal expansion coefficient and molecular structure between the partially imidized film at 150° C and the fully cured film at 400° C. Similar behavior was observed for curing PI5878 up to 220° C. Other researchers have looked at the development of stresses in a soluble amide-imide polymer.[67] Using a bending beam method they report room temperature stresses around 140 MPa after curing at 200° C with cracking occurring in the material.

3.5.2 Energy Approach to Solvent Removal

In the 1940's and 1950's, Flory, Rehner and Treloar observed and modeled the increase in swelling of organic liquids into rubber samples with and without an applied external load.[68,69] This behavior was predicted using an energy balance approach. As an extension of this, Sternstein studied the swelling of filled elastomers.[70] Such liquid swelling is similar to the stress coupled behavior observed with solvent removal in coatings, where liquid is removed from the sample instead of being added. This type of stress dependence has also been reported for the absorbance of water vapor into hair, cellulose fibers and Kapton ribbons.[71-73]

An energy balance like that used by Treloar may also be used to explain the solvent removal process in polyamic acid coatings.[69] The total energy for solvent removal, the molar Gibbs free energy ($\overline{\Delta G}_{SR}$), may be expressed as the sum of the molar free energy for unmixing the solvent from the polymer, $\overline{\Delta G}_{unmix}$, plus the strain energy on a molar basis, $\overline{W} = \partial W / \partial n_1$, with n_1 being the number of moles of solvent:

$$\overline{\Delta G}_{SR} = \overline{\Delta G}_{unmix} + \overline{W}. \qquad (3.4)$$

The free energy of unmixing is equal to the negative of the free energy of mixing. The Flory-Huggins relation for free energy of mixing may be used giving:

$$\overline{\Delta G}_{unmix} = -\overline{\Delta G}_{mix} = RT[\ln\phi_1 + (1 + x^{-1})(1 - \phi_1) + \chi_1(1 - \phi_1)^2] \qquad (3.5)$$

where

R = gas constant, 8.314 J mole^{-1} K^{-1},

T = temperature, K,

ϕ_1 = volume fraction solvent,

x = number of units in the polymer chain,

χ_1 = Chi parameter.

The strain energy over the volume of the material is defined as

$$W = \int_{V_T} \tfrac{1}{2}\, \sigma_{ij}\, \epsilon_{ij}\, dV, \tag{3.6}$$

where V_T is the total volume of the material. For a coating under biaxial tension with $\sigma_{33} = 0$, and $\sigma_{11} = \sigma_{22} = \sigma$, and no shear stresses, the strain energy is

$$W = \int_{V_T} \tfrac{1}{2}\, (\sigma_{11}^2 + \sigma_{22}^2 - 2\nu\, \sigma_{11}\sigma_{22})/E\, dV = \sigma^2(1-\nu)V_T/E. \tag{3.7}$$

The stress may be expressed as

$$\sigma = E[\epsilon - \alpha(T - T_0) + \beta(c + c_0)]/(1-\nu). \tag{3.8}$$

To arrive at a relationship for stress in terms of volume fraction, consider an unconstrained coating. Then a relationship developed by Croll may be used:[51]

$$\Delta V = \phi_s V_T - \phi_1 (V_T - \Delta V), \tag{3.9}$$

where ΔV is the volume of solvent removed after solidification and ϕ_s is the volume fraction at solidification. Rearranging eqn. 3.9 gives eqn. 3.10.

$$\Delta V/V_T = (\phi_s - \phi_1)/(1 - \phi_1) = -3\beta(c - c_0) \tag{3.10}$$

For isotropic swelling, this equals 3 times the swelling strain, $\beta(c - c_0)$. This is then substituted into equation 3.8. If $\Delta T = 0$ and $\epsilon = 0$ then

$$\sigma = \frac{E}{3(1-\nu)} \frac{\phi_s - \phi_1}{1 - \phi_1}. \tag{3.11}$$

This expression is plotted in Figures 3.28 and 3.29 with $E = 2$ GPa, $\nu = 0.4$ and $\phi_s = 0.462$ (determined from propagating wave results). These are values typical for a PAA film.

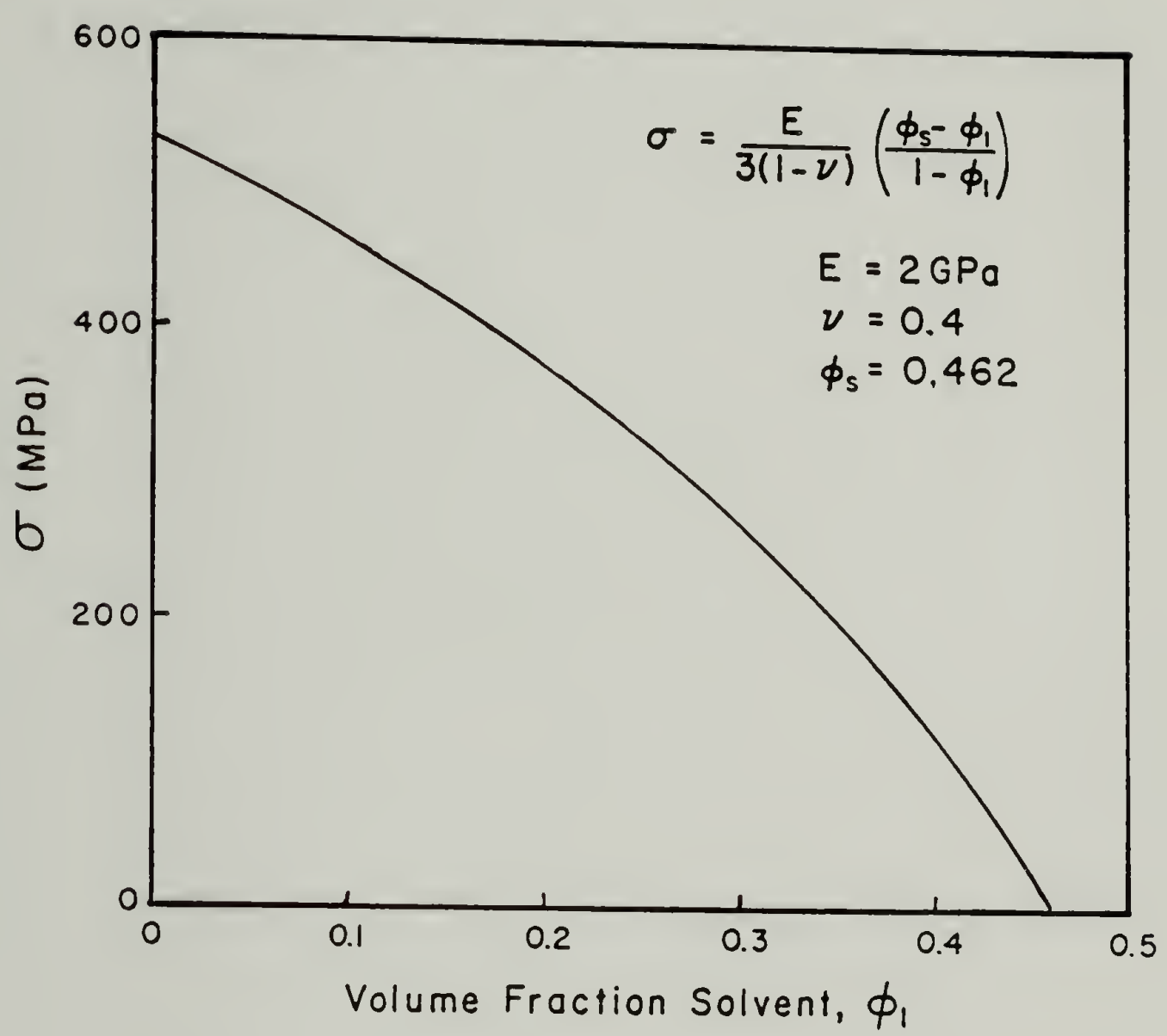

Figure 3.28. Shrinkage stress in a PAA film as a function of volume fraction solvent (from 0 to 0.5).

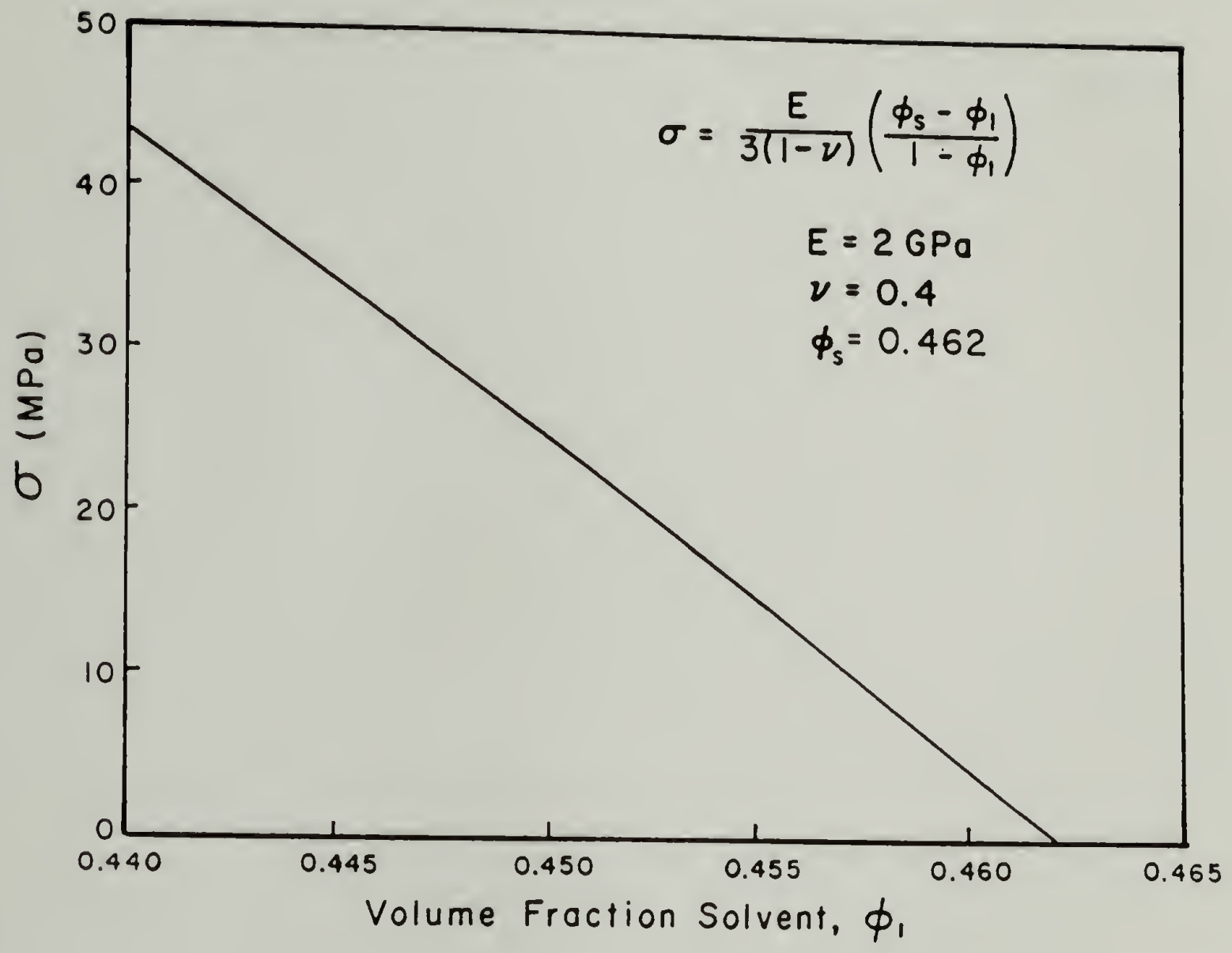

Figure 3.29. Shrinkage stress in a PAA film as a function of volume fraction solvent (from 0.440 to 0.465).

Substituting eqns. 3.8 and 3.10 into 3.7 gives the following expression for strain energy:

$$W = \frac{EV_T}{(1-\nu)}\left[\epsilon^2 + (\alpha\,\Delta T)^2 + \frac{(\phi_s-\phi_1)^2}{9(1-\phi_1)^2} - 2\left[\epsilon\alpha\,\Delta T - \frac{(\epsilon - \alpha\,\Delta T)(\phi_s-\phi_1)}{3(1-\phi_1)}\right]\right] \tag{3.12}$$

Then $\overline{W}$ may be found using the chain rule (eqn. 3.13).

$$\overline{W} = \partial W/\partial n_1 = (\partial W/\partial\phi_1)(\partial\phi_1/\partial n_1). \tag{3.13}$$

The volume fraction of solvent may be defined as: $\phi_1 = 1 - \phi_2$. Then $1/(1-\phi_1) = 1 + n_1\overline{V}_1/V_2$, where ϕ_2 = volume fraction polymer, $\overline{V}_1$ = molar volume of the solvent and V_2 = volume of polymer. This assumes additivity of the volumes, $V_T = V_1 + V_2$. The derivative of ϕ_1 with respect to n_1 may be written as

$$\frac{\partial\phi_1}{\partial n_1} = \frac{\overline{V}_1}{V_2}(1-\phi_1)^2. \tag{3.14}$$

Taking the derivative of eqn. 3.12 with respect to ϕ_1 and multiplying by eqn. 3.15 gives eqn. 3.15.

$$\overline{W} = \frac{E\overline{V}_1}{(1-\nu)}\,\frac{(\phi_s-1)}{(1-\phi_1)}\left[\frac{2(\phi_s-\phi_1)}{9(1-\phi_1)} - \frac{2(\alpha\,\Delta T-\epsilon)}{3}\right] \tag{3.15}$$

At equilibrium, $\overline{\Delta G_{mix}} - \overline{W} = 0$. To demonstrate how equilibrium shifts with changing temperature and concentration the function $\overline{\Delta G_{mix}} - \overline{W}$ is plotted versus ϕ_1. For the PAA/NMP system studied the material parameters are:

$E = 2$ GPa,

$\nu = 0.4$,

$\phi_s = 0.462$ (experimentally measured),

$\alpha = 2.5 \times 10^{-5} \circ C^{-1}$,

$\overline{V}_1 = 9.649 \times 10^{-5}\ m^3\ mole^{-1}$ (for NMP).

Figures 3.30 and 3.31 show plots of this function at 85° C for $\chi_1 = 0$ and 0.5 respectively for $\Delta T = 0$ and 20° C, and $\epsilon = 0$, -0.0032, -0.006 and -0.01. These demonstrate that if the temperature is increased or the strain is decreased (lowering the load), the volume fraction of solvent decreases or more solvent is removed. Table 3.2 shows comparison of experimental results from the propagating wave method to those predicted from this analysis. There is good agreement for the initial drying at 85° C, however the analysis does not predict the change in volume fraction for the second condition. This may be attributed to large, nonisotropic deformation behavior of the material during swelling.

Table 3.2. Volume fraction of solvent after processing

	Volume fraction solvent		
		Theory	
condition	Expt.	$\chi_1 = 0$	$\chi_1 = 0.5$
dry at 85° C	0.456	0.456	0.460
manually decrease load (ϵ = -0.006) dry at 85° C	0.375	0.446	0.454

3.5.3 Conclusions

From the various experiments performed, it has been shown that it is necessary to apply an incremental linear elastic approach to these materials. This technique is extremely useful because of the shifting stress-free reference state. Because of the large shrinkage that occurs with solvent removal and imidization, the stress free temperature is continually moved to higher values. It is not simply the highest temperature that the material has experienced.

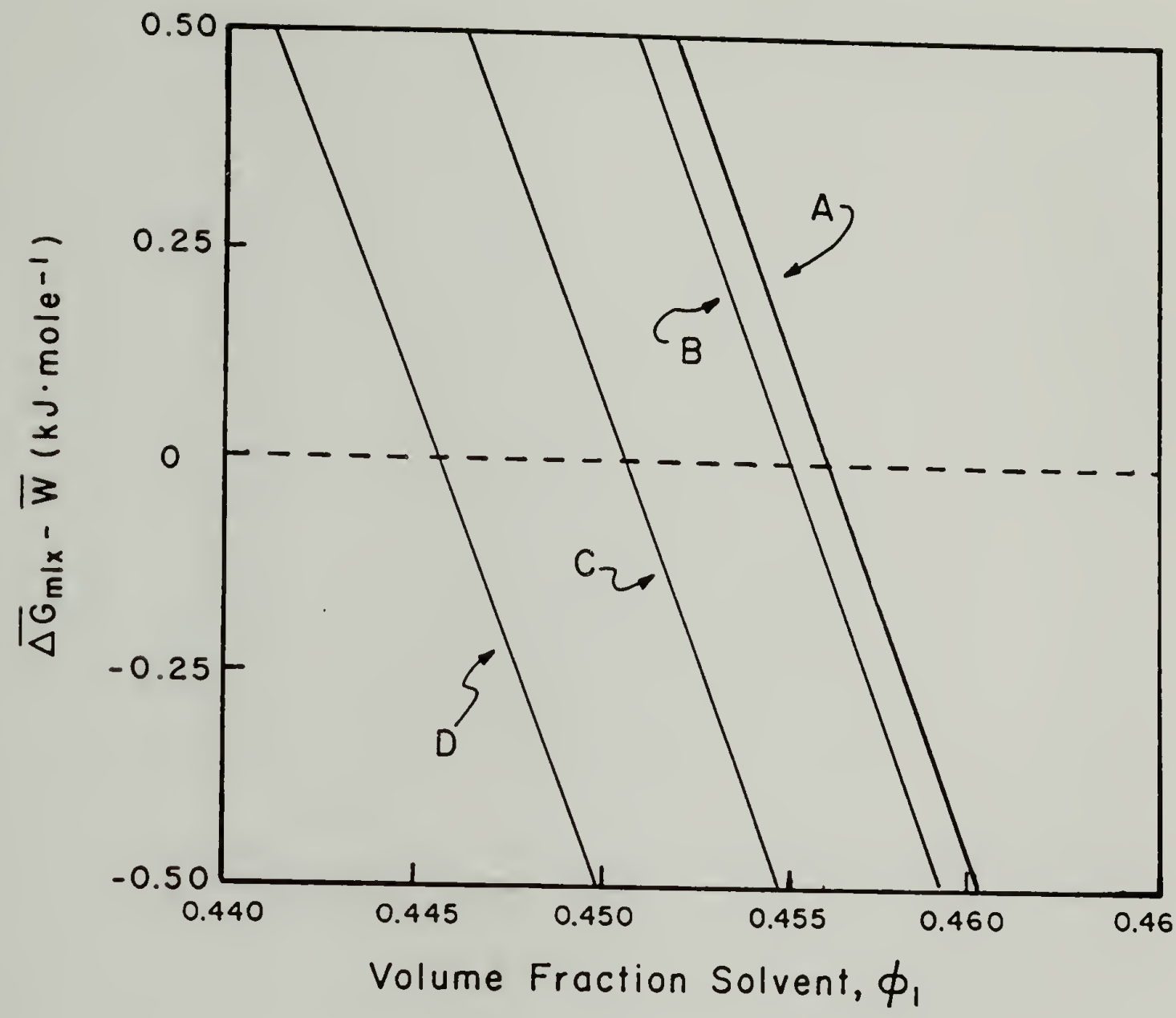

Figure 3.30. Swelling energy as a function of volume fraction solvent for $\chi_1 = 0$ at 85° C; A: $\Delta T = 0, \epsilon = 0$; B: $\Delta T = 20°$ C, $\epsilon = 0$; C: $\Delta T = 0$, $\epsilon = -0.032$; D: $\Delta T = 0, \epsilon = -0.006$.

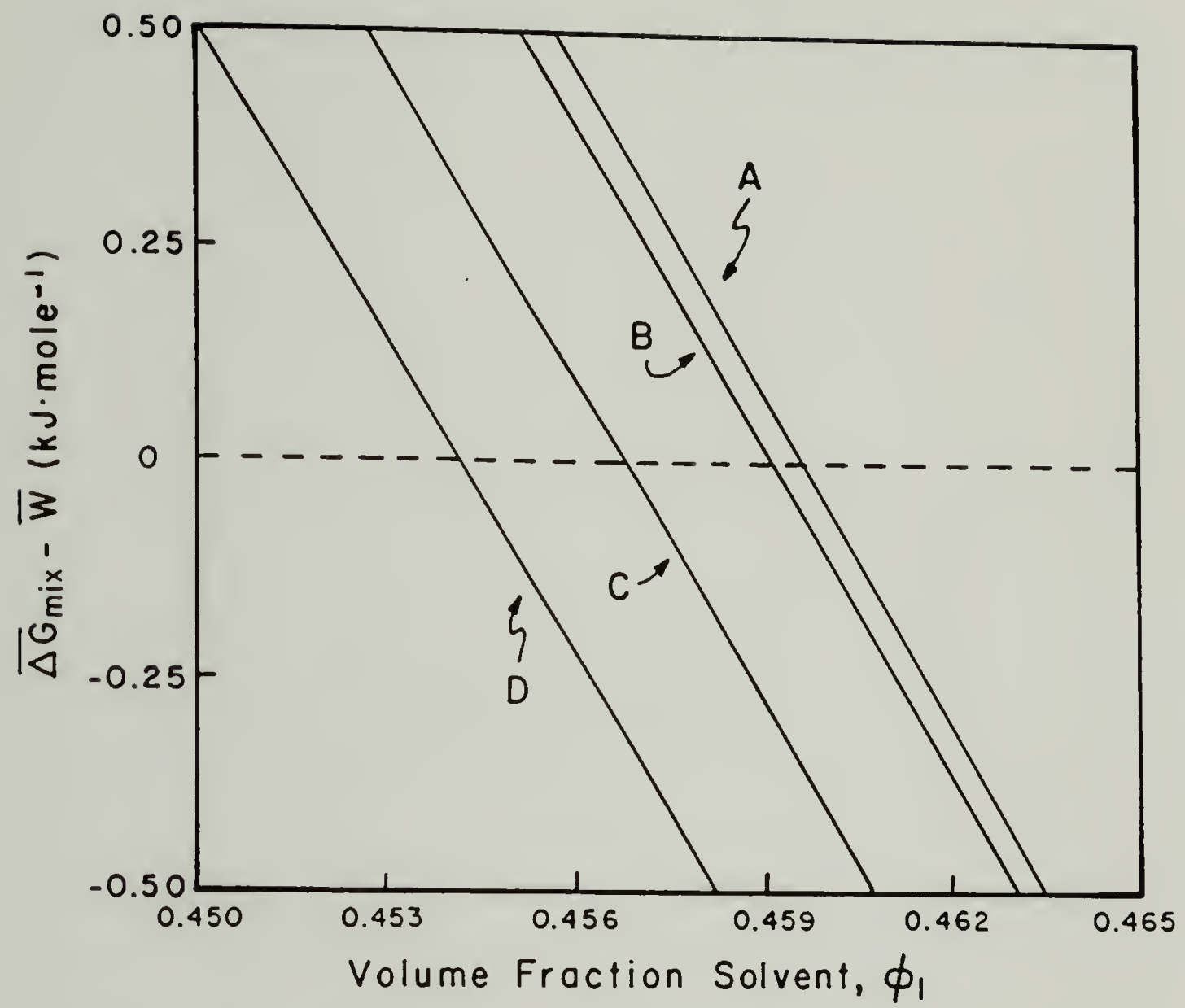

Figure 3.31. Swelling energy as a function of volume fraction solvent for $\chi_1 = 0.5$ at 85° C; A: $\Delta T = 0, \epsilon = 0$; B: $\Delta T = 20°$ C, $\epsilon = 0$; C: $\Delta T = 0$, $\epsilon = -0.032$; D: $\Delta T = 0, \epsilon = -0.006$.

Using this incremental approach the change in stress for a uniaxial experiment may be written as

$$d\sigma = E(T,c)\,[d\epsilon - \alpha(T)dT - \beta(c)dc] \tag{3.16}$$

If the strain and concentration are held constant the change in stress with temperature is related to the product $E\alpha$:

$$(\partial\sigma/\partial T)_{\epsilon,c} = -E\alpha \tag{3.17}$$

Using the cooling curves of the force-temperature data, $E\alpha$ is calculated to be 4.78×10^4 Pa/° C.

In a similar manner the change in stress with concentration at constant strain and temperature is proportional to the product $E\beta$. From the propagating wave results $E\beta$ was found to be 11.45×10^6 Pa/g solvent/g polymer. These values may then be used to predict the change in stress for the first drying cycle of PAA at 85° C using equation 3.16.

CHAPTER 4

MECHANICAL PROPERTIES

4.1 Introduction

To accurately design with thin film or coating materials it is necessary to know their mechanical properties as a function of temperature and concentration. Values for such materials tested in bulk may not apply to thin films of the same material. There are few commercial instruments available to directly measure many of the required properties for coatings, and even these require careful handling of the thin coatings. One of the easier methods is uniaxial tensile tests.

Most researchers characterize the mechanical properties of polyimides using tensile tests or dynamic mechanical experiments.[2,5,6] The physical, thermal, electrical and chemical properties of Kapton materials have also been reported.[4] Typically these properties are only measured at room temperature and as discussed in Chapter 2, it is important to characterize polyimides as a function of temperature and concentration. In this chapter results are presented to attain this objective. In particular the following behavior has been investigated: thermal expansion coefficient as a function of temperature, tensile modulus as function of temperature or solvent concentration, Poisson's ratio and compressive properties.

4.2 Film Preparation

Thin films of polyimide were prepared by spinning either a concentrated solution of polyamic acid or polyimide solution onto glass plates using a Headway Research EC101 photoresist spinner. The polyamic acid solution was a DuPont material, PI5878, based on PMDA-ODA. The soluble polyimide used was Ciba-Geigy's Probimide 293. Typical spinning conditions were 1200 rpm for 30 sec. The following cure schedule was generally applied:

Step 1 85° C for 30 min.

Step 2 150° C for 30 min.

Step 3 220° C for 30 min.

Step 4 400° C for 30 min. under nitrogen

Film thicknesses were measured using either a Tencor Instruments Alpha-Step Surface Profiler or a micrometer with resolution of one micron.

4.3 Thermal Behavior

To investigate the influence of curing temperatures on mechanical properties, spin-coated films of PI5878 dried for thirty minutes at 85° C were exposed to temperatures of approximately 150° C and then tensile properties were determined. These films were exposed to a force-temperature profile as illustrated in Figure 4.1. The starting stress was 2 MPa and three heating cycles were performed in a similar manner as discussed in Chapter 3. After the second cycle, the load was manually decreased to 5.5 MPa and then the sample is reheated to approximately 150° C. The mechanical properties are listed in Table 4.1

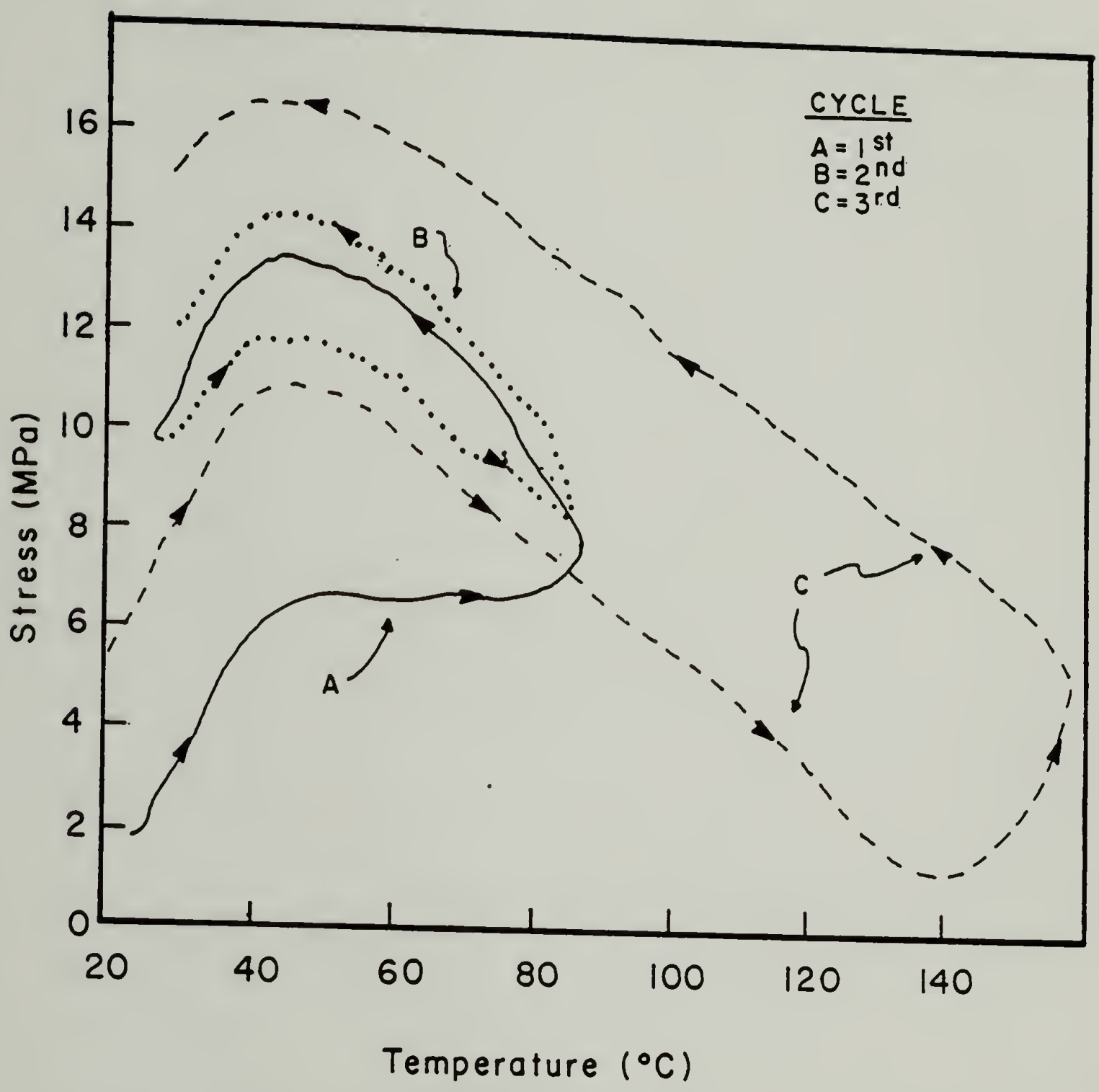

Figure 4.1. Stress versus temperature for a free-standing PAA film dried at 85° C for 30 min.

Table 4.1. Mechanical properties for a thermally treated PAA film

Property	Before Thermal Treatment	After Thermal Treatment
modulus	2.72 ± 0.15	2.99 ± 0.50
tensile strength (MPa)	58 ± 6	90 ± 14

Due to solvent loss and cyclization in the film, an increase in stress of 6 MPa is accompanied by a 10% increase in modulus and a 55% increase in tensile strength. As reported in Chapter 3 the tensile modulus does not change to a great extent after formation of the PAA film. Thermal treatments, however, do greatly alter the tensile strength of the film.

Using the Impulse Method described in the previous chapter, the equilibrium modulus of a Kapton 50H ribbon was obtained. A ribbon of Kapton 50H 77.6 cm x 3 mm x 16 μm was placed in the pulsing apparatus. Data collected over a temperature range of 25 to 375° C permitted the modulus to be calculated at different temperatures and is presented in Figure 4.2. From room temperature to 100° C the modulus decreased slightly from 3.1 to 2.8 GPa and then continually decreases to 1 GPa as the temperature was increased to 280° C. At 375° C the sample began to degrade and therefore the value for E_{eq} should be discarded. In comparison, reported moduli for a 25 μm Kapton film at 23 and 200° C are 3.0 and 1.86 GPa respectively.[4]

The thermal expansion coefficient was also obtained for films cured on glass plates using a Perkin-Elmer TMA-1. The PAA solution was spin-coated onto glass plates and then heated on a hot plate for 30 min. at 85° C, 30 min. at 150° C, and 30 min. at 220° C. The thermal expansion of these films with temperature is shown in Figure 4.3 compared to that of 30H Kapton film.

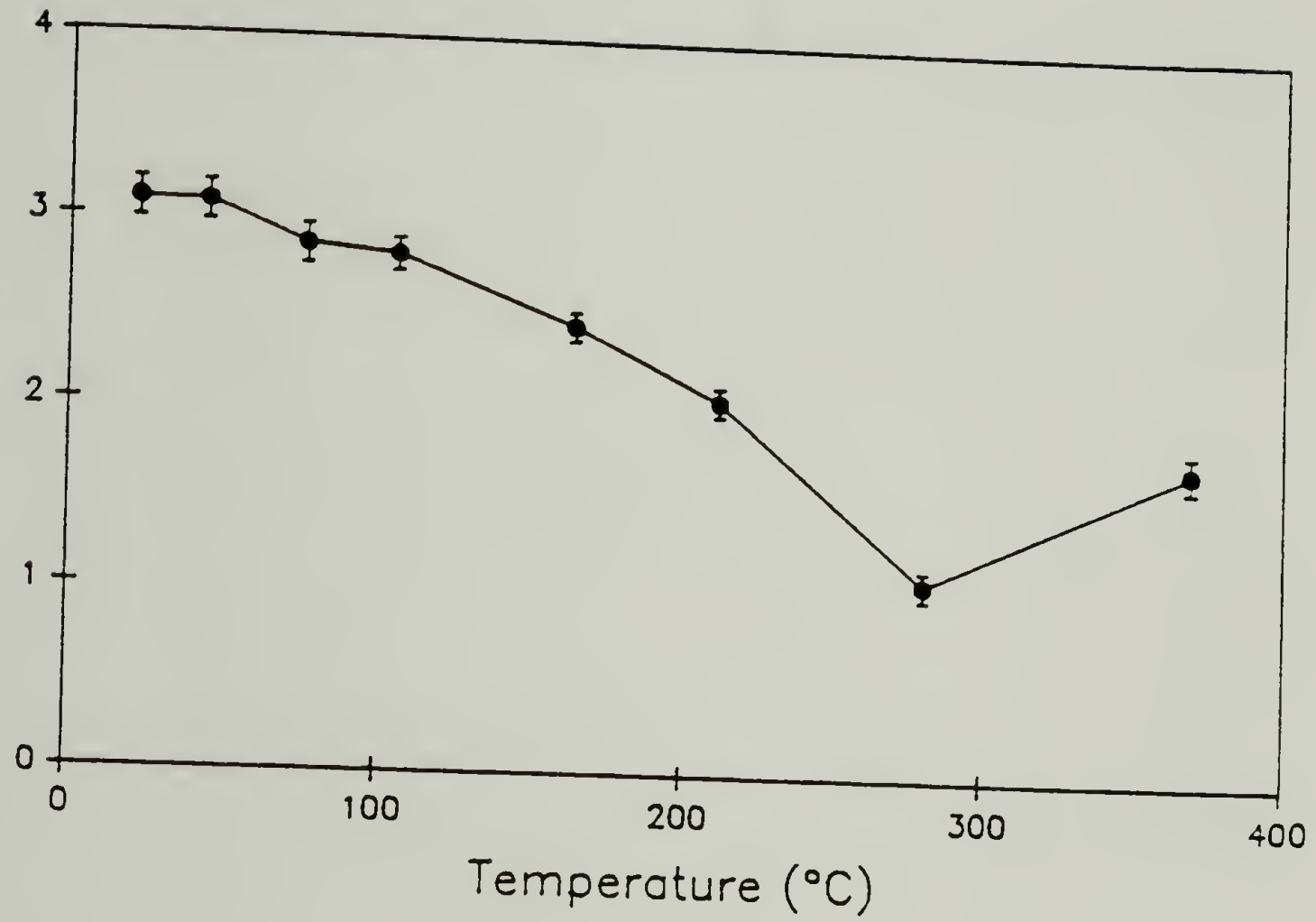

Figure 4.2. Apparent equilibrium modulus for Kapton ribbon as a function of temperature.

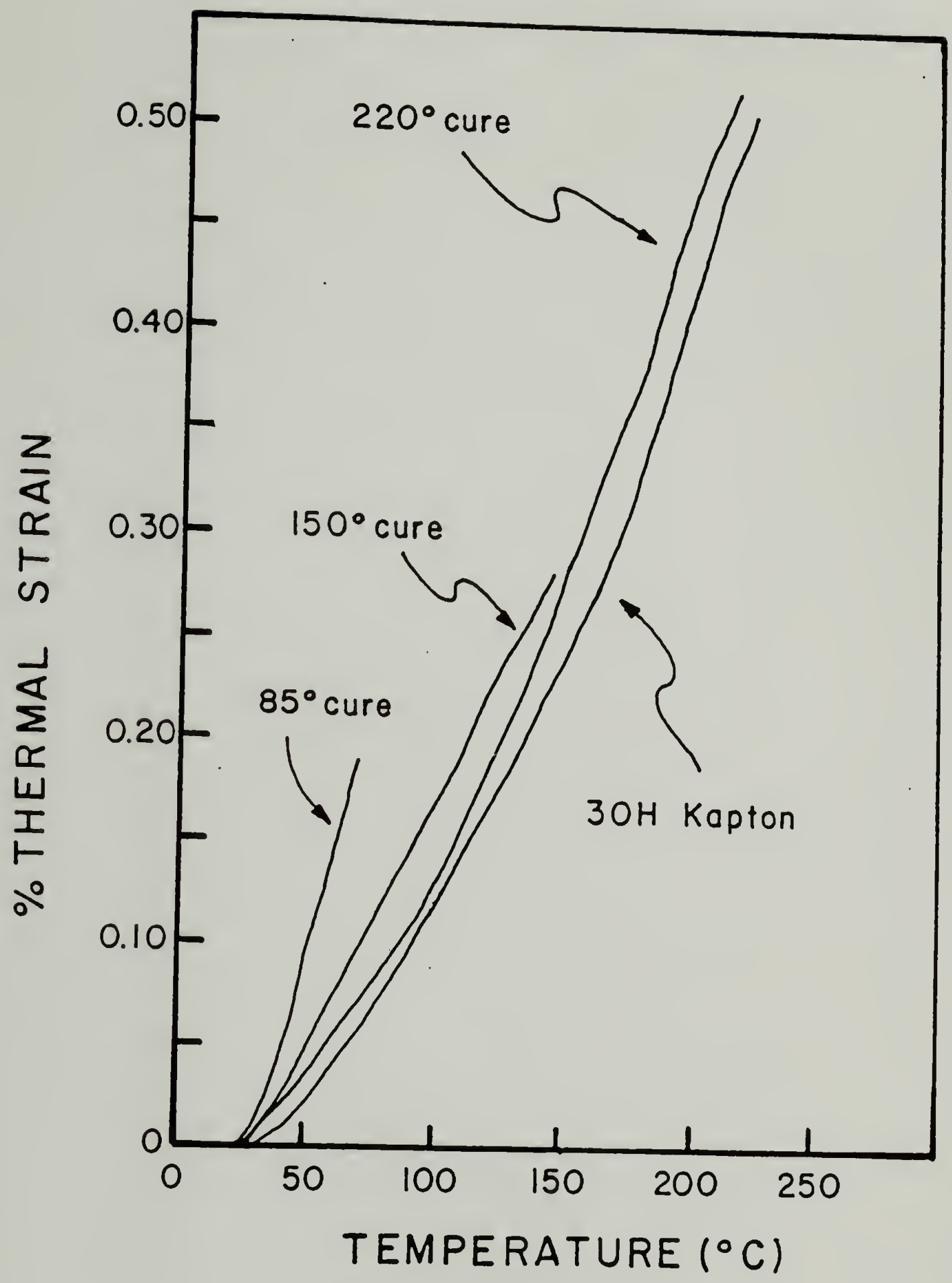

Figure 4.3. Thermal expansion as a function of temperature for PI5878 films after 85° , 150° and 220° C cure stages and for a 30H Kapton film.

Table 4.2 compares expansion coefficients calculated from this data over three temperature intervals. (The error for the thermal expansion coefficient is ±5%.)

Table 4.2. Thermal expansion coefficients of PI films

Sample	T interval (° C)	$\alpha \times 10^5$ (cm/cm/° C)
85° C cure	20 - 85	4.87
150° C cure	20 - 85	2.42
	85 - 150	2.32
220° C cure	20 - 85	1.85
	85 - 150	2.79
	150 - 220	3.81
30H Kapton	20 - 85	1.84
	85 - 150	2.55
	150 - 220	3.80

After heat treating at 220° C the PI has thermal expansion behavior identical to that of the fully cured PI, 30H Kapton. The PAA film, 85° C cured sample, has a thermal expansion coefficient about twice that of the 150° C cured material, which is already partially imidized. If these results are compared to values in Table 4.1 it is probable that the change is due to loss of solvent or morphological changes rather than imidization. Over this temperature range the thermal expansion coefficient is not independent of temperature. The change with temperature may be incorporated into constitutive relations using an incremental elastic approach.

4.4 Tensile Behavior in Liquid Environments

4.4.1 Experimental

The Tensilon Tester was adapted with a stainless steel cylinder on top of a piston with two quad-ring seals to form a solvent environment for the sample (see Figures 4.4 and 4.5). This allowed tensile tests to be performed in various liquid environments such as water, methanol, acetone and N-methylpyrrolidinone. For safety precautions, this tester is located inside a laboratory fume hood.

Tensile tests were performed on various thin films (15 μm in thickness) by first mounting the samples on manila tabs. Windows, 8 cm x 1 cm, were cut into manila sheets, 10 cm x 1.5 cm. The thin film sample was placed on top of this opening and then glued in place with a short manila tab using Devcon 5 min. epoxy. After drying the samples overnight in a vacuum oven at room temperature, the samples were placed into the tensile tester, gripped and then the window frames were cut off prior to testing.

4.4.2 Results

The effect of water on the modulus of Kapton-H was determined as a function of exposure time to water. Samples of Kapton (3 mil $\approx$ 76 μm) were placed in the tensile tester equipped with a solvent bath. All tests were performed while the sample was in the liquid environment, thus a buoyancy correction for the clamps was needed. Results are shown in Figure 4.6 along with percent weight change as a function of exposure time. The mass changes were obtained in separate experiments by weighing by difference.

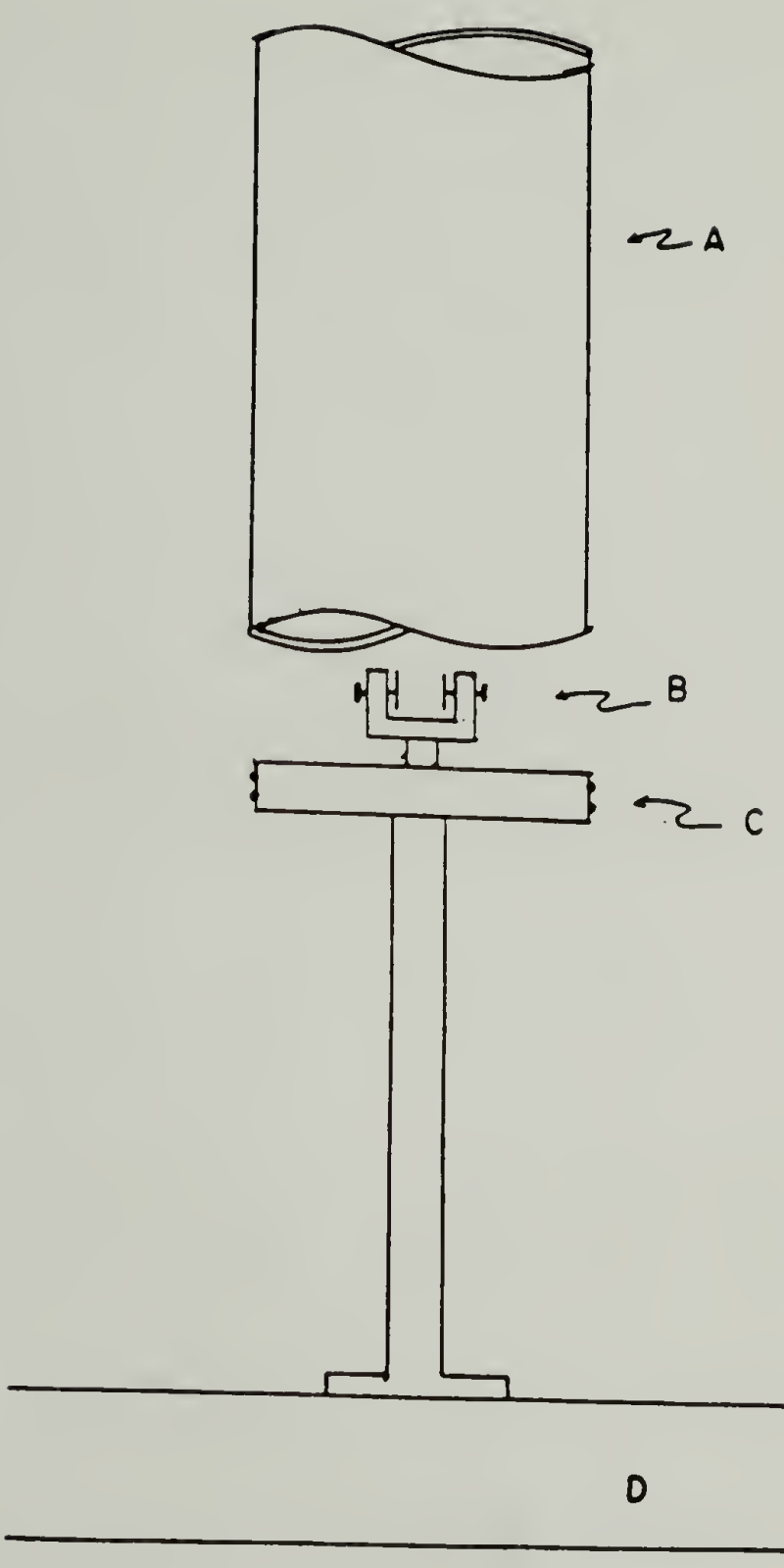

Figure 4.4. Schematic diagram of solvent bath for tensile tester. A = stainless steel cylinder, B = clamp, C = piston with quad-ring seals, D = crossarm of tensile tester.

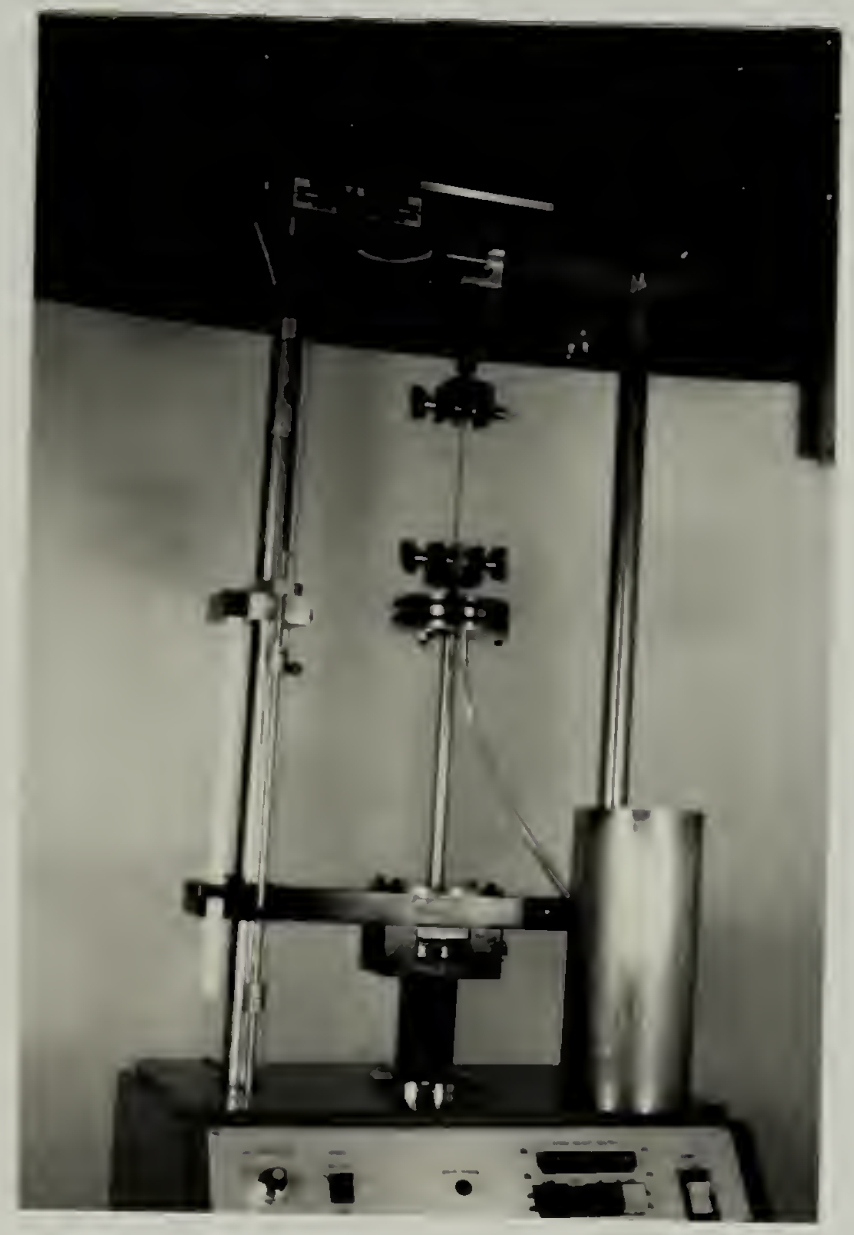

Figure 4.5. Photographs of solvent bath and tensile tester.

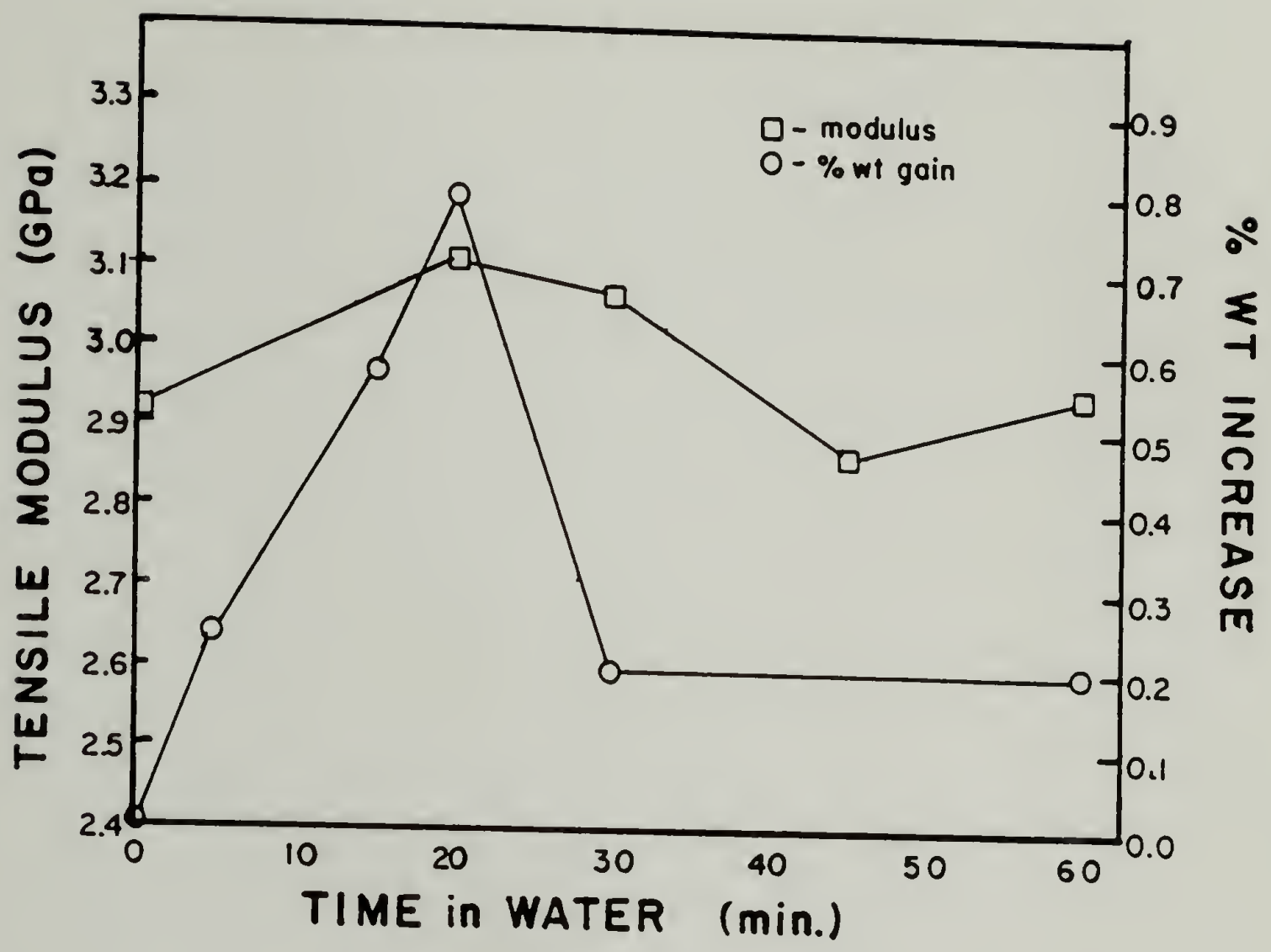

Figure 4.6. Change in modulus and weight gain for a Kapton film as a function of exposure time to water.

These results indicate that after approximately twenty minutes exposure to water, maxima in modulus and percent weight change occur. Due to experimental error in determining the modulus, the changes presented fall just outside error limits. Therefore this increase should be taken with some skepticism. The weight change may be explained by a removal of low molecular weight impurities from the Kapton. As water first enters and swells the material, the weight initially increases but as impurities are removed the weight decreases and approaches a steady value. To check this hypothesis, the 3 mil Kapton film was exposed to water for 20 min. then dried in a vacuum oven to constant weight. A 2% weight decrease was noted.

Other organic liquids (methanol, NMP) were investigated for their effect on the modulus of Kapton films. Samples were exposed to the liquid for 20 min. in the same manner as before. See Figure 4.7. Again an increase in modulus with weight gain is observed. The scales in these figures are exaggerated and the difference in moduli approaches experimental error (± 5%). One possible explanation for the indicated trend is that as the material swells, the internal pressure increases causing an increase in stiffness. Then as impurities are removed the modulus decreases.

The loss in weight due to extraction of impurities by water should be followed by some degree of shrinkage on drying the film. Table 4.3 shows the results of immersing the film one hour in water, applying a stress of approximately 2 MPa, removing the liquid and following the stress with time during air drying. All samples show approximately the same change in stress. Since the impurities would be extracted while the samples were unstressed in the water, this increase in stress is attributed to the removal of water from the sample.

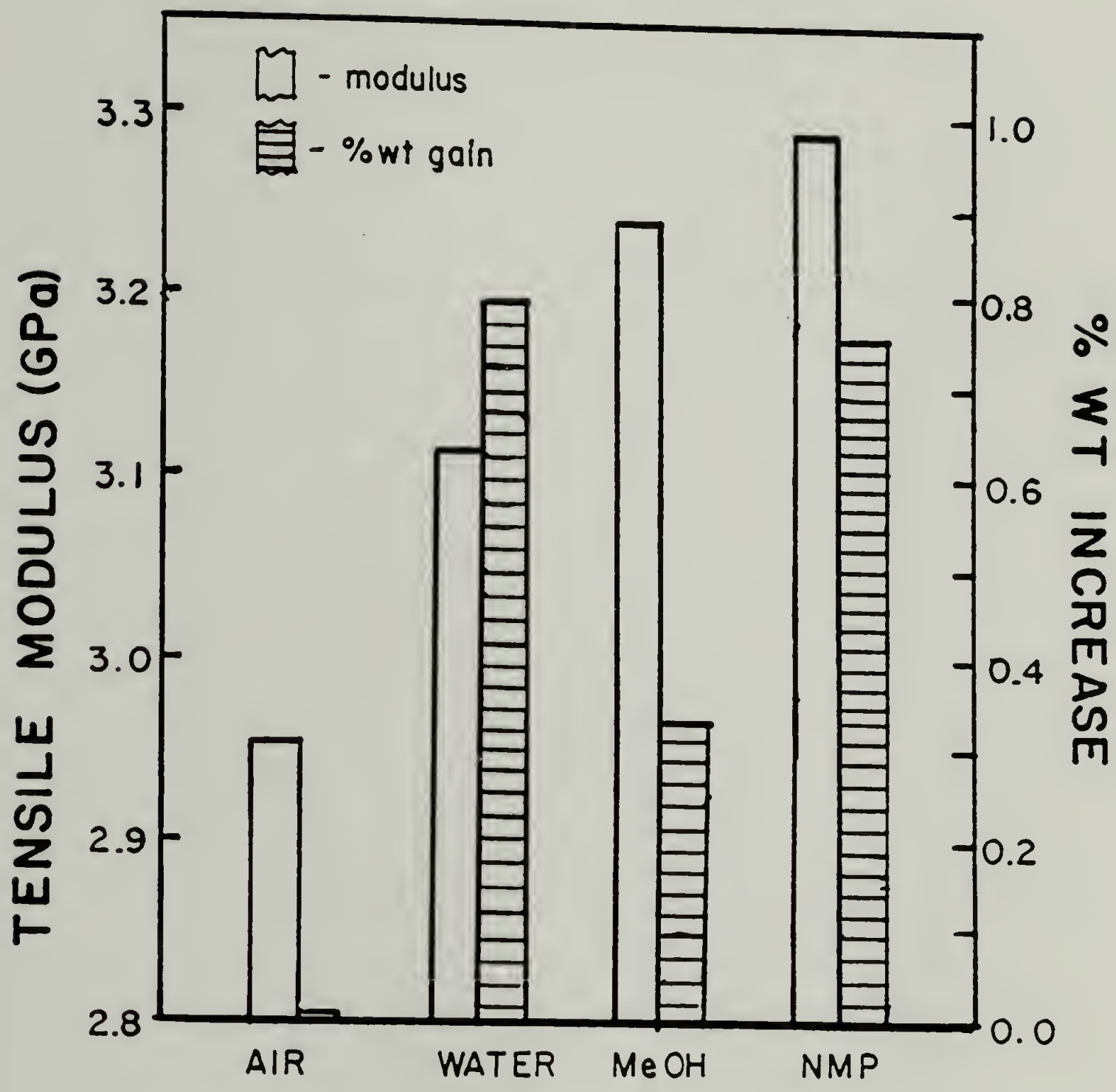

Figure 4.7. Tensile modulus and percent weight increase for a Kapton film immersed for 20 min. in various liquids.

Table 4.3. Shrinkage on drying of wet polyimide films

Sample	% increase in stress
3 mil Kapton	8
0.5 mil Kapton	7
PI cured at 200° C	6

Fully cured, spin-coated films of PI5878 and CG293, approximately 15 μm in thickness, were also tested in different liquid environments. The results are summarized in Table 4.4. These values indicate that the given liquid exposure times have no apparent effect on the tensile properties of the polyimide films. Within experimental error, a tensile modulus of 3 GPa and strength of 100 MPa were obtained for PI5878 regardless of environmental conditions. In comparison, the tensile modulus of Kapton film changes with exposure to liquids as seen above. Furthermore, Kapton has approximately a 2% loss in mass with exposure to water and similar behavior was also observed with PI5878.

Removal of the films from the substrates may result in some variation in the properties. For the PI5878 a slight peel force had to be applied which may deform the material. If the sample is not continuously removed from the plate, marks or lines appear on the film where the peeling was stopped. During mounting, the film removal was stopped 2 cm into the sample to attach the tab. This latter was the site of failure for many of the samples. Film removal for the CG293 coatings did not present such a problem since once the material is cut along the edges of the adhered film, it self-peels off the plate.

Table 4.4. Influence of liquid environments on tensile properties

Material	Test Condition	E (GPa)	σ_B (MPa)	ϵ_B (%)
PI5878	in air	3.14 ± 0.04	101 ± 9	12 ± 2
	30 min. water	3.00 ± 0.17	111 ± 12	29 ± 10
	30 min. NMP	3.19 ± 0.35	135 ± 6	34 ± 7
	30 min. MeOH	2.94 ± 0.24	86 ± 19	32 ± 17
CG293	in air	2.78 ± 0.37	92 ± 10	5 ± 1
	30 min. water	2.62 ± 0.67	81 ± 16	6 ± 2

4.5 Compressive Behavior

The compressive strength of polyimides may be obtained using a hollow fiber test.[74] In this method a hollow fiber is threaded with a thin wire (Figure 4.8) One end of the sample is sealed with epoxy binding the wire to the hollow fiber. The other end of the fiber (~1 cm from the top) is placed between two grooved PMMA tabs and epoxied together. With this arrangement, only the hollow fiber is attached to the PMMA tab and the wire remains free. After allowing the epoxy to set overnight, the sample was placed in an Instron. The top grip clamps the wire extending out of the sample and the bottom grips clamps onto the PMMA tab. As the Instron grips move apart a compressive force is applied to the sample. The force-elongation curve resembles a normal tensile test; however, the forces are now compressive instead of tensile. The presence of the wire inside the hollow fiber prevents buckling of the sample.

This technique was used on PAA hollow fibers. The hollow fibers were obtained by coating rubber thread with a PAA solution as for the propagating wave technique. After drying the coated rubber for several hours at 85° C the rubber support was removed from the coating leaving hollow fibers of PAA. These fibers had a thickness of approximately 20 μm and the resulting compressive strength ranged between 40 and 60 MPa.

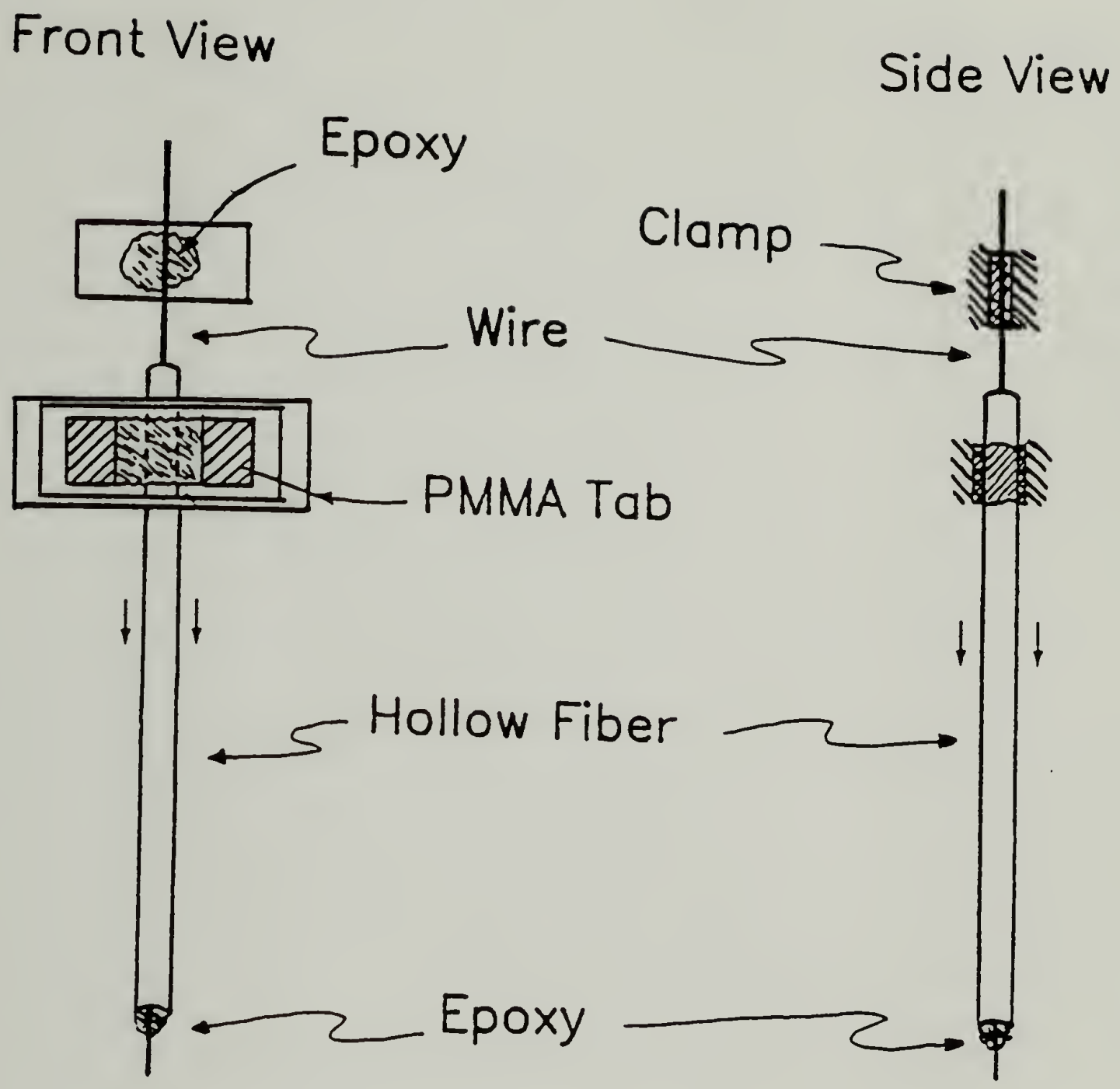

Figure 4.8. Illustration for hollow fiber compression test.

4.6 Poisson's Ratio

4.6.1 Introduction

For a homogeneous, isotropic material, the constitutive relationship between stress and strain is simply

$$\sigma_{ij} = 2G\epsilon_{ij} + \lambda \delta_{ij} \epsilon_{kk}, \tag{4.1}$$

where G and λ are the two independent elastic constants, the Lamé constants.[75,76] Poisson's ratio, ν, is defined as

$$\nu = \frac{\lambda}{2(\lambda + G)} . \tag{4.2}$$

The physical interpretation of this becomes apparent for a uniaxial loaded sample. In this case, Poisson's ratio is the ratio of the transverse strain to the longitudinal strain:

$$\nu = -\epsilon_{22}/\epsilon_{11} = -\epsilon_{33}/\epsilon_{11}. \tag{4.3}$$

This provides the standard method of obtaining ν for relatively large samples.[77] Poisson's ratio may also be determined for an isotropic material by measuring any two elastic constants which can be related to ν, such as E and G where ν = (E/2G) - 1.

These methods are adequate for large samples but are difficult to apply to thin films. The only elastic constant that can be reliably measured for thin films is the tensile modulus, E. As discussed in Chapter 2, the value of Poisson's ratio can dramatically alter the stress state in constrained coatings. This demonstrates the importance of a reliable method of characterizing Poisson's ratio.

A pressure technique was developed to obtain Poisson's ratio for thin films. If a sample is held at constant length (strain) in the 1-direction and a hydrostatic

pressure is applied, the stresses are then written using an incremental approach as:

$$d\sigma_{11} = d\sigma_{applied} - dP, \tag{4.4}$$

$$d\sigma_{22} = d\sigma_{33} = - dP. \tag{4.5}$$

The stress-strain relation in the 1-direction is

$$Ed\epsilon_{11} = d\sigma_{11} - \nu\ (d\sigma_{22} - d\sigma_{33}). \tag{4.6}$$

Substituting eqns. 4.2 and 4.3 into eqn. 4.4 gives

$$Ed\epsilon_{11} = d\sigma_{applied} - dP + 2\nu\ dP. \tag{4.7}$$

Since the sample is held at constant length $d\epsilon_{11} = 0$, then

$$0 = d\sigma_{applied} - dP + 2\nu\ dP, \text{ at constant strain, } \epsilon_{11}. \tag{4.8}$$

Rearranging

$$d\sigma_{applied}/dP = 1 - 2\nu. \tag{4.9}$$

By following the change in stress with pressure, Poisson's ratio is obtained. The applied stress is used rather than σ_{11} since the load cell for the instrument is within the pressure vessel and only measures $\sigma_{applied}$.

4.6.2 Experimental

A High Pressure Gas Dilatometer by Farris Instruments was used to measure the stress as a function of pressure. This instrument allows a uniaxial tension superimposed with a hydrostatic pressure to be applied to a sample. The basic design of this instrument has been described previously by Farris.[78] To attain the sensitivity needed for use with films, a 25 lb load cell was used. Figures 4.9 A and B picture this instrument. Compressed pre-purified nitrogen gas was used to pressurized the system. A thin film sample is placed in the instrument and an initial strain was applied to the film. Before testing, the stress was

A

B

Figure 4.9. Photographs of dilatometer and samples. A - Top plate removed showing location of load cell. B - dilatometer positioned in Instron for testing.

allowed to relax to a constant value. Both the uniaxial load and pressure are measured independently. From the slope of the stress-pressure trace, ν is calculated. An error analysis of this method gives a 10% error. This large error results from the 7% error in measuring the area of the sample. Each experiment was repeated 5 times to give a statistical average for ν with a standard deviation of $\pm$ 2%.

4.6.3 Results

Using a high pressure gas dilatometer, the Poisson's ratio of films was obtained. With this technique the change in load on a sample is measured as a function of superimposed pressure. The response for the 25 lb. load cell is presented in Figure 4.10. This was used as a baseline correction for all the data. As a check of the technique a natural rubber sheet was tested (as shown in Figure 4.11). The slope of the stress pressure trace from 3 to 7 MPa is approximately zero giving Poisson's ratio of 0.5. The stress response from 0 to 3 MPa may be due to the collapse of voids in the rubber.

This method was then used to determine the Poisson's ratio of several polyimide films (Figures 4.12 and 4.13). At about 1% strain, Poisson's ratio for a 76 μm Kapton film and a fully cured PI5878 film was determined to be approximately 0.34. The Poisson's ratio for a 25 μm Kapton film at 7-10% strain has been reported to be 0.34.[4] The diffusion of nitrogen gas into the polyimide is assumed to have a negligible effect on the stress.

By increasing the strain on the PI5878 sample the Poisson's ratio increased to 0.48 at 3.8% strain (Figure 4.14). This supports earlier results on PI5878 where a logarithmic based Poisson's number was measured to be 0.48 at strains

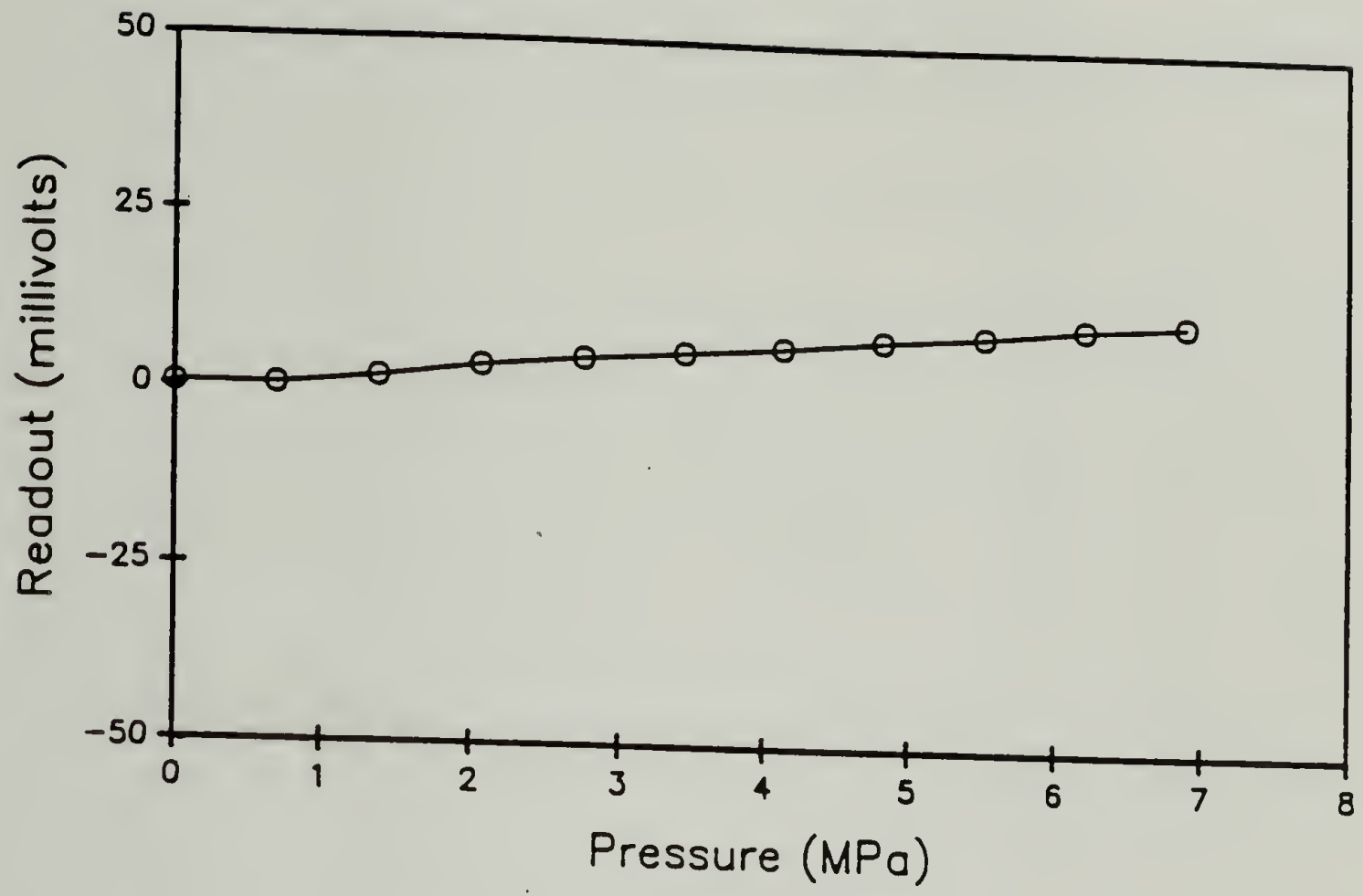

Figure 4.10. Response of 25 lb. load cell to pressure.

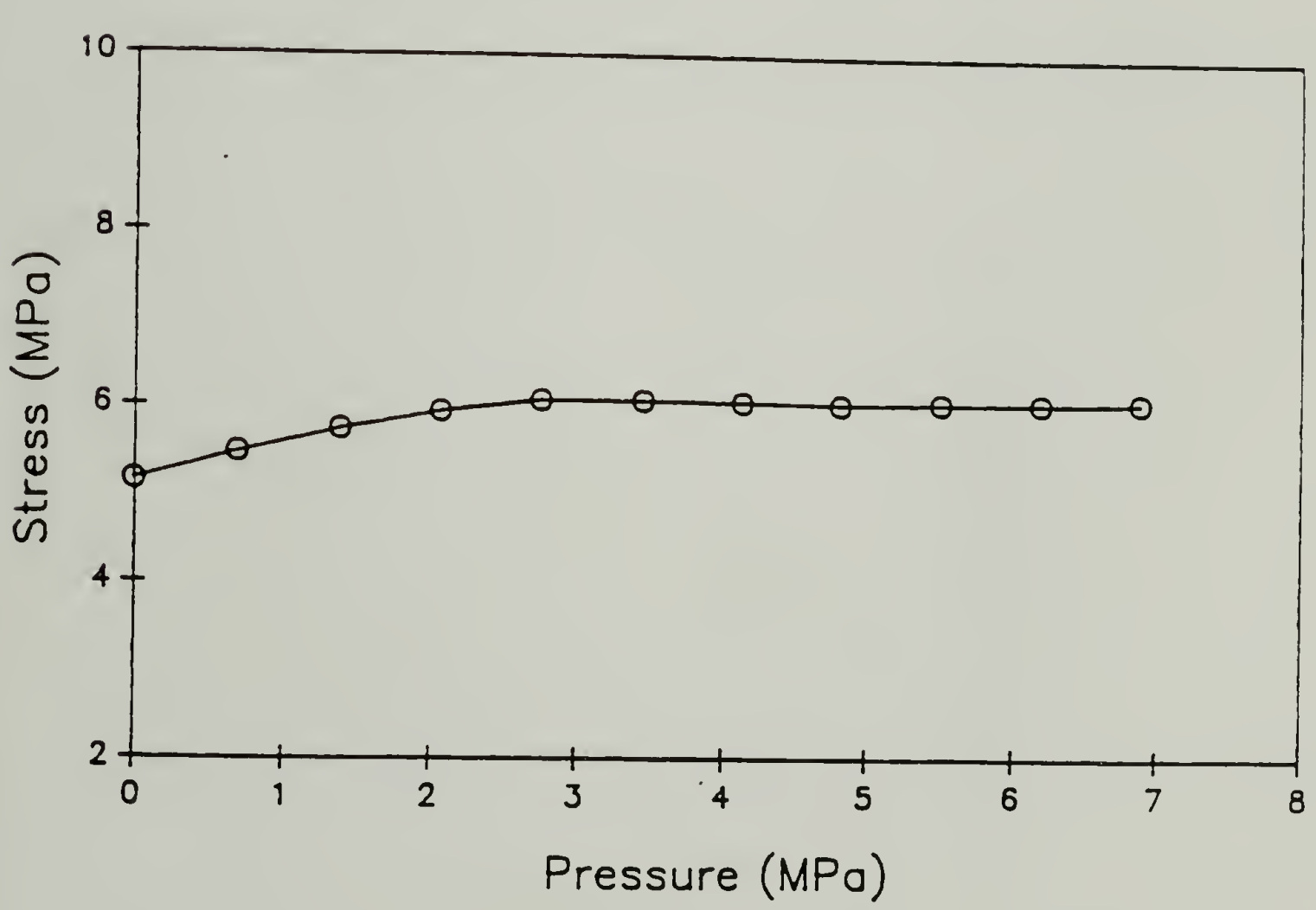

Figure 4.11. Stress versus pressure for natural rubber.

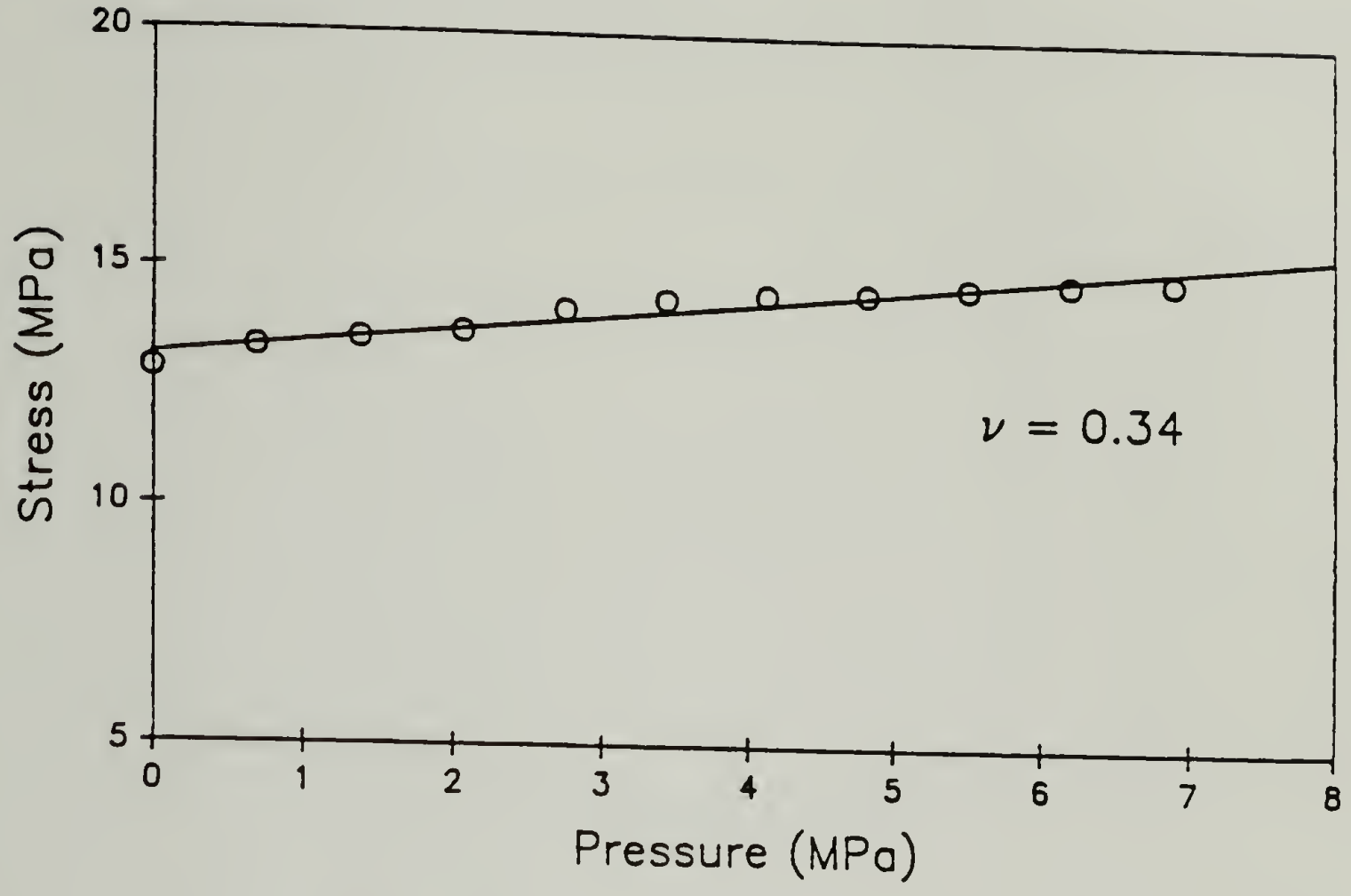

Figure 4.12. Stress versus pressure for Kapton film.

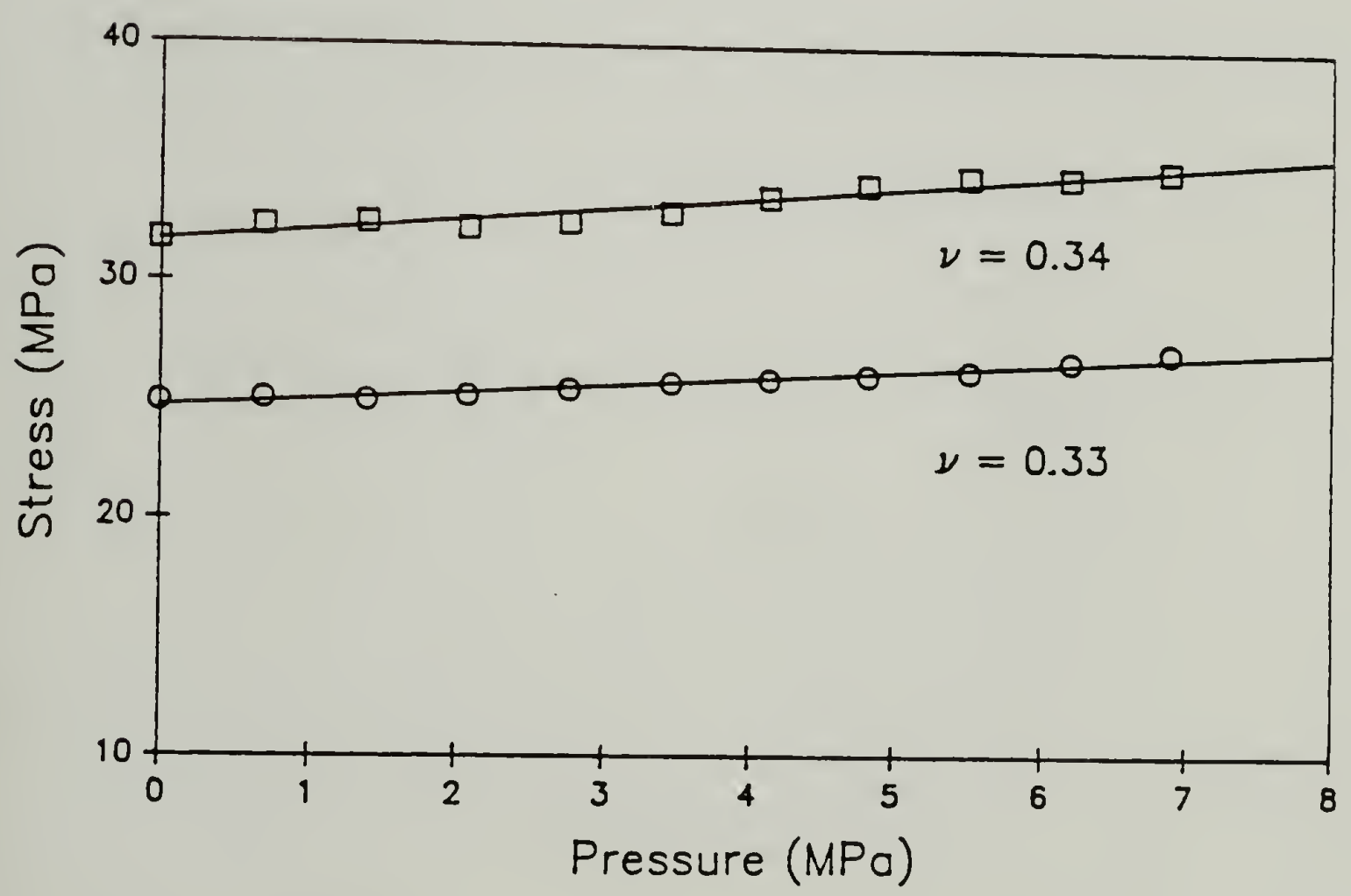

Figure 4.13. Stress versus pressure for fully cured PI5878.

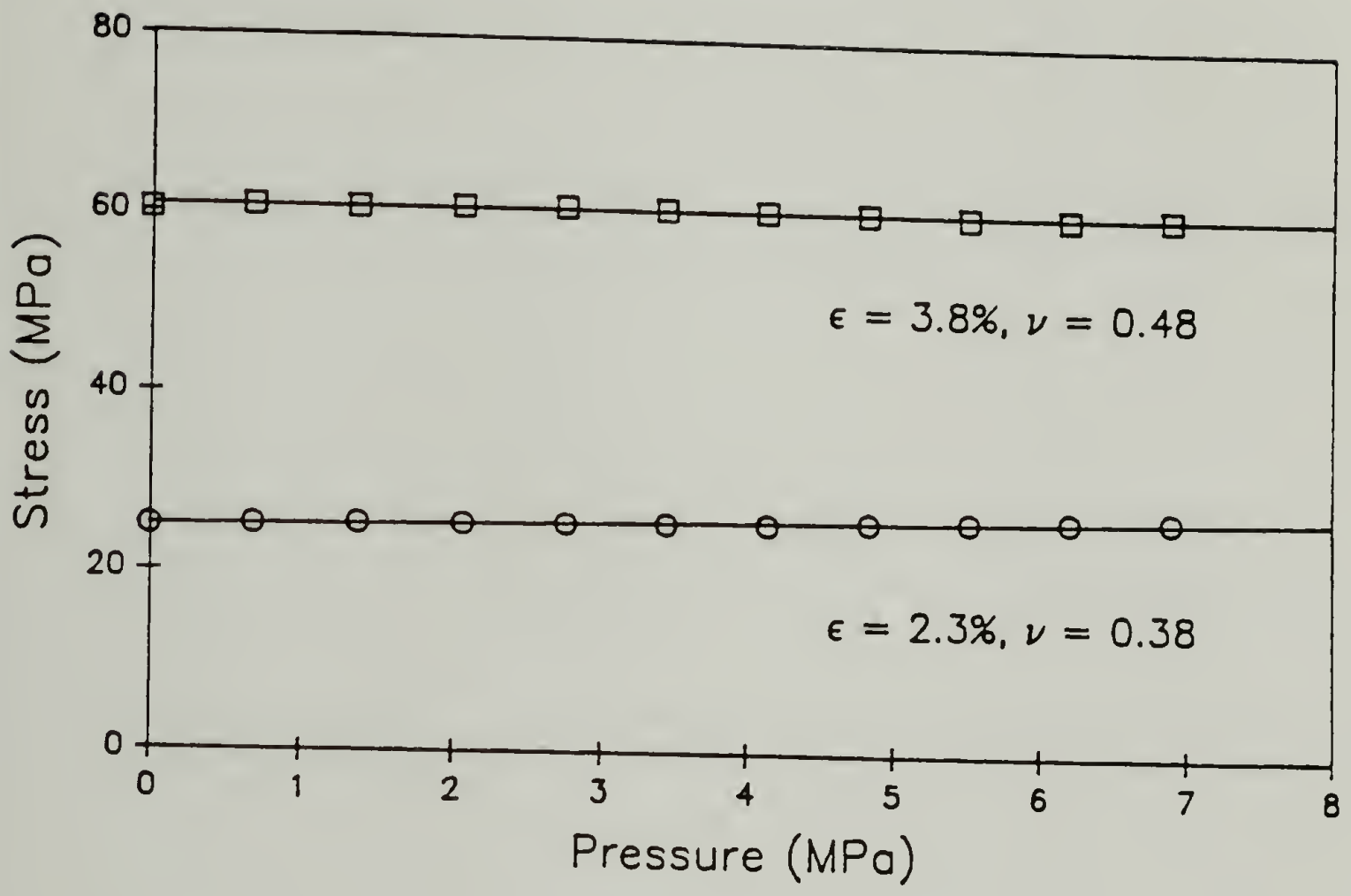

Figure 4.14. Stress versus pressure for fully cured PI5878 films at 2.3% and 3.8% strain.

greater than 5%.[79] This value was obtained by measuring dimensional changes of a film due to uniaxial stretching. This change in Poisson's ratio with strain is similar to metals where at low strains $\nu = 1/3$ and as the strain increases, reaching the plastic zone, ν approaches 0.5.[80]

Stress as a function of pressure for PI5878 at different cure stages is presented in Figure 4.15. At the early stages of processing, 85° and 150° C, ν is around 0.41. These values were difficult to obtain probably because of the residual solvent content. After the 220° C cure stage, the Poisson's ratio is 0.25 and 0.34 after 400° C. These results were very reproducible. The changes in Poisson's ratio during curing can have an appreciable effect on the room temperature stresses in constrained materials as noted in Chapter 2.

The analysis presented for ν is applicable for isotropic materials. For anisotropic materials, this technique provides information on the combinations of these parameters. For an anisotropic material with orthotropic symmetry, the stress-strain relation may be written as:[81]

$$\begin{bmatrix} \epsilon_{11} \\ \epsilon_{22} \\ \epsilon_{33} \\ \epsilon_{12} \\ \epsilon_{13} \\ \epsilon_{23} \end{bmatrix} = \begin{bmatrix} 1/E_{11} & -\nu_{12}/E_{11} & -\nu_{13}/E_{11} & 0 & 0 & 0 \\ -\nu_{12}/E_{22} & 1/E_{22} & -\nu_{23}/E_{22} & 0 & 0 & 0 \\ -\nu_{13}/E_{33} & -\nu_{23}/E_{33} & 1/E_{33} & 0 & 0 & 0 \\ 0 & 0 & 0 & 1/G_4 & 0 & 0 \\ 0 & 0 & 0 & 0 & 1/G_5 & 0 \\ 0 & 0 & 0 & 0 & 0 & 1/G_6 \end{bmatrix} \begin{bmatrix} \sigma_{11} \\ \sigma_{22} \\ \sigma_{33} \\ \sigma_{12} \\ \sigma_{13} \\ \sigma_{23} \end{bmatrix} \tag{4.10}$$

Then using an analysis similar to that above for an applied stress in the 1-direction with a superimposed pressure, eqn. 4.11 is obtained.

$$(d\sigma_{applied}/dP)_{\epsilon 11} = 1 - (\nu_{12} + \nu_{13}) \tag{4.11}$$

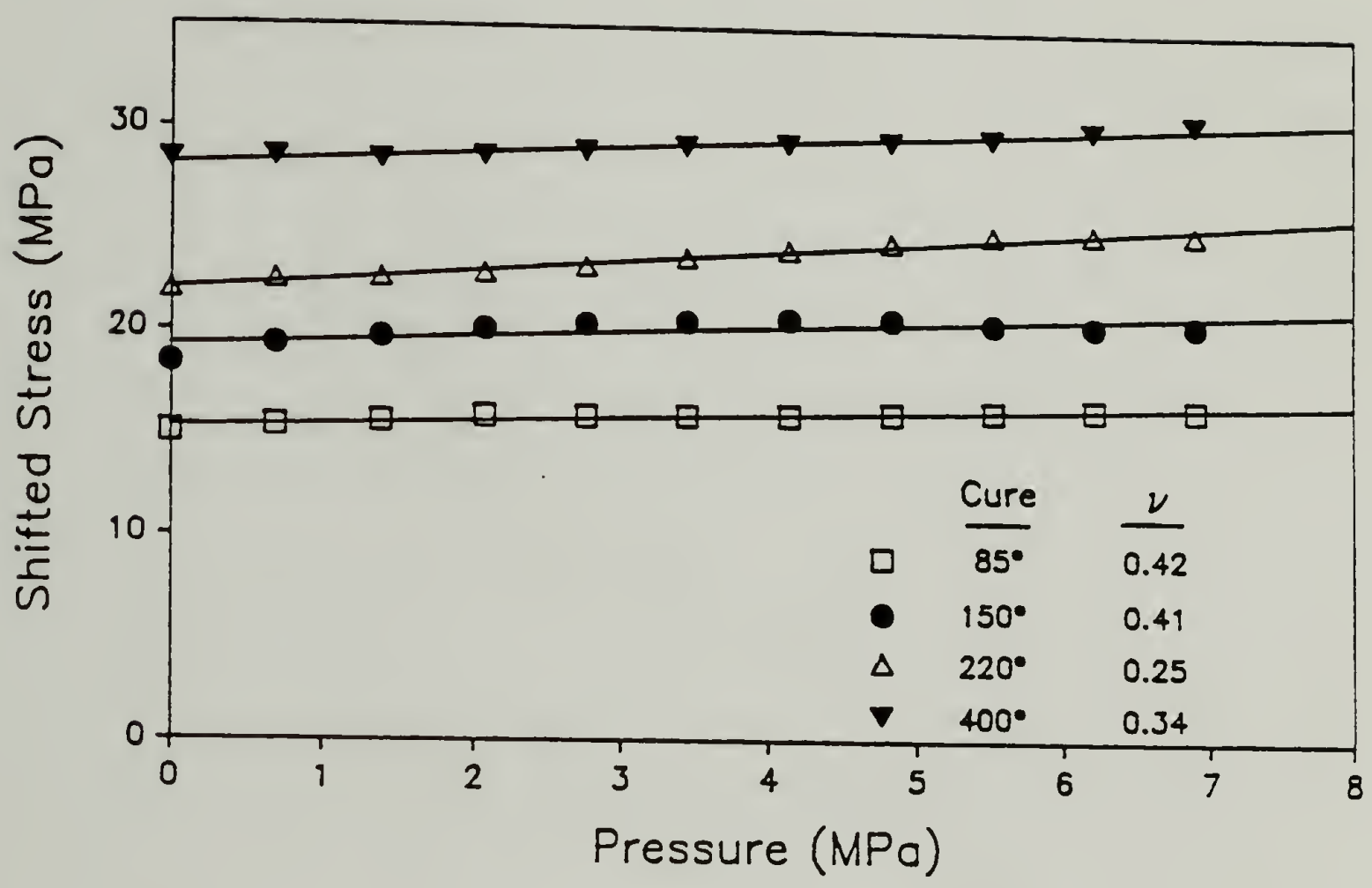

Figure 4.15. Stress versus pressure for PI5878 films after indicated stages of curing. Stress values have been shifted by a constant to make graph legible.

Therefore, the calculated value of Poisson's ratio using eqn. 4.9 gives the averaged value of ν_{12} and ν_{13}. Likewise, when the load is applied in the 2-direction, information is obtained on the combination of ν_{12} and ν_{23}. If the dilatometric test could be performed by applying the stress in three direction, it would be possible to uncouple these expressions. However, for 15 μm films, this becomes impracticable and other approaches must be developed to achieve this goal.

CHAPTER 5

SURFACE ENERGY OF ADHESION

5.1 Introduction

Thin coatings adhered to rigid substrates may be considered to be under plane stress conditions. This signifies that there are no stresses across the interface except at edges. Cuts or cracks in the coating create such free edges. The stresses acting across the interface near these cuts or cracks may then lead to delamination of the coating.

A usage criterion for coatings on substrates is difficult to define. Merely reporting the stiffness of a material or the adhesion strength of a coating does not fully describe the coating. Strong, high modulus films are generally preferred over softer coatings. However, these strong materials can develop large residual stresses that may result in failure of the coating such as delamination or cracking of the film. A reliable assessment of a coating compares the mechanical properties and residual stress to the adhesion of the coating.

An energy balance approach has been successfully used to relate the adhesion of a coating to internal stress.[82-85] Typical experiments involve T-peel or pull-off tests. From these measurements the surface energy of adhesion may be determined, taking into account the effect of residual stress in the film. This stress actually decreases the force needed to remove a coating since it increases the energy of the system. If the stress is sufficiently large compared to the coating dimensions there may be enough energy to crack or self-delaminate the film.[43]

Without any external constraints, the coating can completely delaminate as observed with PI5878 cured at 220° C on glass which was cut along the edges of the glass to create a free edge (Figure 5.1).

A method has been developed that takes advantage of the spontaneous delamination by constraining the extent of debonding. This allows a unique method of measuring the surface energy of adhesion of coatings.

5.2 Analysis

It has been indicated that spontaneous peeling of a coating from its substrate provides a measurement of the surface energy of adhesion.[82,83] A simplified analysis relates the surface energy, γ , to the stress: $\gamma = t_{cr} \sigma_o^2/(2\,E)$, where t_{cr} is the critical thickness required for debonding at a constant residual stress, σ_o, E is the tensile modulus and Poisson's ratio assumed to be 0.5.

Existing methods to measure surface energy require a series of coatings of various thicknesses above and below the critical thickness to assess the surface energy. By inducing an internal geometrical constraint, a method has been developed to measure γ with the condition that $t > t_{cr}$. The constraint is due to a circular hole (radius 'a') cut in the material. If $t > t_{cr}$, the inner circular piece will completely debond while the material on the outer portion of the cut will only partially debond to a radius 'b' (see Figure 5.2). The analysis for the determination of γ for this problem is given below. For a homogeneous, isotropic media the constitutive relation between stress and strain that includes thermal effects can be expressed using indicial notation as

$$E(\epsilon_{ij} - \delta_{ij}\alpha\,\Delta T) = (1+\nu)\sigma_{ij} - \nu\delta_{ij}\sigma_{kk} \qquad (5.1)$$

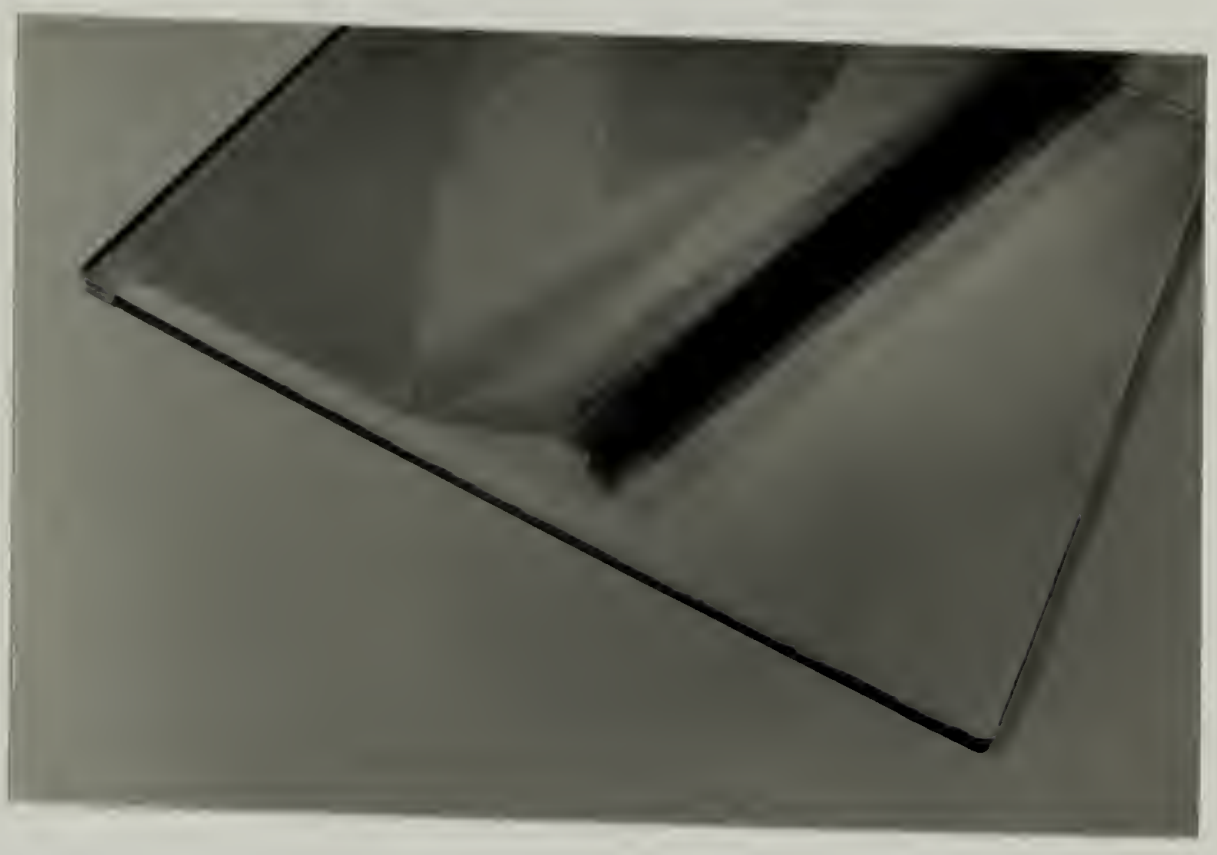

Figure 5.1. Photograph of self-delamination of 200° C cured PI5878 from glass plate due to cuts (free edges) near ends of plate.

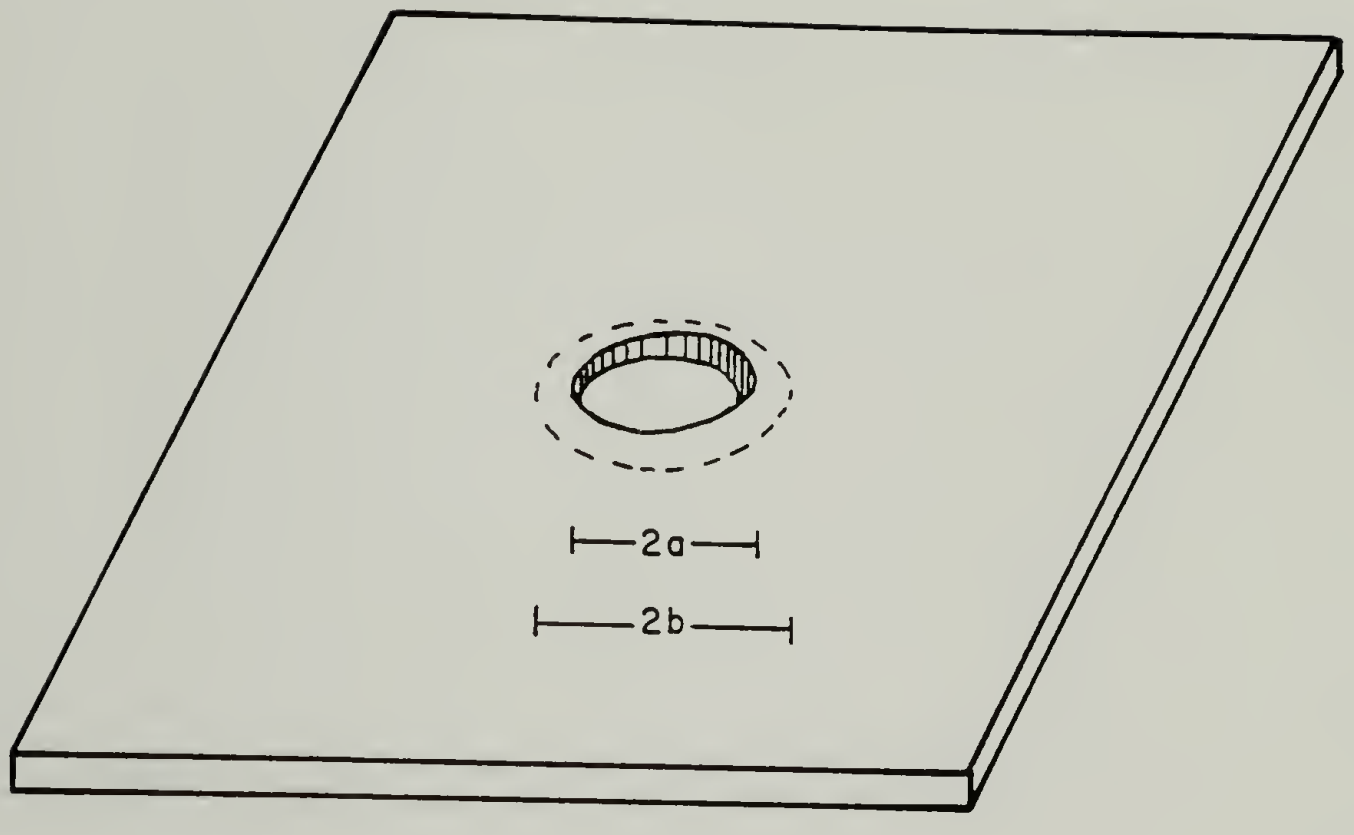

Figure 5.2. Illustration of delamination due to presence of circular cut in a coating on a substrate.

where

σ_{ij} = stress,

ϵ_{ij} = strain,

δ_{ij} = Kronecker delta,

E = tensile modulus,

ν = Poisson's ratio,

α = thermal expansion coefficient,

ΔT = change in temperature.

Similar expressions may be written to include any non-mechanical displacements such as swelling.

For a thin coating on an infinitely flat plate, plane stress conditions may be applied; thus, there are no shear or interfacial stresses acting on the interface ($\sigma_{33} = \sigma_{13} = \sigma_{23} = 0$). Equation 5.1 may then be expanded in cylindrical coordinates as:

$$E(\epsilon_{rr} - \alpha \Delta T) = \sigma_{rr} - \nu \sigma_{\theta\theta}, \tag{5.2a}$$

$$E(\epsilon_{\theta\theta} - \alpha \Delta T) = \sigma_{\theta\theta} - \nu \sigma_{rr}, \tag{5.2b}$$

$$E(\epsilon_{zz} - \alpha \Delta T) = -\nu (\sigma_{rr} + \sigma_{\theta\theta}). \tag{5.2c}$$

Solving eqn. 5.2 for the principal stresses in the plane of the film gives:

$$\sigma_{rr} = [\epsilon_{rr} + \nu \epsilon_{\theta\theta} - \alpha \Delta T(1 + \nu)]E/(1 - \nu^2), \tag{5.3a}$$

$$\sigma_{\theta\theta} = [\epsilon_{\theta\theta} + \nu \epsilon_{rr} - \alpha \Delta T(1 + \nu)]E/(1 - \nu^2). \tag{5.3b}$$

Initially the coating is in uniform tension and there are no displacements in the plane such that $\epsilon_{rr} = \epsilon_{\theta\theta} = 0$. With these conditions eqns. 5.3 become

$$\sigma_{rr} = \sigma_{\theta\theta} = -E \alpha \Delta T/(1 - \nu). \tag{5.4}$$

As described above, when a circular hole of radius 'a' is cut in the film it may partially debond to a radius 'b'. The stress in the coating may be obtained by using the plane stress solution for a hollow cylinder under pressure:

$$u_r = A/r + Br, \tag{5.5}$$

(u_r = radial displacement, A, B = constants).

At r = b, the film remains bonded to the plate, therefore $u_r = 0$. With this boundary condition, on solving for A, u_r can be expressed as

$$u_r = B(r - b^2/r). \tag{5.6}$$

Using this to obtain the strains (ϵ_{rr}, $\epsilon_{\theta\theta}$) and inserting these into eqn. 5.3a gives:

$$\sigma_{rr}' = \frac{E}{(1-\nu^2)} [B(1+b^2/r^2) + \nu B(1- b^2/r^2) - \alpha \Delta T(1+\nu)]. \tag{5.7}$$

where the prime indicates the partially debonded case.

With the other boundary condition, $\sigma_{rr} = 0$ at r = a (free surface), eqn. 5.7 becomes

$$\sigma_{rr}' = \frac{-E\alpha\Delta T b^2(1 - a^2/r^2)}{b^2(1-\nu) + a^2(1+\nu)} \qquad \text{for } a \le r \le b. \tag{5.8}$$

Similarly it can be shown that

$$\sigma_{\theta\theta}' = \frac{-E\alpha\Delta T b^2(1 + a^2/r^2)}{b^2(1-\nu) + a^2(1+\nu)} \qquad \text{for } a \le r \le b. \tag{5.9}$$

The stored energy in a material is defined over a volume element as

$$U = \int_V \tfrac{1}{2}\sigma_{ij}\epsilon_{ij}\, dV \tag{5.10}$$

which for a thin film, neglecting shear stresses becomes

$$U = 1/(2E) \int_0^t \int_0^{2\pi} \int_{r_1}^{r_2} (\sigma_{rr}^2 + \sigma_{\theta\theta}^2 - 2\nu\sigma_{rr}\sigma_{\theta\theta}) r\, dr\, d\theta\, dz. \tag{5.11}$$

For the bonded case in the region from r_1 = a to r_2 = b, the internal energy is found by using eqn. 5.4 in eqn. 5.11:

$$U = \frac{t E \pi (b^2 - a^2)(\alpha \Delta T)^2}{(1-\nu)}. \tag{5.12}$$

For the debonded case between $a \le r \le b$, by using eqns. 5.5 and 5.9 for the stresses, eqn. 5.11 gives the energy as

$$U' = \frac{t\,E\,\pi\,(b^2 - a^2)(\alpha\,\Delta T)^2\,b^2}{b^2(1-\nu) + a^2(1+\nu)}. \tag{5.13}$$

The difference between the two states is equal to the energy required to form two new surfaces over the debonded area:

$$U' - U = -2\gamma\,\pi\,(b^2 - a^2) \tag{5.14}$$

with γ = surface energy of adhesion.

Using eqns. 5.12 and 5.13 in eqn. 5.14 and solving for γ gives:

$$\gamma = \frac{E\,t\,(\alpha\,\Delta T)^2}{2} \quad \frac{a^2(1+\nu)}{b^2(1-\nu)^2 + a^2(1-\nu^2)}. \tag{5.15}$$

Since $\sigma_{rr} = \sigma_{\theta\theta} = -E\,\alpha\,\Delta T/(1-\nu)$ (eqn. 5.4) is the residual stress, σ_o, in the unbonded state, eqn. 5.15 simplifies to

$$\gamma = \frac{\sigma_o^2 \cdot t}{2E} \quad \frac{a^2(1-\nu^2)}{b^2(1-\nu) + a^2(1+\nu)}. \tag{5.16}$$

From this expression the surface energy of adhesion may be determined if the tensile modulus, Poisson's ratio, coating thickness, residual stress in the film and the debonded area are known.

5.3 Discussion

This technique was demonstrated using polyimide coatings on glass. These films were prepared by spin-coating a polyamic acid solution, PAA, [poly (N,N'-bis(phenoxyphenyl)-pyromellitamic acid)] in NMP onto glass plates. The thickness was altered by varying the spinning speeds. The PAA coatings were heat treated at 85° C for 30 min., 150° C for 30 min. and 220° C for 30 min. under nitrogen to remove solvent and thermally imidize the material.

A circular hole of radius 0.7 cm ('a') was cut in a coating of thickness 35 μm. After a 24 hour period the inner circular piece completely delaminated

and the film on the outside of the circle partially debonded to a radius 'b' which for this example is 1.05 cm (see Figure 5.3).

For the PI coating the tensile modulus was determined to be 3 GPa, Poisson's ratio determined to be 0.25 and the residual stress estimated to be 30 MPa.[62] With these values the surface energy was calculated to be 1.68 Nm^{-1} using eqn. 5.16.

To illustrate that this method is independent of hole size, a circle of radius 0.55 cm was used. From the measured delamination (b = 0.8 cm) γ was found to be 1.73 Nm^{-1}.

For comparison, 180° peel tests were performed on these samples. Strips of the 220° C cured material were peeled off the glass in an Instron to obtain peel energies between 0.3 and 1.4 Nm^{-1}. This is good agreement considering the assumed value for σ_o and that it influences peel behavior. However, these values are two orders of magnitude less than adhesive energies for polyimides reported in the literature as determined by a blister method and a T-peel test.[86,87] The literature values were obtained for PI cured at 400° C on silicon wafers while our results were obtained for a 220° C cured PI film on glass. This method for determining the surface energy considers only initial and final states and does not incorporate any energy release rate.

Several other coatings were prepared using the same PAA material except curing steps or thicknesses were varied. A 20 μm coating cured up to 220° C as before showed no signs of delamination with this method. This indicates that the critical thickness for self-peeling lies between 20 and 30 μm. However on applying this technique to a 20 μm film cured only at 85° C for 30 min., slight debonding was observed and the surface energy was determined to 0.52 Nm^{-1}. In comparison thin films cured up to 400° C had a final thickness of 15 μm and

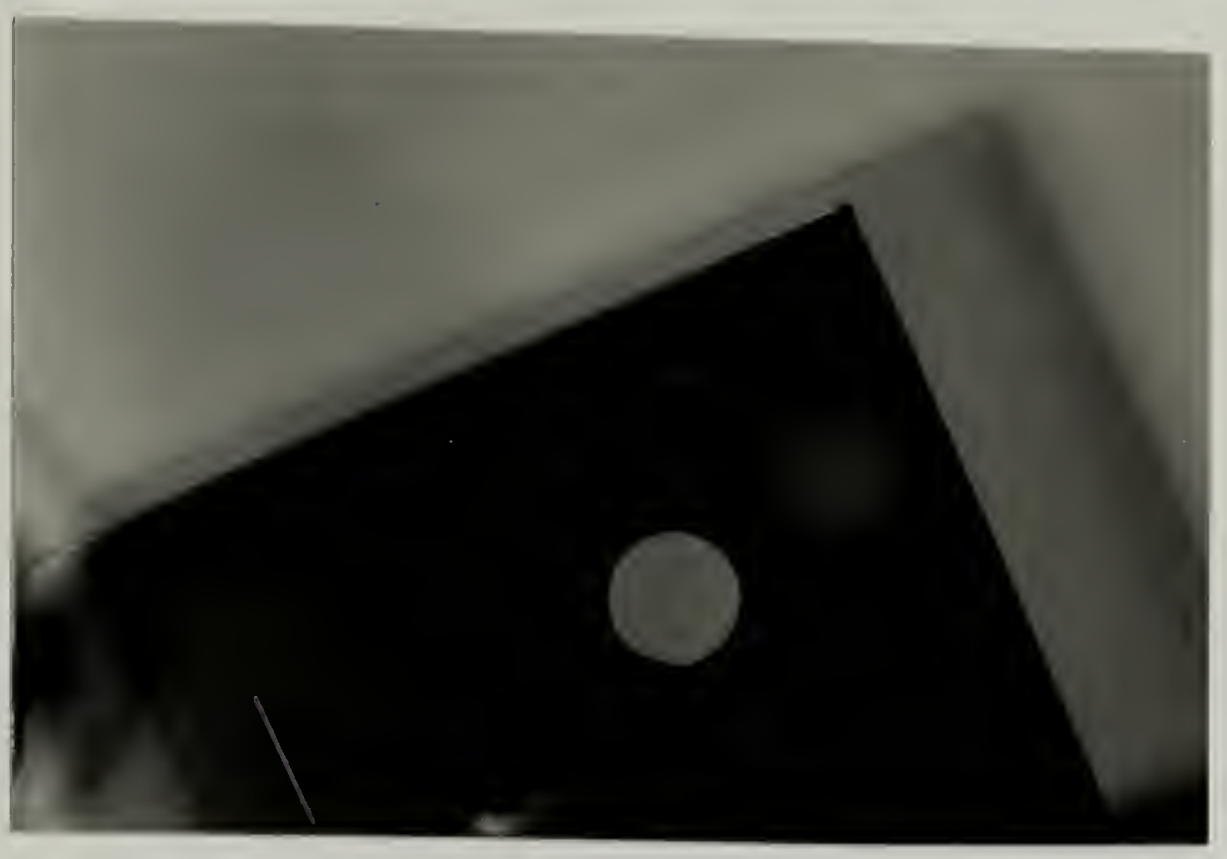

Figure 5.3. Photograph of self-delamination of 200° C cured PI5878 due to presence of circular hole and slit.

showed no signs of delamination upon inscribing a hole in the material. After the 85° C cure step, the coating remains as poly(amic acid). Only after higher heat treatments is it thermally cyclized to the polyimide. Therefore, the difference in results between 85° and 400° C cure may be attributed a chemical change in the material which alters the properties such as surface energy. Also, after imidization, the thickness has been reduced to a value below the critical thickness for self-delamination. It should then be possible to use this technique to follow the change in surface energy throughout the processing history.

The approach described above for attaining γ is not restricted to circular cuts. Cuts of varied shape and size may be used for this technique such as a straight slit. In this case, semi-circular debonding was observed on both sides of the slit. Although such geometries are easier to inscribe in the film the energy and stress analysis becomes more difficult especially at corners.

Experimentally, to improve this technique, new methods of cutting holes in coatings without disturbing the stress state of the film are required. Since the inner piece of film completely debonds it should be possible to obtain the residual stress in the film using strain analysis techniques. These methods such as Moire fringes or digital-image-correlation techniques allow determination of small planar displacements of the film due to delamination.[88,89] With these displacements and mechanical properties of the coating, the residual stress may be obtained for the film for each individual delamination test.

5.4 Summary

A method of assessing the surface energy of coatings has been presented. This method is applicable when the thickness of the coating is greater than a

critical debond thickness such that there is sufficient energy in the film for self-delamination. This technique is ideal for coatings which experience several processing steps, since one coated plate may be used for several tests. It should be possible to repeat this method on the same film after each processing stage providing a direct means of following the change in stress and adhesive strength throughout a coatings processing history. This technique was demonstrated using a polyimide film cured at 220° C for which a surface energy of 1.6 Nm^{-1} was obtained. This technique may also be generalized for multilayered coatings.

CHAPTER 6

SUMMARY

6.1 Conclusions

Polyimides used as coatings in the electronics industry undergo several harsh processing stages to achieve the final product. These include a series of heat treatments to remove solvent and cure the material. Because the properties and stress state are continually changing throughout this processing, a simple linear constitutive relation for stress and strain cannot be used in designing complicated structures utilizing these materials. Therefore, finite stress analysis techniques are needed and require the material properties as a function of processing history.

Standard methods of determining the properties of thin films or coatings as a function of their thermal and solvent history are not available. Therefore it was necessary to develop new techniques or adapt existing methods to characterize the mechanical behavior of coatings from the initial solvent casting to high temperature curing to post-curing thermal and solvent treatments. These include methods to:

* measure the stress-strain properties of materials in liquid environments.

* measure the stress-temperature response of axially constrained films.

* measure the stress-solvent response of axially constrained films.

* measure the stress developed due to solidification of solvent-based coatings and subsequent thermal and chemical treatments.

* measure Poisson's ratio for thin films as a function of stress or strain level.

* simultaneously measure shrinkage stress, modulus, and mass (hence solvent content) during constrained film solidification and subsequent thermal and chemical treatments.

* measure the surface energy of adhesion in coatings using a self-peeling geometry.

These techniques are not limited to use with polyimides. They are applicable to most solvent-based coatings and any thin film material or fiber. In addition, it has been demonstrated that an incremental linear elastic approach may be used to describe the constitutive behavior in these materials. The incremental approach includes dilatational phenomena associated with solidification, swelling, thermal and pressure effects and therefore may be applied to other systems.

This research dealt primarily with development of properties during formation of the polyimide coatings. The room temperature properties after four processing stages for a PI5878 material are summarized in Table 6.1. The modulus of this material after the 85° C solvent evaporation step (PAA) is similar

to that of the fully cured PI (after 400° C). The additional thermal treatments, however, do have an effect on the tensile strength (30 MPa at 85° C and 110 MPa at 400° C). The thermal expansion behavior of PI5878 is not fully developed until after the 220° C curing. The greatest change in this property occurs during the conversion of the PAA to PI when heated at 150° C. Probably the most important parameter to have acquired is Poisson's ratio, which was determined to be 0.34.

Table 6.1. Room temperature properties of PI5878

Processing T(° C)	E (GPa)	$\alpha \times 10^5$ (° C^{-1})	ν (at 1% strain)
85	2	4.9	0.42
150	3	2.4	0.41
220	3	1.8	0.25
400	3	1.8	0.34

Limited studies were performed on post-treatment effects on the properties of polyimides. Exposure of PI5878 and CG293 to water, NMP and methanol has no apparent effect on the tensile properties. The modulus of PI5878 is a nonlinear function of temperature decreasing from 3 to 1 GPa over a 300° C temperature span.

Shrinkage stresses due to solidification have been measured directly. Under uniaxial constraints a shrinkage stress of 8 MPa is measured in PAA films due to solvent removal at 85° C. An additional 6 MPa of stress is incurred due to further removal of solvent and imidization at 150° C. The removal of solvent at

85° C was observed to be dependent on the stress level in the coating and temperature. An energy balance approach predicts this type of coupling.

The residual stress level can alter the performance of the coating by facilitating failure mechanisms such as delamination. To assess a coatings performance, some knowledge of the surface energy is required. A self-delamination technique was used to determine the surface energy of adhesion of PI5878 to glass.

Once the polyimides are coated on a substrate they are not manually deformed. The stresses that develop are due solely to changes in the material. It does not appear possible to significantly relieve these stresses by changing processing history. Then, structures using these materials must be designed accordingly to accommodate the stresses.

The easiest solution to the large stresses that develop in PI5878 coatings would be to find another material. In the microelectronics industry, the ideal material would be one that possess the same thermal stability and electrical properties as PI5878 but has a tensile modulus appreciably lower.

6.2 Future Studies

This work has only been a first attempt at studying the mechanical behavior of polyimides as a function of thermal and solvent history. Currently a more comprehensive study of the influence of chemical environments on the mechanical behavior of these materials is being performed in Dr. Farris's research group. Additional work also needs to be performed high temperature processing ($T > 250°$ C) of these polyimides. This includes determining Poisson's ratio as a function of temperature.

It is now possible to follow the development of shrinkage stress with changes in mass of the sample. To understand this process on a molecular level changes in chemical structure need to be assessed. Fourier Transform Infra-red spectroscopy may be used to determine the degree of imidization during processing. However, at imide conversions greater than 97% this method is unreliable. Analysis of evolved gases (such as solvent and water) from the coating by gas chromatography may provide additional information on chemical interactions.

Probably one of the more unusual properties observed in Kapton is it plastic deformation behavior. Some polyimides may be elongated up to 70% without failure at room temperature.[2] Argon and Bessonov developed a theory of plastic deformation for polyimides or any glassy polymer. Their explanation considers that the deformation is due to orientation of a thermally activated complex to a given strain, where the complex is a cooperative bundle of chain segments.[90] As these increase in size with increasing chemical complexity, the activate complex also increases and thus local plasticization is decreased. Russell used X-ray scattering techniques to study this type of deformation in polyimides.[91] He observed no changes in diffraction profiles up to 30% elongation. After this point he was able to characterize the change in diffraction as due to a distortion of the ether bond angles in the PMDA-ODA molecule. His results confirm the Argon-Bessonov model.

Preliminary data (Table 6.2) indicates that the yield stress in PI5878 depends on the chemical environment.

Table 6.2. Yield stress of PI5878 films

Test Condition	Yield Stress (MPa)
in air	83 ± 9
30 min. in NMP	103 ± 6
30 min. in water	80 ± 4
30 min. in methanol	55 ± 4

Since the yielding phenomena is an energy dissipation mechanism, some insight into this process may be obtained using deformation calorimetry. This technique has been developed in Farris's research group and provides information on the total internal energy change during deformation.[92,93] Figure 6.1 shows the internal energy change (U), work (W) and heat (Q) corresponding to the given stress strain curve for a Kapton film. Work done on the sample is positive and heat flow into the sample is positive. This data indicates that most of the work goes into an internal energy change where $U = Q + W$.

This technique appears to be a promising method to study the deformation mechanisms of polyimides. Deformation calorimetry may also be used to measure the total energy involved in peeling films from their substrates to provide another method of obtaining surface energy.

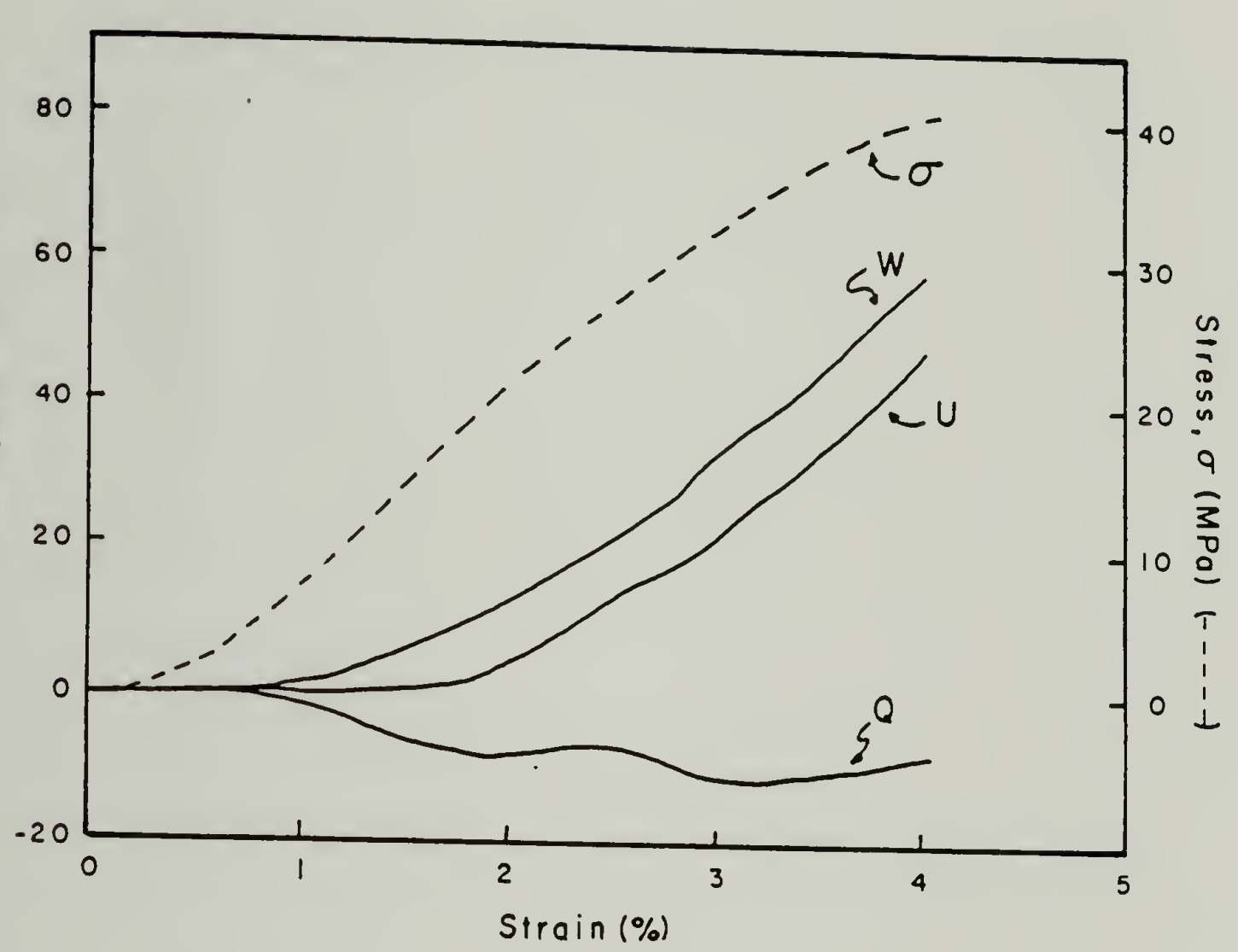

Figure 6.1. Work (W), heat (Q) and internal energy change (U) corresponding to given stress-strain curve for Kapton film.

APPENDIX

Figures A.1 through A.7 are transmission IR spectra of polyimide films after different stages of cure. The N-H stretching of the polyamic acid appears at 3247 cm^{-1} and the imide bands occur at 1776 and 722 cm^{-1}.

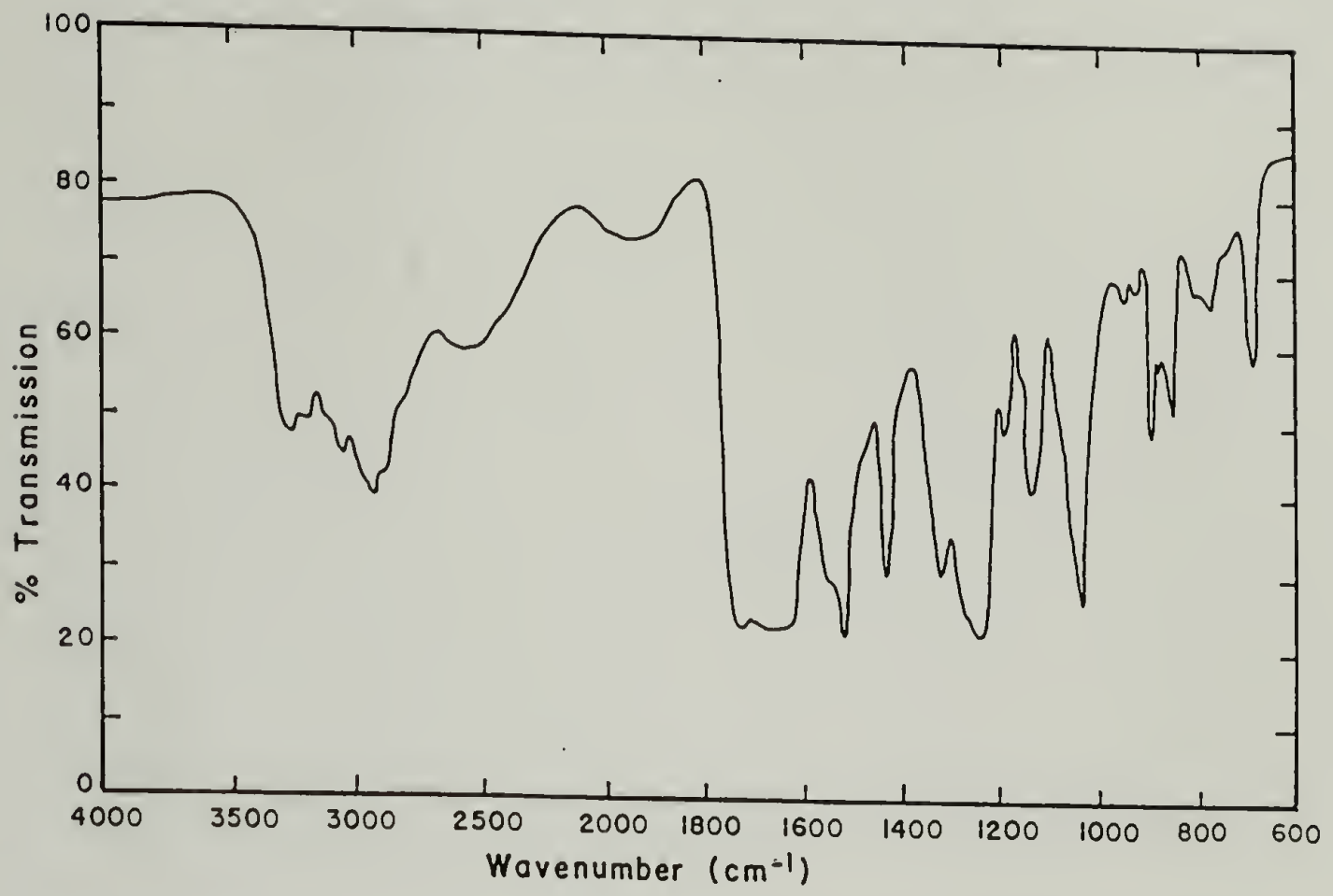

Figure A.1. Transmission IR of air dried PAA coating on rubber.

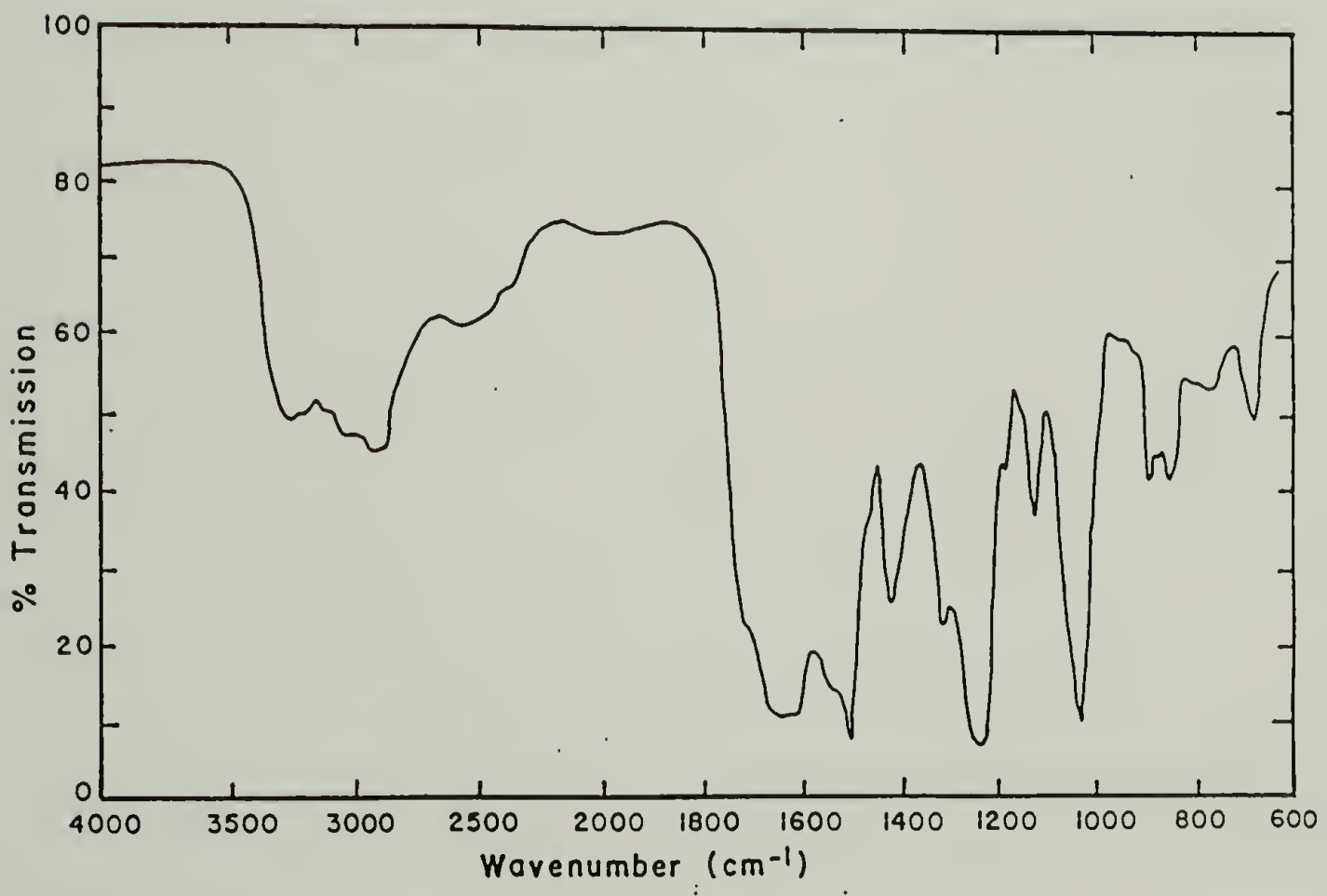

Figure A.2. Transmission IR of PAA film after one drying cycle at 85° C in force-temperature experiment.

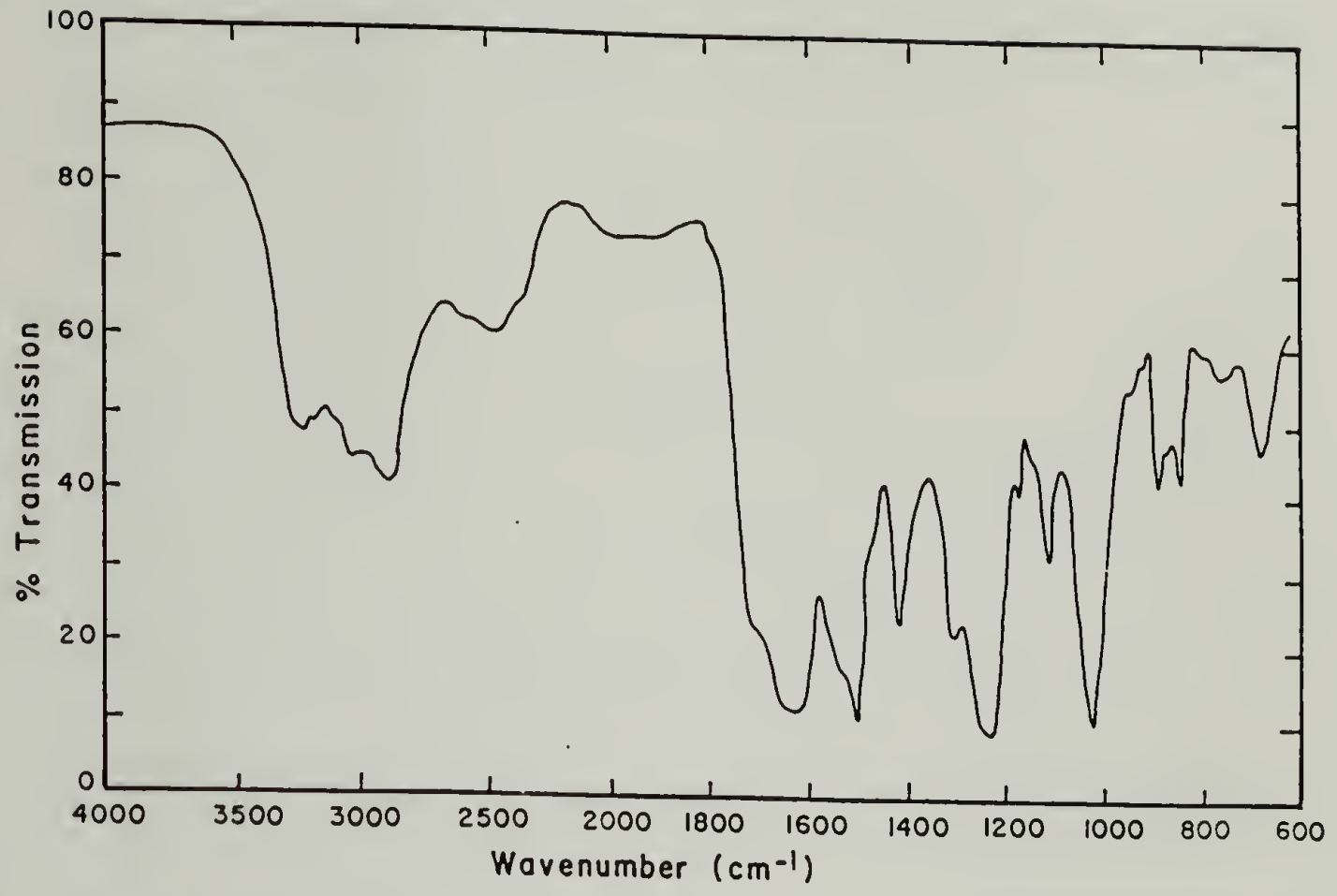

Figure A.3. Transmission IR of PAA film after two drying cycles at 85° C in force-temperature experiment.

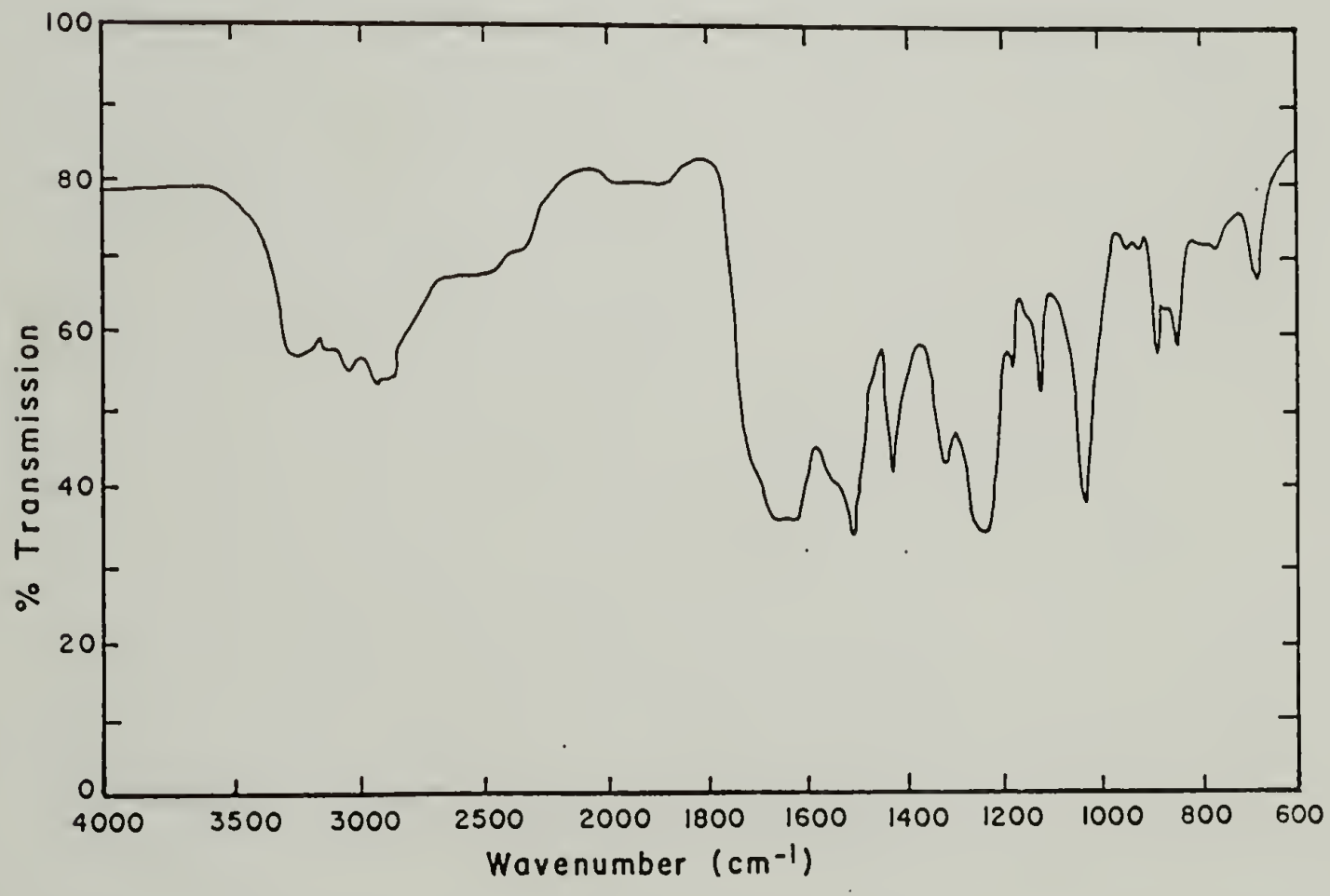

Figure A.4. Transmission IR of PAA film after three drying cycles at 85° C in force-temperature experiment.

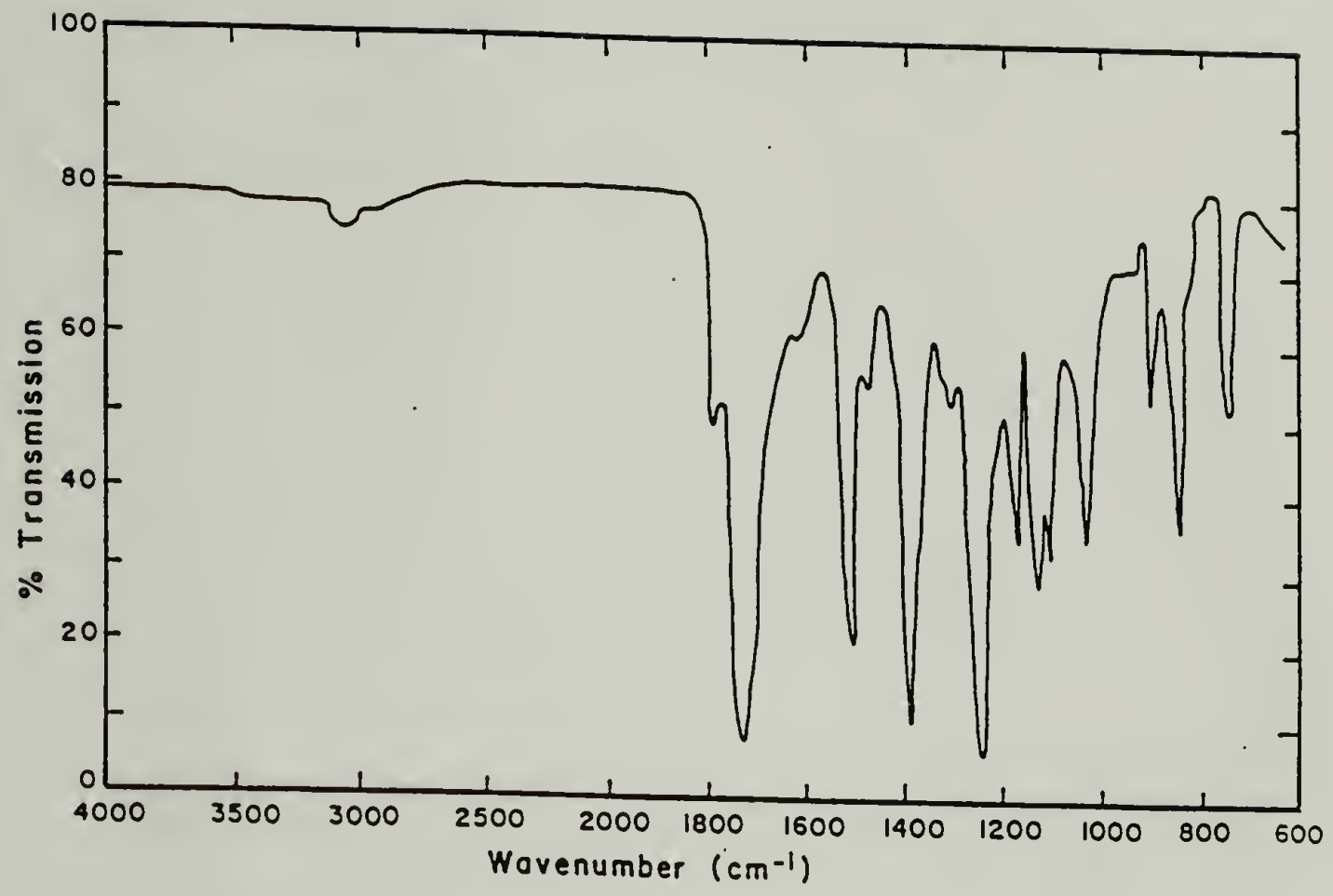

Figure A.5. Transmission IR of PAA film after curing at 160° C.

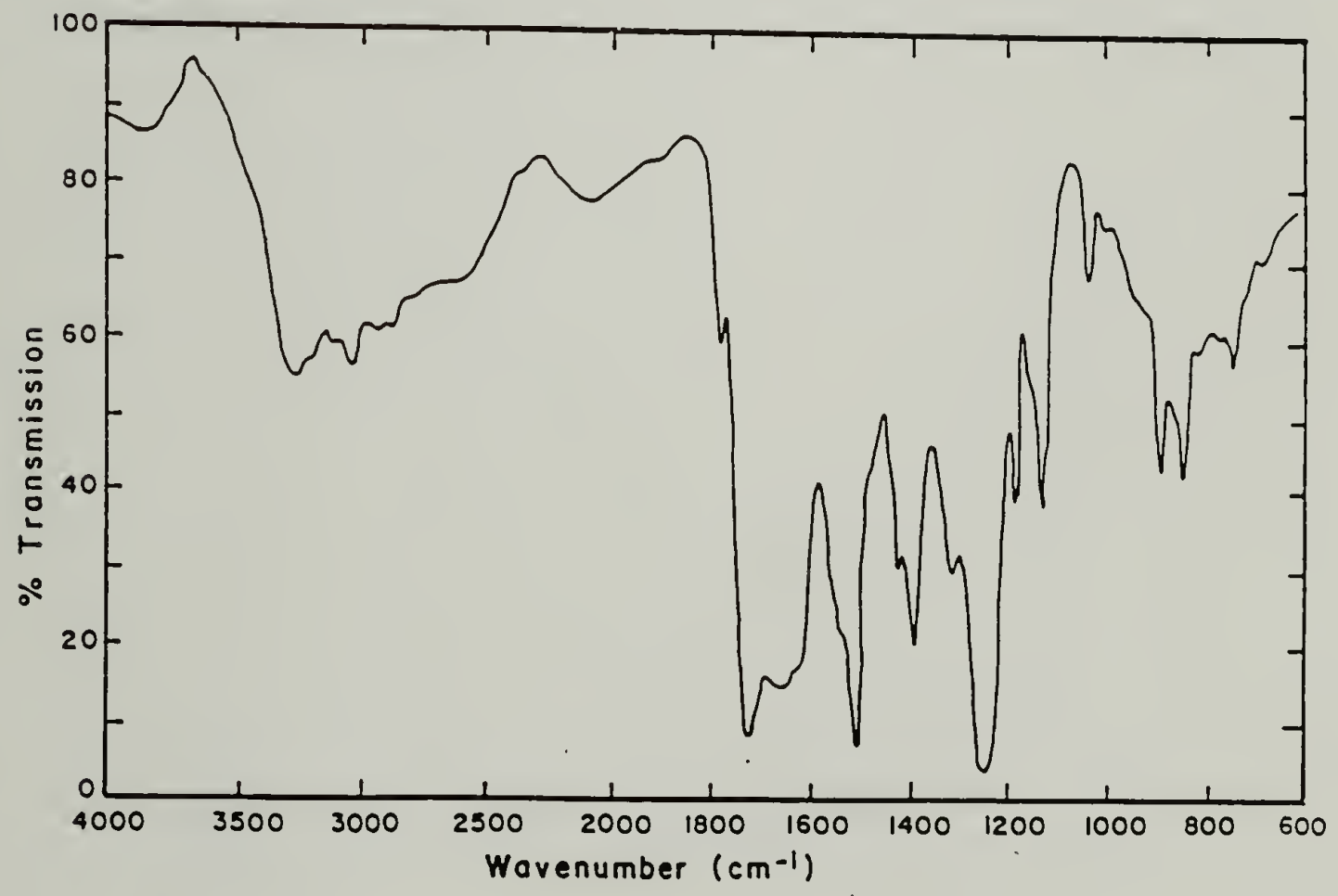

Figure A.6. Transmission IR of PAA coating after curing at 150° C on glass.

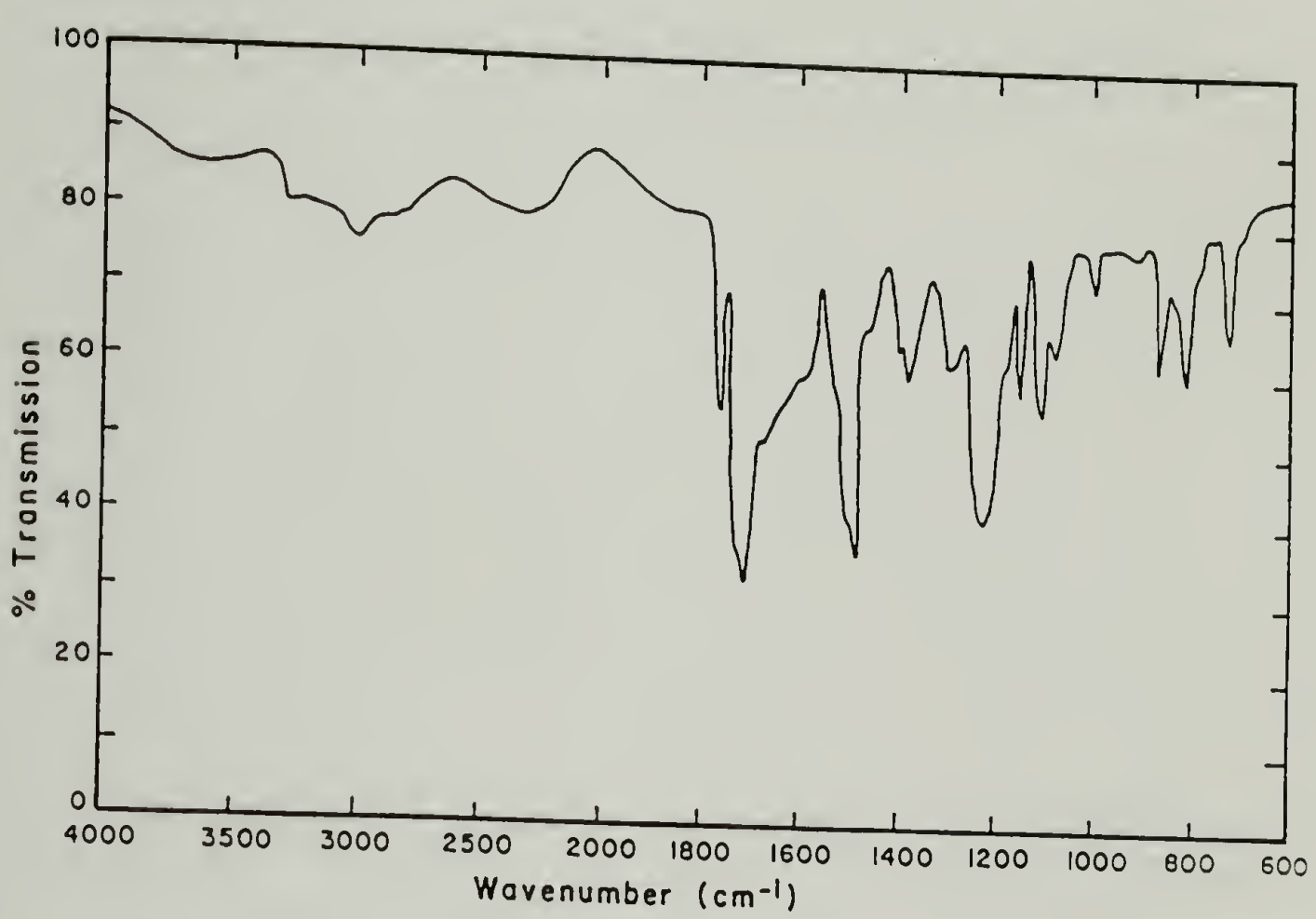

Figure A.7. Transmission IR of PAA film after curing at 220° C.

REFERENCES

1. D. Y. Perera and D. V. Eynde, "Moisture and Temperature Induced Stresses (Hygothermal Stresses) in Organic Coatings", J. Coat. Technol., 59 (748), 55 (1987).

2. N. A. Adrova, M. I. Bessonov, et al., Polyimides: A New Class of Thermally Stable Polymers, Technomic Pub. Co., Stamford, Conn. (1970).

3. S. D. Senturia, "Polyimides in Microelectronics", in ACS Symposium Series 346, Polymers for High Technology, M. J. Bowden and S. R. Turner eds., ACS, Washington D.C. (1987), Chapter 36.

4. "Kapton Polyimide Film: Summary of Properties", DuPont Technical Information Bulletin, E-50533 (1982).

5. C. E. Sroog, "Polyimides", J. Polym. Sci., Macrom. Reviews, 11, 161 (1976).

6. M. L. Wallach, "Structure-Property Relations of Polyimide Films", J. Polym. Sci., A-2, 6, 953 (1968).

7. D. R. Day and S. R. Senturia, "In-Situ Monitoring of Polyamic Acid Imidization with Microdlelectrometry", in Polyimides: Synthesis, Characterization and Applications, Vol 1, K. L. Mittal ed., Plenum Press, NY (1984), pp 249-258.

8. S. G. Anderson, H. M. Meyer, Lj. Atanasoska and J. H. Weaver, "Dynamics of Polyimide Curing and Degradation: An In-situ X-Ray Photoemission Study", J. Vac. Sci. Technol., A6, 38 (1988).

9. G. R. Palmese and J. K. Gillham, "Time-Temperature-Transformation (TTT) Cure Diagrams: Relationship between Tg and the Temperature and Time of Cure for a Polyamic Acid/Polyimide System", J. Appl. Polym. Sci., 34, 1925 (1987).

10. R. M. Ikeda, "A Mechanical Effect of Orientation", J. Poly. Sci., Polym. Letters, 4, 353 (1966).

11. G. A. Bernier and D. E. Kline, "Dynamic Mechanical Behavior of a Polyimide", J. Appl. Polym. Sci, 12, 593 (1968).

12. E. Butta, S. DePetris and M. Pasquini, "Young's Modulus and Secondary Mechanical Dispersions in Polypyromellitimide", J. Appl. Polym. Sci., 13, 1076 (1969).

13. W. Wrasidlo, "Motion in Poly(4,4'-oxydiphenylene)-pyromellitimide, J. Macromol. Sci-Phys, B6 (3), 559 (1972).

14. T. Lim, V. Frosini, V. Zaleckas, D. Morrow and J. A. Sauer, "Mechanical Relaxation Phenomena in Polyimide and Poly(2,6-dimethyl-p-phenyleneoxide) from 100 K to 700 K", Polym. Eng. Sci., 13 (1), 51 (1973).

15. J. A. Sauer and T. Lim, "Influence of Diluents on Mechanical Relaxation Behavior of Nylon 6 and Polyimide", Preprint ACS Div. Polym. Sci., 17 (2), 43 1976).

16. W. J. Wrasidlo, "The Nature of Dielictric Losses in H-Film", J. Polym. Sci., Polym. Phys. Ed., 11, 2143 (1973).

17. R. P. Chartoff and T. W. Chiu, "A Study of Crosslinking in Polyimides by Viscoelasctic and Diffusion Techniques", Proc. ACS Div. PMSE, 39, 129 (1978).

18. P. Metzger Cotts and W. Volksen, "Solution Characterization of Polyamic Acids and Polyimides", in ACS Symposium Series 242, Polymers in Electronics, T. Davidson ed., ACS, Washington, D.C. (1984), pp 227-237.

19. C. Conte, L. D'Ilario and N. V. Pavel, "An X-Ray and Conformational Study of Kapton-H", J. Polym Sci., Polym. Phys. Ed., 14, 1553 (1976).

20. S. Isoda, H. Shimada and M. Kochi, "Molecular Aggregation of Solid Aromatic Polymers. I. Small Angle X-Ray Scattering from Aromatic Polyimide Film", J. Polym. Sci., Polym. Phys. Ed., 19, 1293 (1981).

21. Sh. Tuichiev, L. N. Korzhavin, O. Ye. Prokhorov, B. M. Ginzburg, and S. Ya. Frenkel, "X-Ray Diffraction Study of the Structure of Some Aromatic Polyimide Fibers", Polym. Sci. USSR, 13, 1645 (1971). (Vysokomol. Soyed., A13, 1463 (1971)).

22. L. G. Kazaryan, D. Ya. Tsvankin, B. M. Ginzburg, Sh. Tuichiev, L. N. Korzhavin, and S. Ya. Frenkel, "X-Ray Diffraction Study of the Crystalline Structure of Aromatic Polyimides", Polym. Sci. USSR, 14, 1344 (1972). (Vysokomol. Syoed., A14, 1199 (1972)).

23. M. Kochi, H. Shimada and H. Kambe, "Molecular Aggragation and Mechanical Properties of Kapton H", J. Polym. Sci., Polym. Phys. Ed., 22, 1979 (1984).

24. N. Takahashi, D. Y. Yoon and W. Parrish, "Molecular Order in Condensed States of Semiflexible Poly(amic acid) and Polyimide", Macromolecules, 17, 2583 (1984).

25. T. P. Russell, "A Small Angle X-Ray Scattering Study of an Aromatic Polyimide", J. Polym. Sci., Polym. Phys. Ed., 22, 1105 (1984).

26. T. P. Russell, H. Gugger and J. D. Swalen, "In Plane Orientation of Polyimide", J. Polym. Sci., Polym. Phys. Ed., 21, 1745 (1983).

27. T. P. Russell, "Concerning Voids in Polyimide", Polym. Eng. Sci., 24 (5), 345 (1984).

28. B. F. Blumentritt, "Anisotropy and Dimensional Stability of Polyimide Films", Polym. Eng. Sci., 18, 1216 (1978).

29. R. F. Boehme and G. S. Cargill, "X-Ray Scattering Measurements Demonstrating In-Plane Anisotropy in Kapton Polyimide Films", in Polyimides: Synthesis, Characterization and Applications, Vol 1, K. L. Mittal ed., Plenum Press, NY (1984), pp 461-476.

30. R. M. Felder, C. J. Patton and W. J. Koros, "Dual Mode Sorption and Transport of Sulfur Dioxide in Kapton Polyimide", J. Polym. Sci., Polym. Phys. Ed., 19, 1895 (1981).

31. L. Iler, W. J. Koros, D. Y. Yang and R. Yui, "Sorption and Transport of Physically Interacting Penetrants in Kapton Polyimide", in Polyimides: Synthesis, Characterization and Applications, Vol 1, K. L. Mittal ed., Plenum Press, NY (1984), pp 443-460.

32. T. L. Smith and R. E. Adam, "Effect of Tensile Deformation on Gas Transport in Glassy Polymer Films", Polymer, 22, 299 (1981).

33. D. K. Yang, et al, "Sorption and Transport Studies of Water in Kapton Polyimide", J. Appl. Poly. Sci., 30, 1035 (1985).

34. D. K. Yang, et al, "The Effect of Morphology and Hygrothermal Aging on Water Sorption and Transport in Kapton Polyimide", J. Appl. Polym. Sci., 31, 1619 (1986).

35. J. F. Romanelli, J. W. Mayer, E. J. Kramer and T. P. Russell, "Rutherford Backscattering Spectroscopy Studies of Iodine Diffusion in Polyimide", J. Polym. Sci., Polym. Phys. Ed., 24, 263 (1986).

36. D. D. Denton, D. R. Day, D. F. Priore and S. D. Senturia, "Moisture Diffusion in Polyimide Films in Integrated Circuits", J. Elect. Mat., 14 (2), 119 (1985).

37. E. Sacher and J. R. Susko, "Water Permeation of Polymer Films. I. Polyimide", J. Appl. Polym. Sci., 23, 2355 (1979).

38. E. Sacher and J. R. Susko, "Water Permeation of Polymer Films. III. High Temperature Polyimides", J. Appl. Polym. Sci., 26, 679 (1981).

39. C. J. Wolf and R. S. Soloman, "Aging of Aromatic Polyimide Insulated Electrical Wire", SAMPE Journal, 20 (1), 16 (1984).

40. D. R. Askins, "Hydrolytic Degradation of Kapton Film", ANTEC, 395 (1984).

41. C. J. Wolf, D. L. Fanter and R. S. Soloman, "Environmental Degration of Aromatic Polyimide Insulated Electrical Wires", IEEE Trans. Electrical Insulation, EI-19 (4), 265 (1984).

42. B. J. Aleck, "Thermal Stresses in a Rectangular Plate Clamped Along an Edge", J. Appl. Mech., 16, 118 (1949).

43. S. G. Croll, "Internal Strain in Solvent-Cast Coatings", J. Coat. Technol., 51 (648), 64 (1979).

44. K. Sato, "The Internal Stress of Coating Films", Prog. Org. Coat., 8, 143 (1980).

45. D. Y. Perera and D. V. Eynde, "Effect of Organic Solvents on Internal Stress in Latex Coatings", J. Coat. Technol., 56 (718), 69 (1984).

46. D. Y. Perera, "Internal Stress in Latex Coatings", J. Coat. Technol., 56 (716), 111 (1984).

47. R. F. Eaton and F. G. Willeboordse, "Evaporation Behavior of Organic Cosolvents in Water-Bourne Formulations", J. Coat. Technol., 52 (660), 63 (1980).

48. J. Holten-Anderson and C. M. Hansen, "Solvent and Water Evaporation from Coatings", Prog. Org. Coat., 11, 219 (1983).

49. S. G. Croll, "Heat and Mass Transfer in Latex Paints During Drying", J. Coat. Technol., 59 (751), 81 (1987).

50. H. P. Blandin, et al., "Modelling of Drying of Coatings: Effect of the Thickness, Temperature and Concentration of Solvent", Prog. Org. Coat., 15, 163 (1987).

51. S. G. Croll, "The Origin of Residual Internal Stress in Solvent-Cast Thermoplastic Coatings", J. Appl. Polym. Sci., 23, 847 (1979).

52. D. S. Campbell, "Mechanical Properties of Thin Films", in Handbook of Thin Film Technology, L. I. Maissel and R. Glang eds., McGraw Hill, NY (1970), Chapter 12.

53. E. M. Corcoran, "Determining Stresses in Organic Coatings Using Plate Beam Deflection", J. Paint Technol., 41 (538), 635 (1969).

54. S. G. Croll, "Internal Stress in a Solvent-Cast Thermoplastic Coating", J. Coat. Technol., 50 (638), 33 (1978).

55. R. N. O'Brien and W. Michalik, "Laser Interferometry Method for Internal Stress Measurement in Coatings", J. Coat. Technol., 58 (735), 25 (1986).

56. D. Y. Perera and D. V. Eynde, "Considerations on a Cantilever (Beam) Method for Measuring the Internal Stress in Organic Coatings", J. Coat. Technol., 53 (677), 39 (1981).

57. M. Chipalkatti, J. Hutchinson and R. J. Farrris, "Development of the Vibrational Time-Delay Technique and the Study of Stress/Strain Coupled Diffusion in Polymers", Rev. Sci. Instrum., 58, 112 (1987).

58. C. R. Wylie and L. C. Barrett, Advanced Engineering Mathematics, 5th ed., McGraw Hill, NY (1982).

59. M. S. Vratsanos, Studies of Polymer Solidification Using the Technique of Impulse Viscoelasticity, Ph.D. Thesis, University of Massachusetts, Amherst, MA, (1987).

60. N. L. Yarym-Agaev, L. D. Afanasenko, V. P. Kalinichenko and G. B. Tolmacheva, "The Liquid-Vapor Equilibrium of N-Methylpyrrolidone and γ -Butyrolactone", Ukrain. Khim. Zh., 46, 1331 (1980).

61. C. Goldsmith, P. Geldermans, F. Bedetti and G. A. Walker, "Measurement of Stresses Generated in Cured Polyimide Films", J. Vac. Sci. Technol., A1 (2), 407 (1983).

62. P. Geldermans, C. Goldsmith and F. Bedetti, "Measurement of Stresses Generated During Curing and in Cured Polyimide Films", in Polyimides: Synthesis, Characterization and Applications, Vol 2, K. L. Mittal ed., Plenum Press, NY (1984), pp 695-711.

63. T. S. Chow, C. A. Liu and R. C. Penwall, "Strains Induced upon Drying Thin Films Solvent-Cast on Flexible Substrates", J. Polym. Sci., Polym. Phys. Ed., 14, 1311 (1976).

64. C. Feger, "Curing of Polyimides", SPE ANTEC, 32, 967 (1987).

65. M.-J. Brekner and C. Feger, "Curing Studies of a Polyimide Precursor", J. Polym. Sci., Polym. Chem. Ed., 25, 2005 (1987).

66. M.-J. Brekner and C. Feger, "Curing Studies of a Polyimide Precursor. II. Polyamic Acid", J. Polym. Sci., Polym. Chem. Ed., 25, 2479 (1987).

67. H. M. Tong, C.-K. Hu, C. Feger, and P. S. Ho, "Stress Development in Supported Polymer Films During Thermal Cycling", Polym. Eng. Sci., 26, 1213 (1986).

68. P. J. Flory and J. Rehner, "Effect of Deformation on the Swelling Capacity of Rubber", J. Chem. Phys., 12, 412 (1944).

69. L. R. G. Treloar, The Physics of Rubber Elasticity, 3rd ed., Oxford Univ. Press, London (1975).

70. S. S. Sternstein, "Inhomogeneous Swelling in Filled Elastomers", J. Macromol. Sci.-Phys., B6, 243 (1972).

71. L. R. G. Treloar, "The Absorbance of Water by Hair, and its Dependence on Applied Stress", Trans. Faraday Soc., 48, 567 (1952).

72. L. R. G. Treloar, "The Absorption of Water by Cellulose, and its Dependence on Applied Stress", Trans. Faraday Soc., 49, 816 (1953).

73. M. Chipalkatti, R. J. Farris and J. M. Ottino, "History Dependence of Stress Coupled Transport in Polymer Fibers and Ribbons", Proc. ACS Div. PMSE, 55, 831 (1986).

74. L. A. Pottick, "The Influence of Drying on the Structure and Mechanics of Poly(p-phenylene benzobisthiazole) Fibers', Ph.D. Thesis, University of Massachusetts, Amherst, MA (1986).

75. I. S. Sokolnikoff, Mathematical Theory of Elasticity, 2nd ed., McGraw Hill, NY (1956).

76. S. P. Timoshenko and J. N. Goodier, Theory of Elasticity, 3rd ed., McGraw Hill, NY (1970).

77. ASTM E132-61, "Standard Test Method for Poisson's Ratio at Room Temperature".

78. R. J. Farris, "Dilatation of Granular Filled Elastomers under High Rates of Strain", J. Appl. Polym. Sci., 8, 25 (1964).

79. H. Lee and T. L. Smith, IBM San Jose Research Laboratories, unpublished results.

80. S. H. Crandall, N. C. Dahl and T. J. Lardner, An Introduction to the Mechanics of Solids, 2nd ed., McGraw Hill, NY (1978).

81. L. E. Malvern, Introduction to the Mechanics of a Continuous Medium, Prentice-Hall, NJ (1969).

82. S. G. Croll, "Adhesion Loss Due to Internal Strain", J. Coat. Technol., 52 (665), 35 (1980).

83. S. G. Croll, "Adhesion and Internal Strain in Polymeric Coatings", in Adhesion Aspects of Polymeric Coatings, K. L. Mittal ed., Plenum Press, NY (1983), pp 107-129.

84. K. Kendall, "The Adhesion and Surface Energy of Elastic Solids", J. Phys. D, Appl. Phys., 4, 1186 (1971).

85. K. Kendall, "Shrinkage and Peel Strength of Adhesive Joints", J. Phys. D, Appl. Phys., 6, 1782 (1973).

86. M. G. Allen and S. D. Senturia, "Microfabicated Structures for the Measurement of Adhesion and Mechanical Properties of Polymer Films" Proc. ACS Div. PMSE, 56, 735 (1987).

87. D. Suryanarayana and K. L. Mittal, "Effect of Polyimide Thickness on its Adhesion to Silicon Nitride Substrate with and without Adhesion Promoter", J. Appl. Polym. Sci., 30, 3107 (1985).

88. A. J. Durelli and V. J. Parks, Moire Analysis of Strains, Prentice-Hall, Inc., New Jersey (1970).

89. T. C. Chu, W. F. Ransom, M. A. Sutton, and W. H. Peters, "Applications of Digital-Image-Correlation Techniques to Experimental Mechanics", Exp. Mech., 25, 232 (1985).

90. A. S. Argon and M. I. Bessonov, "Plasitic Deformation in Polyimides, with New Implications on the Theory of Plastic Deformation of Glassy Polymers", Phil. Mag., 35, 917 (1977).

91. T. P. Russell and H. R. Brown, "X-ray Studies on the Deformation of an Aromatic Polyimide", J. Polym. Sci.: Polym. Phys., 25, 1129 (1987).

92. R. E. Lyon, Thermodynamics of Deformation, Ph.D. Thesis, University of Massachusetts, Amherst, MA (1985).

93. G. W. Adams, The Thermodynamics of Deformation for Thermoplastic Polymers, Ph.D. Thesis, University of Massachusetts, Amherst, MA (1987).

BIBLIOGRAPHY

Adams, Gary W., The Thermodynamics of Deformation for Thermoplastic Polymers, Ph.D. Thesis, University of Massachusetts, Amherst, MA (1987).

Adrova, N. A., Bessonov, M. I., et al., Polyimides: A New Class of Thermally Stable Polymers, Technomic Pub. Co., Stamford, Conn. (1970).

Aleck, B. J., "Thermal Stresses in a Rectangular Plate Clamped Along an Edge", J. Appl. Mech., 16, 118 (1949).

Allen, Mark G. and Senturia, Stephen D., "Microfabicated Structures for the Measurement of Adhesion and Mechanical Properties of Polymer Films" Proc. ACS Div. PMSE, 56, 735 (1987).

Anderson, Stephen G., Meyer, H. M., Atanasoska, Lj. and Weaver, J. H., "Dynamics of Polyimide Curing and Degradation: An In-situ X-Ray Photoemission Study", J. Vac. Sci. Technol., A6, 38 (1988).

Argon, A. S. and Bessonov, M. I., "Plasitic Deformation in Polyimides, with New Implications on the Theory of Plastic Deformation of Glassy Polymers", Phil. Mag., 35, 917 (1977).

Askins, D. Robert, "Hydrolytic Degradation of Kapton Film", ANTEC, 395 (1984).

ASTM E132-61, "Standard Test Method for Poisson's Ratio at Room Temperature".

Bernier, G. A. and Kline, D. E., "Dynamic Mechanical Behavior of a Polyimide", J. Appl. Polym. Sci, 12, 593 (1968).

Blandin, H. P., et al., "Modelling of Drying of Coatings: Effect of the Thickness, Temperature and Concentration of Solvent", Prog. Org. Coat., 15, 163 (1987).

Blumentritt, Bruce F., "Anisotropy and Dimensional Stability of Polyimide Films", Polym. Eng. Sci., 18, 1216 (1978).

Boehme, R. F. and Cargill, G. S., "X-Ray Scattering Measurements Demonstrating In-Plane Anisotropy in Kapton Polyimide Films", in Polyimides: Synthsis, Characterization and Applications, Vol 1, Mittal, K. L. ed., Plenum Press, NY (1984), pp 461-476.

Brekner Michael-Joachim and Feger Clausius, "Curing Studies of a Polyimide Precursor", J. Polym. Sci., Polym. Chem. Ed., 25, 2005 (1987).

Brekner, Michael-Joachim and Feger, Claudius, "Curing Studies of a Polyimide Precursor. II. Polyamic Acid", J. Polym. Sci., Polym. Chem. Ed., 25, 2479 (1987).

Butta, Enzo, DePetris, Silvano and Pasquini, Mario, "Young's Modulus and Secondary Mechanical Dispersions in Polypyromellitimide", J. Appl. Polym. Sci., 13, 1076 (1969).

Campbell, D. S., "Mechanical Properties of Thin Films", in Handbook of Thin Film Technology, Maissel, L. I. and Glang, R. eds., McGraw Hill, NY (1970), Chapter 12.

Chartoff, Richard P. and Chiu, Tai W., "A Study of Crosslinking in Polyimides by Viscoelasctic and Diffusion Techniques", Proc. ACS Div. PMSE, 39, 129 (1978).

Chipalkatti, Makarand, Farris, Richard J., and Ottino, Julio M., "History Dependence of Stress Coupled Transport in Polymer Fibers and Ribbons", Proc. ACS Div. PMSE, 55, 831 (1986).

Chipalkatti, Makarand, Hutchinson, John and Farrris, Richard J., "Development of the Vibrational Time-Delay Technique and the Study of Stress/Strain Coupled Diffusion in Polymers", Rev. Sci. Instrum., 58, 112 (1987).

Chow, T. S., Liu, C. A. and Penwall, R. C., "Strains Induced upon Drying Thin Films Solvent-Cast on Flexible Substrates", J. Polym. Sci., Polym. Phys. Ed., 14, 1311 (1976).

Chu, T. C., Ransom, W. F., Sutton, M. A., and Peters, W. H., "Applications of Digital-Image-Correlation Techniques to Experimental Mechanics", Exp. Mech., 25, 232 (1985).

Conte, C., D'Ilario, L. and Pavel, N. V., "An X-Ray and Conformational Study of Kapton-H", J. Polym Sci., Polym. Phys. Ed., 14, 1553 (1976).

Corcoran, E. M., "Determining Stresses in Organic Coatings Using Plate Beam Deflection", J. Paint Technol., 41 (538), 635 (1969).

Cotts, P. Metzger and Volksen, W., "Solution Characterization of Polyamic Acids and Polyimides", in ACS Symposium Series 242, Polymers in Electronics, Davidson, T. ed., ACS, Washington, D.C. (1984), pp 227-237.

Crandall, Stephen H., Dahl, Norman C. and Lardner, Thomas J., An Introduction to the Mechanics of Solids, 2nd ed., McGraw Hill, NY (1978).

Croll, Stuart G., "Adhesion and Internal Strain in Polymeric Coatings", in Adhesion Aspects of Polymeric Coatings, K. L. Mittal ed., Plenum Press, NY (1983), pp 107-129.

Croll, Stuart G., "Adhesion Loss Due to Internal Strain", J. Coat. Technol., 52 (665), 35 (1980).

Croll, Stuart G., "Heat and Mass Transfer in Latex Paints During Drying", J. Coat. Technol., 59 (751), 81 (1987).

Croll, Stuart G., "Internal Strain in Solvent-Cast Coatings", J. Coat. Technol., 51 (648), 64 (1979).

Croll, Stuart G., "Internal Stress in a Solvent-Cast Thermoplastic Coating", J. Coat. Technol., 50 (638), 33 (1978).

Croll, Stuart G., "The Origin of Residual Internal Stress in Solvent-Cast Thermoplastic Coatings", J. Appl. Polym. Sci., 23, 847 (1979).

Day, D. R. and Senturia, S. R., "In-Situ Monitoring of Polyamic Acid Imidization with Microdlelectrometry", in Polyimides: Synthsis, Characterization and Applications, Vol 1, Mittal, K. L. ed., Plenum Press, NY (1984), pp 249-258.

Denton, D. D., Day, D. R., Priore, D. F. and Senturia, S. D., "Moisture Diffusion in Polyimide Films in Integrated Circuits", J. Elect. Mat., 14 (2), 119 (1985).

Durelli, Augusto J. and Parks, Vincent J., Moire Analysis of Strains, Prentice-Hall, Inc., New Jersey (1970).

Eaton, R. F. and Willeboordse, F. G., "Evaporation Behavior of Organic Cosolvents in Water-Bourne Formulations", J. Coat. Technol., 52 (660), 63 (1980).

Farris, Richard J., "Dilatation of Granular Filled Elastomers under High Rates of Strain", J. Appl. Polym. Sci., 8, 25 (1964).

Feger, Claudius, "Curing of Polyimides", SPE ANTEC, 32, 967 (1987).

Felder, R. M., Patton, C. J. and Koros, W. J., "Dual Mode Sorption and Transport of Sulfur Dioxide in Kapton Polyimide", J. Polym. Sci., Polym. Phys. Ed., 19, 1895 (1981).

Flory, Paul J., Principles of Polymer Chemistry, Cornell University Press, Ithica (1953).

Flory, Paul J. and Rehner, John, "Effect of Deformation on the Swelling Capacity of Rubber", J. Chem. Phys., 12, 412 (1944).

Geldermans, P., Goldsmith, C., and Bedetti, F., "Measurement of Stresses Generated During Curing and in Cured Polyimide Films", in Polyimides: Synthsis, Characterization and Applications, Vol 2, Mittal, K. L. ed., Plenum Press, NY (1984), pp 695-711.

Goldsmith, C., Geldermans, P., Bedetti, F. and Walker, G. A., "Measurement of Stresses Generated in Cured Polyimide Films", J. Vac. Sci. Technol., A1 (2), 407 (1983).

Holten-Anderson, John and Hansen, Charles M., "Solvent and Water Evaporation from Coatings", Prog. Org. Coat., 11, 219 (1983).

Ikeda, Richard M., "A Mechanical Effect of Orientation", J. Poly. Sci., Polym. Letters, 4, 353 (1966).

Iler, L., Koros, W. J., Yang, D. Y. and Yui, R., "Sorption and Transport of Physically Interacting Penetrants in Kapton Polyimide", in Polyimides: Synthsis, Characterization and Applications, Vol 1, Mittal, K. L. ed., Plenum Press, NY (1984), pp 443-460.

Isoda, Satoru, Shimada, Hiromichi and Kochi, Masakatsu, "Molecular Aggregation of Solid Aromatic Polymers. I. Small Angle X-Ray Scattering from Aromatic Polyimide Film", J. Polym. Sci., Polym. Phys. Ed., 19, 1293 (1981).

"Kapton Polyimide Film: Summary of Properties", DuPont Technical Information Bulletin, E-50533 (1982).

Kazaryan, L. G., Tsvankin, D. Ya., Ginzburg, B. M., Tuichiev, Sh., Korzhavin, L. N., and Frenkel, S. Ya., "X-Ray Diffraction Study of the Crystalline Structure of Aromatic Polyimides", Polym. Sci. USSR, 14, 1344 (1972). (Vysokomol. Syoed., A14, 1199 (1972)).

Kendall, K., "Shrinkage and Peel Strength of Adhesive Joints", J. Phys. D, Appl. Phys., 6, 1782 (1973).

Kendall, K., "The Adhesion and Surface Energy of Elastic Solids", J. Phys. D, Appl. Phys., 4, 1186 (1971).

Kinloch, Anthony J. and Young, Robert J., Fracture Behavior of Polymers, Applied Science Publishers, London (1983).

Kochi, Masakatsu, Shimada, Hiromichi and Kambe, Hirotaro, "Molecular Aggragation and Mechanical Properties of Kapton H", J. Polym. Sci., Polym. Phys. Ed., 22, 1979 (1984).

Lee, H. and Smith, T. L., IBM San Jose Research Laboratories, unpublished results.

Lim, T., Frosini, V., Zaleckas, V., Morrow, D. and Sauer, J. A., "Mechanical Relaxation Phenomena in Polyimide and Poly(2,6-dimethyl-p-phenyleneoxide) from 100 K to 700 K", Polym. Eng. Sci., 13 (1), 51 (1973).

Lyon, Richard E., Thermodynamics of Deformation, Ph.D. Thesis, University of Massachusetts, Amherst, MA (1985).

Malvern, Lawrence E., Introduction to the Mechanics of a Continuous Medium, Prentice-Hall, NJ (1969).

O'Brien, R. N. and Michalik, W., "Laser Interferometry Method for Internal Stress Measurement in Coatings", J. Coat. Technol., 58 (735), 25 (1986).

Palmese, G. R. and Gillham, J. K., "Time-Temperature-Transformation (TTT) Cure Diagrams: Relationship between Tg and the Temperature and Time of Cure for a Polyamic Acid/Polyimide System", J. Appl. Polym. Sci., 34, 1925 (1987).

Perera, Dan Y., "Internal Stress in Latex Coatings", J. Coat. Technol., 56 (716), 111 (1984).

Perera, Dan Y. and Eynde, D. Vanden, "Considerations on a Cantilever (Beam) Method for Measuring the Internal Stress in Organic Coatings", J. Coat. Technol., 53 (677), 39 (1981).

Perera, Dan Y. and Eynde, D. Vanden., "Effect of Organic Solvents on Internal Stress in Latex Coatings", J. Coat. Technol., 56 (718), 69 (1984).

Perera, Dan Y. and Eynde, D. Vanden, "Moisture and Temperature Induced Stresses (Hygothermal Stresses) in Organic Coatings", J. Coat. Technol., 59 (748), 55 (1987).

Pottick, Lorelle A., "The Influence of Drying on the Structure and Mechanics of Poly(p-phenylene benzobisthiazole) Fibers', Ph.D. Thesis, University of Massachusetts, Amherst, MA (1986).

Romanelli, J. F., Mayer, J. W., Kramer, E. J. and Russell, T. P., "Rutherford Backscattering Spectroscopy Studies of Iodine Diffusion in Polyimide", J. Polym. Sci., Polym. Phys. Ed., 24, 263 (1986).

Russell, T. P. and Brown, H. R., "X-ray Studies on the Deformation of an Aromatic Polyimide", J. Polym. Sci.: Polym. Phys., 25, 1129 (1987).

Russell, T. P., "A Small Angle X-Ray Scattering Study of an Aromatic Polyimide", J. Polym. Sci., Polym. Phys. Ed., 22, 1105 (1984).

Russell, T. P., "Concerning Voids in Polyimide", Polym. Eng. Sci., 24 (5), 345 (1984).

Russell, T. P., Gugger, H. and Swalen, J. D., "In Plane Orientation of Polyimide", J. Polym. Sci., Polym. Phys. Ed., 21, 1745 (1983).

Sacher, E. and Susko, J. R., "Water Permeation of Polymer Films. I. Polyimide", J. Appl. Polym. Sci., 23, 2355 (1979).

Sacher, E. and Susko, J. R., "Water Permeation of Polymer Films. III. High Temperature Polyimides", J. Appl. Polym. Sci., 26, 679 (1981).

Sato, Kozo, "The Internal Stress of Coating Films", Prog. Org. Coat., 8, 143 (1980).

Sauer, J. A. and Lim, T., "Influence of Diluents on Mechanical Relaxation Behavior of Nylon 6 and Polyimide", Preprint ACS Div. Polym. Sci., 17 (2), 43 1976).

Senturia, Stephen D., "Polyimides in Microelectronics", in ACS Symposium Series 346, Polymers for High Technology, Bowden, M. J. and Turner, S. R. eds., ACS, Washington D.C. (1987), Chapter 36.

Smith, T. L. and Adam, R. E., "Effect of Tensile Deformation on Gas Transport in Glassy Polymer Films", Polymer, 22, 299 (1981).

Sokolnikoff, Ivan S., Mathematical Theory of Elasticity, 2nd ed., McGraw Hill, NY (1956).

Sroog, C. E., "Polyimides", J. Polym. Sci., Macrom. Reviews, 11, 161 (1976).

Sternstein, Sanford S., "Inhomogeneous Swelling in Filled Elastomers", J. Macromol. Sci.-Phys., B6, 243 (1972).

Suryanarayana, D. and Mittal, K. L., "Effect of Polyimide Thickness on its Adhesion to Silicon Nitride Substrate with and without Adhesion Promoter", J. Appl. Polym. Sci., 30, 3107 (1985).

Takahashi, Noboyuki, Yoon, Do Y. and Parrish, William, "Molecular Order in Condensed States of Semiflexible Poly(amic acid) and Polyimide", Macromolecules, 17, 2583 (1984).

Timoshenko, Stephen P. and Goodier, John N., Theory of Elasticity, 3rd ed., McGraw Hill, NY (1970).

Tong, H. M., Hu, C.-K., Feger, C., and Ho, P. S., "Stress Development in Supported Polymer Films During Thermal Cycling", Polym. Eng. Sci., 26, 1213 (1986).

Treloar, L. R. G., "The Absorbance of Water by Hair, and its Dependence on Applied Stress", Trans. Faraday Soc., 48, 567 (1952).

Treloar, L. R. G., "The Absorption of Water by Cellulose, and its Dependence on Applied Stress", Trans. Faraday Soc., 49, 816 (1953).

Treloar, L. R. G., The Physics of Rubber Elasticity, 3rd ed., Oxford Univ. Press, London (1975).

Tuichiev, Sh., Korzhavin, L. N., Prokhorov, O. Ye., Ginzburg, B. M., and Frenkel, S. Ya., "X-Ray Diffraction Study of the Structure of Some Aromatic Polyimide Fibers", Polym. Sci. USSR, 13, 1645 (1971). (Vysokomol. Soyed., A13, 1463 (1971)).

Vratsanos, Menas S., Studies of Polymer Solidification Using the Technique of Impulse Viscoelasticity, Ph.D. Thesis, University of Massachusetts, Amherst, MA, (1987).

Wallach, M. L., "Structure-Property Relations of Polyimide Films", J. Polym. Sci., A-2, 6, 953 (1968).

Wolf, Clarence J., Fanter, Dale L. and Soloman, Ronald S., "Environmental Degration of Aromatic Polyimide Insulated Electrical Wires", IEEE Trans. Electrical Insulation, EI-19 (4), 265 (1984).

Wolf, Clarence J. and Soloman, Ronald S., "Aging of Aromatic Polyimide Insulated Electrical Wire", SAMPE Journal, 20 (1), 16 (1984).

Wrasidlo, Wolfgang, "Motion in Poly(4,4'-oxydiphenylene)-pyromellitimide", J. Macromol. Sci-Phys, B6 (3), 559 (1972).

Wrasidlo, W. J., "The Nature of Dielictric Losses in H-Film", J. Polym. Sci., Polym. Phys. Ed., 11, 2143 (1973).

Wylie, C. Ray and Barrett, Louis C., Advanced Engineering Mathematics, 5th ed., McGraw Hill, NY (1982).

Yang, D. K., et al., "Sorption and Transport Studies of Water in Kapton Polyimide", J. Appl. Poly. Sci., 30, 1035 (1985).

Yang, D. K., et al., "The Effect of Morphology and Hygrothermal Aging on Water Sorption and Transport in Kapton Polyimide", J. Appl. Polym. Sci., 31, 1619 (1986).

Yarym-Agaev, N. L., Afanasenko, L. D., Kalinichenko, V. P. and Tolmacheva, G. B., "The Liquid-Vapor Equilibrium of N-Methylpyrrolidone and γ-Butyrolactone", Ukrain. Khim. Zh., 46, 1331 (1980).